uOttawa

L'Université canadienne
Canada's university

**FACULTÉ DES ÉTUDES SUPÉRIEURES ET POSTOCTORALES**

uOttawa

L'Université canadienne
Canada's university

**FACULTY OF GRADUATE AND POSDOCTORAL STUDIES**

Hadi D. Toeg
AUTEUR DE LA THÈSE / AUTHOR OF THESIS

M.Sc. (Biochemistry)
GRADE / DEGREE

Department of Biochemistry, Microbiology and Immunology
FACULTÉ, ÉCOLE, DÉPARTEMENT / FACULTY, SCHOOL, DEPARTMENT

Role of Connexin 30 in Directing Adult Neural Progenitor Cell Fate

TITRE DE LA THÈSE / TITLE OF THESIS

Steffany Bennett
DIRECTEUR (DIRECTRICE) DE LA THÈSE / THESIS SUPERVISOR

CO-DIRECTEUR (CO-DIRECTRICE) DE LA THÈSE / THESIS CO-SUPERVISOR

EXAMINATEURS (EXAMINATRICES) DE LA THÈSE / THESIS EXAMINERS

Kristen Baetz

Marc Ruel

Gary W. Slater
Le Doyen de la Faculté des études supérieures et postdoctorales / Dean of the Faculty of Graduate and Postdoctoral Studies

# Role of Connexin 30 in Directing Adult Neural Progenitor Cell Fate

Hadi D. Toeg

A thesis submitted to the Faculty of Graduate and
Postdoctoral studies in partial fulfillment of the
requirements for the degree of Masters of Science.

Department of Biochemistry, Microbiology, and Immunology
University of Ottawa
Ottawa, ON, Canada

*Your file Votre référence*
*ISBN: 978-0-494-48645-0*
*Our file Notre référence*
*ISBN: 978-0-494-48645-0*

**Abstract**

This thesis tested the hypothesis that the gap junction protein connexin 30 (Cx30) plays a role in regulating adult neural progenitor cell (NPC) fate. Cx30, previously shown to be expressed by postnatal astrocytes, was localized, for the first time, to adult NPCs specifically to a subset of multipotential nestin$^{+}$/glial fibrillary acidic protein$^{+}$ (GFAP)$^{+}$ NPCs in the subventricular zone (SVZ) of adult mice. When bromodeoxyuridine (BrdU) labelling was performed in Cx30$^{(-/-)}$ mice, the transition of early NPCs to a neuronal lineage was reduced. Increased BrdU cell number in the rostral migratory stream and the olfactory bulb was observed in Cx30$^{(-/-)}$ mice which suggested enhanced survival or migration of these immature progeny. Enhanced neuronal specification, induced by co-culture with NPCs and astrocytes, was blocked by pharmacological inhibition of gap junction intercellular communication. Together, these results suggest a role for Cx30 in regulating adult NPC fate by promoting neurogenesis through direct cell-cell communication.

**Acknowledgments**

I wish to sincerely thank Dr. Steffany Bennett for all the support, wisdom, guidance, encouragement, and endless enthusiasm that she has brought into my masters research project. I owe all my success and future achievements to the love and support from Stef and her lab. It has been an honour and pleasure to be part of the Neural Regeneration Laboratory (NRL). My utmost gratitude goes to Jennifer Hill who helped me with experimental procedures and protocols that I needed to succeed early on in my research and Sophie Imbeault who kindly performed some time course experiments for my project during my leave of absence. I am also sincerely thankful for all the helpful advice that Mario Morin, Sophie Imbeault, Dr. Lysanne Melanson-Drapeau, Dr. Shawn Whitehead, and Lianne Gauvin have given me to further improve my project. Finally, I would like to thank all the past and present members of the NRL (Cathy Sobara, Stephanie Fowler, Ashleigh McLean, Dr. Leigh-Anne Swayne, Dr. Scott Ryan, Vian Peshdary, Cory Harris, Mark Akins, Alexandra Petit) for all the ever-lasting encouragement and friendship that I am so fortunate to have.

**Table of Contents:**

**List of Abbreviations**

ab, antibody
aCSF, artificial cerebrospinal fluid
ANOVA, analysis of variance
ATP, adenosine triphosphate
BrdU, bromodeoxyuridine
cAMP, cyclic adenosine monophosphate
CNS, central nervous system
Cx30, connexin 30
Cy5, cyanine 5
BDNF, brain derived neurotrophic factor
bp, base pair
DCX, doublecortin
DG, dentate gyrus
DIV, days *in vitro*
DLA, dorso-lateral aspect
DMEM/F12, Dulbecco's modified Eagle's medium/ F12
DNA, deoxyribonucleic acid
EGF, epidermal growth factor
FGF2, basic fibroblast growth factor
FITC, fluorescein
GAPDH, glyceraldehyde 3-phosphate dehydrogenase
GFAP, glial fibrillary acidic protein
GJIC, gap junction intercellular communication
GRA, 18 α-glycyrrhetinic acid
GZA, glycyrrhizic acid
$IP_3$, inositol 1,4,5-triphosphate
kDa, kiloDalton
KO, knock-out $^{(-/-)}$
LV, lateral ventricle
NPC, neural progenitor cell
NSP, neurosphere
OB, olfactory bulb
P, postnatal day
PBS, phosphate buffered saline
PCR, polymerase chain reaction
RA, retinoic acid
RMS, rostral migratory stream
RPE, R-phycoerythrin
RT, reverse transcriptase
SEM, standard error of the mean
SGZ, subgranular zone
SVZ, subventricular zone
Tuj1, beta tubulin class III
WT, wild-type

## List of Figures

## List of Tables

## Chapter 1: General Introduction.

### 1.1 Stem and NPCs in the adult and developing mammalian brain.

An adult central nervous system (CNS) neural "stem cell" exhibits three cardinal features: 1) an ability to proliferate by continuing to undergo mitosis throughout the lifespan of an organism; 2) an ability to self renew either through symmetrical or asymmetrical division. Symmetrical division generates two progeny that are indistinguishable from the parental cell. Asymmetrical division generates one daughter cell that retains a stem cell phenotype and a second daughter cell that embarks on a course of terminal specification by themselves generating a series of intermediate NPCs ; and 3) a multipotent nature wherein stem cell progeny can differentiate into different neuronal and glial cell types in the CNS (Emsley et al., 2005). While NPCs have the ability to proliferate, they are limited in their ability to self renew and become increasingly restricted in their ability to differentiate into different CNS lineages as they pass different developmental checkpoints (Abematsu et al., 2006; Gage et al., 1995; Zhao et al., 2008). Lineage-specific NPCs are cells that are restricted to one distinct CNS lineage under normal physiological conditions through either intrinsic and/or extrinsic programs; for example, neuronal, astroglial, or oligodendrocyte progenitor cells (Figure 1.1). The term "neural precursor" is broadly used to refer to all CNS stem cells, multipotential NPCs, and lineage-restricted progenitor cells.

The identification of neural precursor cell populations as undifferentiated, highly mobile, actively proliferating, and able to produce mature neurons and glia has raised new hope for therapeutic cell replacement strategies to treat neurodegenerative disorders. Our

**Figure 1.1 Neural progenitor specification: Antigenic lineage progression from nestin expression to mature cell markers.** This diagram demonstrates the possible CNS cellular phenotypes that can originate from one stem cell-like NPC. Multipotential NPCs, characterized by both nestin and GFAP expression, can either self renew, or specify to intermediate progeny with increasingly restricted potential (*i.e.,* neuronal or glial progenitors, or generate mature astrocytes). There is some suggestion that astrocytes may, themselves, be the source of nestin$^+$/ GFAP$^+$ NPCs in adult brain. NG2$^+$ glial progenitors also specify through a series of intermediate progenitors to become mature Rip$^+$/ CNPase$^+$ oligodendrocytes. For neuronal progenitor cell specification, mature NeuN$^+$ neurons are generated after several intermediate differentiation steps. Specific proteins expressed at different stages of NPC specification are indicated (green). These antigenic markers were used throughout this thesis to identify the cell types expressing Cx30. The main connexins that were previously known to be expressed in various CNS cell types prior to this thesis are indicated (red).

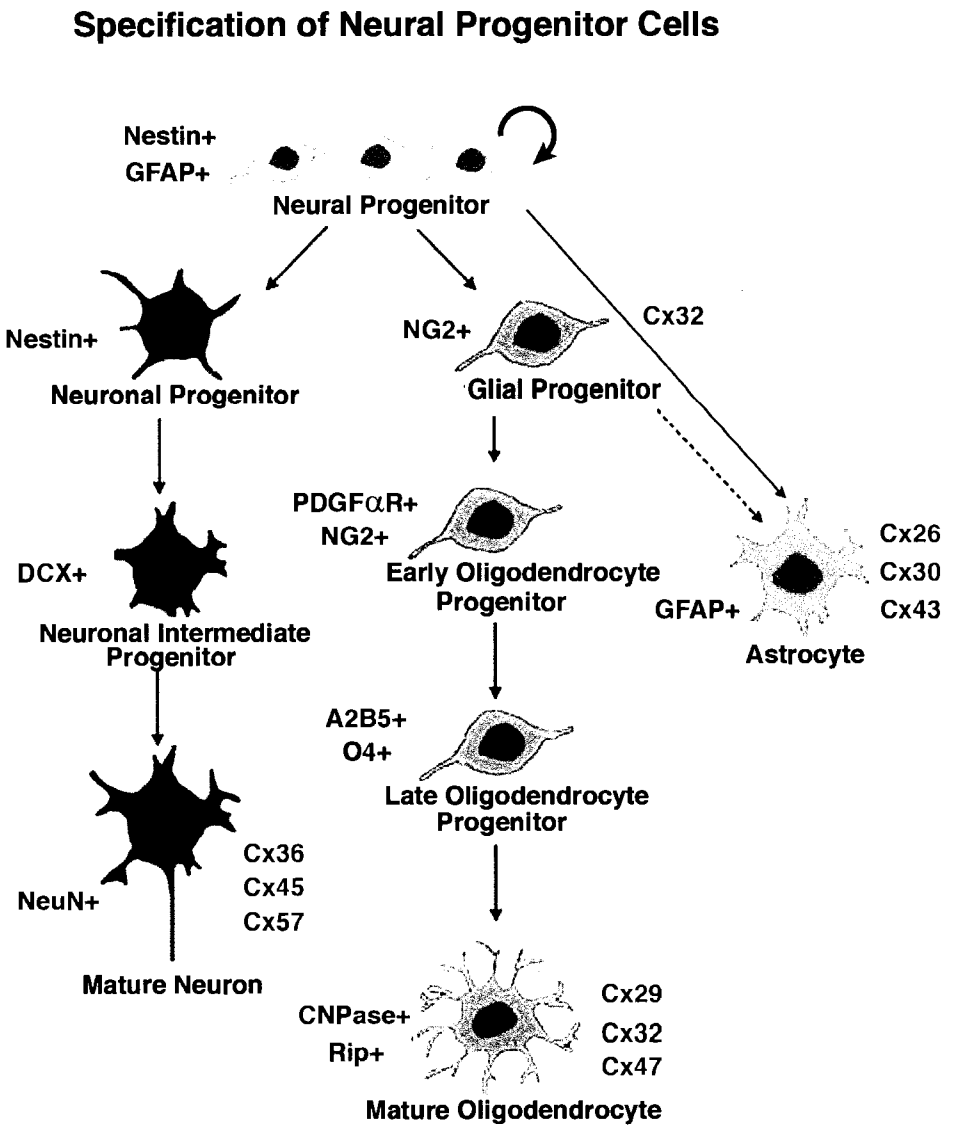
Specification of Neural Progenitor Cells
Nestin+
GFAP+
Neural Progenitor
Nestin+
Neuronal Progenitor
NG2+
Cx32
Glial Progenitor
PDGFαR+
NG2+
Early Oligodendrocyte Progenitor
GFAP+
Cx26
Cx30
Cx43
Astrocyte
DCX+
Neuronal Intermediate Progenitor
A2B5+
O4+
Late Oligodendrocyte Progenitor
NeuN+
Cx36
Cx45
Cx57
Mature Neuron
CNPase+
Rip+
Cx29
Cx32
Cx47
Mature Oligodendrocyte

Figure 1.1

understanding of NPC biology, however, is still in its early days. Clearly, a further insight into how these populations are directed to adopt specific CNS lineages is required if this promise is to be validated.

### 1.1.1 Neurogenesis in the adult CNS.

The discovery of constitutive adult mammalian neurogenesis was established in 1965 by Joseph Altman who was the first to use tritiated thymidine analog as an *in vivo* mitotic label, thereby demonstrating that adult neurogenesis occurs primarily in the hippocampus and the OB of adult brain (Altman, 1969; Altman and Das, 1965). In the absence of neuron-specific antigenic markers, proof that these actively dividing cells terminally differentiated into post-mitotic neurons was based on purely morphological criteria. Acceptance of the adult neurogenic phenomenon was limited. Twenty-seven years later, in 1992, Reynolds and Weiss revived these seminal studies and confirmed the concept of adult mammalian neurogenesis by demonstrating that proliferating adult mouse striatal cells could be differentiated into neurons and glia *in vitro* (Reynolds and Weiss, 1992). More recent work has shown that mitotic precursor populations capable of generating new neurons are enriched mainly in the neurogenic niches of the subgranular zone (SGZ) of the DG in the hippocampal formation, and the SVZ of the LV (Figure 1.2) (Eriksson et al., 1998; Gotz et al., 2002; Gould and Gross, 2002; Zhao et al., 2008). Other neurogenic regions in the adult mammalian brain have been identified, although with less neurogenic potential, and albeit with some controversy, that include the septum, striatum, optic nerve, corpus callosum,

**Figure 1.2 Neurogenic niches of the adult brain.** Schematic illustrations of the neurogenic niches of the adult mouse brain in both coronal and sagittal orientations. NPCs are known to reside in the SGZ of the DG in the hippocampal formation (presented in coronal sections between Bregma -1.68 mm and -2.08 mm) (A). Magnified schematic view of the SGZ with cells labelled G as mature granule cell neurons, blue cells as multipotent NPCs, orange cells as transit amplifying intermediate progeny, and red cells as immature migrating neuronal progenitors (A1). The SVZ including the dorsal lateral tip (DLA) of the LV also contains NPCs (presented in coronal sections between Bregma 1.10 mm and 0.5 mm) (B). Magnified schematic illustration depicts the cellular architecture of the SVZ with multipotential Type B NPCs (blue), transit amplifying Type C progeny (green), and Type A migrating neuroblasts (red) (B1). Cells labelled E are multi-ciliated ependymal cells that line the LV. Depicted in a sagittal cross section (presented at interaural lateral positions 1.0 mm to 1.40 mm), NPCs are able to proliferate, differentiate, and migrate along the RMS and become functional interneurons in the OB (C). Abbreviations include: DG, dentate gyrus; CA1, Cornu Ammonis 1 region; CA3, Cornu Ammonis 3 region; NC, neocortex; CC, corpus callosum; DLA, dorso-lateral aspect of the LV; CB, cerebellum; SVZ, subventricular zone; BV, blood vessel. Coronal sections were adapted from Mouse Brain Library (mbl) online (www.mbl.org) (A, B). Adapted from (Alvarez-Buylla and Garcia-Verdugo, 2002) (B1, C) and (Alvarez-Buylla and Lim, 2004) (A1).

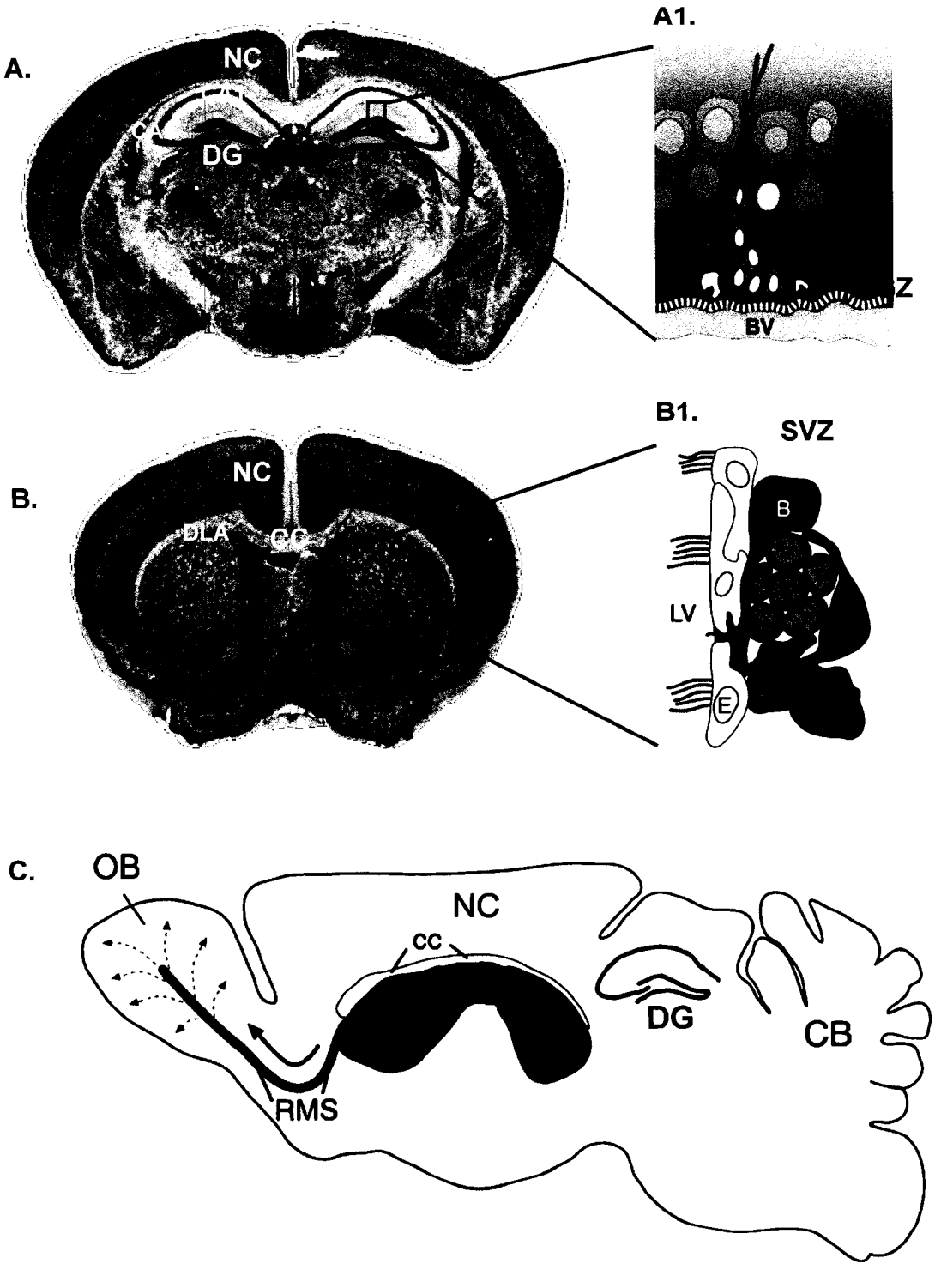


**Figure 1.2**

spinal cord, retina, hypothalamus, and cerebellum (Magavi and Macklis, 2002; Palmer et al., 1995).

### 1.1.2 *In vivo* conceptual models of neurogenesis and *in vitro* validation of these models.

Study of these primary neurogenic niches in the adult rodent brain has lead to the current model of adult neurogenesis (Figures 1.3, 1.4). In the hippocampus, this begins with a multipotential progenitor population, possibly stem-cell like with radial-glial properties denoted as Type 1 progenitors and defined by their ability to proliferate and their expression of nestin and GFAP. Type 1 progenitors are located in the SGZ between the hilus and the granule cell layer of the DG (Figure 1.2). These cells either self renew or undergo a series of differentiation steps into putative transiently amplifying progenitor cells that differ in their proliferative potential and increasing neuronal differentiation restriction. These amplifying cells begin as nestin$^+$ Type 2a cells and differentiate further into Type 2b nestin$^+$ and doublecortin$^+$ (DCX$^+$) cells which finally become Type 3 DCX$^+$ (nestin$^-$) progenitors. Type 2a and 2b are slowly dividing cells; Type 3 cells are rapidly dividing cells. During the proliferation and maturation process of Type 2a/2b/3 cells, they migrate from the SGZ into the granule cell layer where the Type 3 DCX$^+$ early neuronal progenitor cells undergo terminal differentiation into NeuN$^+$ postmitotic neurons that are also calbindin$^+$ and exhibit phenotypic characteristics of mature granule neurons forming axonal projections with pyramidal cells in the CA3 region of the hippocampus (Figure 1.3) (Hastings and Gould, 1999; Kempermann et al., 2004).

**Figure 1.3 Model of adult hippocampal neurogenesis.** Adult hippocampal NPCs localize to the SGZ of the DG (see Figure 1.2) and generate a series of transitional intermediate cells until they become functional neurons in the granule cell layer. The primordial stem-like cell is a $GFAP^+$ astrocyte (Type 1 cell) with putative unlimited potential for self renewal and distinguished from mature astrocytes by $nestin^+$ expression. As these cells undergo several rounds of division and differentiation, the cell marker expression pattern of their progeny changes from $GFAP^+$/ $nestin^+$ (Type 1) cells to $DCX^+$ (Type 3) cells that commit to a postmitotic $NeuN^+$/ $calbindin^+$ mature granule neuron. Adapted from (Kempermann et al., 2004).

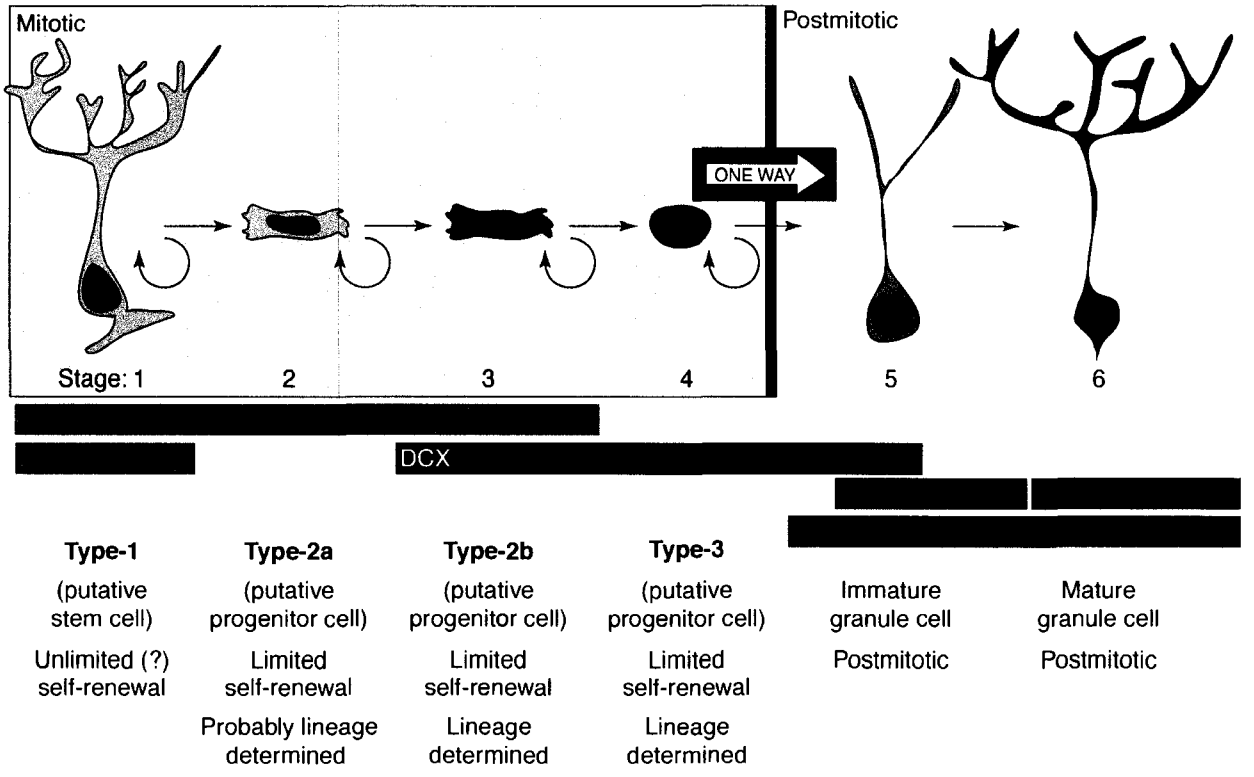
Mitotic
Postmitotic
ONE WAY
Stage: 1
2
3
4
5
6
DCX
Type-1
(putative stem cell)
Unlimited (?) self-renewal
Type-2a
(putative progenitor cell)
Limited self-renewal
Probably lineage determined
Type-2b
(putative progenitor cell)
Limited self-renewal
Lineage determined
Type-3
(putative progenitor cell)
Limited self-renewal
Lineage determined
Immature granule cell
Postmitotic
Mature granule cell
Postmitotic

**Figure 1.3**

**Figure 1.4 Model of adult SVZ neurogenesis**. Adult forebrain NPCs are enriched in the SVZ of the LV indicated in light blue in this coronal schematic of the adult mouse brain at Bregma 1.10 mm to 0.5 mm (A). The cellular architecture of the SVZ includes ciliated ependymal cells (gray) that line the LV and are thought to produce various paracrine regulatory signals involved in neurogenesis. $GFAP^+$/ $nestin^+$ Type B cells (blue) with both astrocytic and stem cell-like properties make contact with the ventricle lumen and the basal lamina (BL, yellow) which extends from a blood vessel (BV, pink) and interdigitates extensively with other SVZ cells. A perivascular macrophage (dotted fill) is also shown (B).Type B cells either undergo self renewal or differentiate into $nestin^+$ transit amplifying Type C cells which can further specify into Type A $DCX^+$ neuroblasts (C). Subsequently, Type A cells can migrate along the RMS and become functional neurons in the OB. Adapted from (Alvarez-Buylla and Lim, 2004).

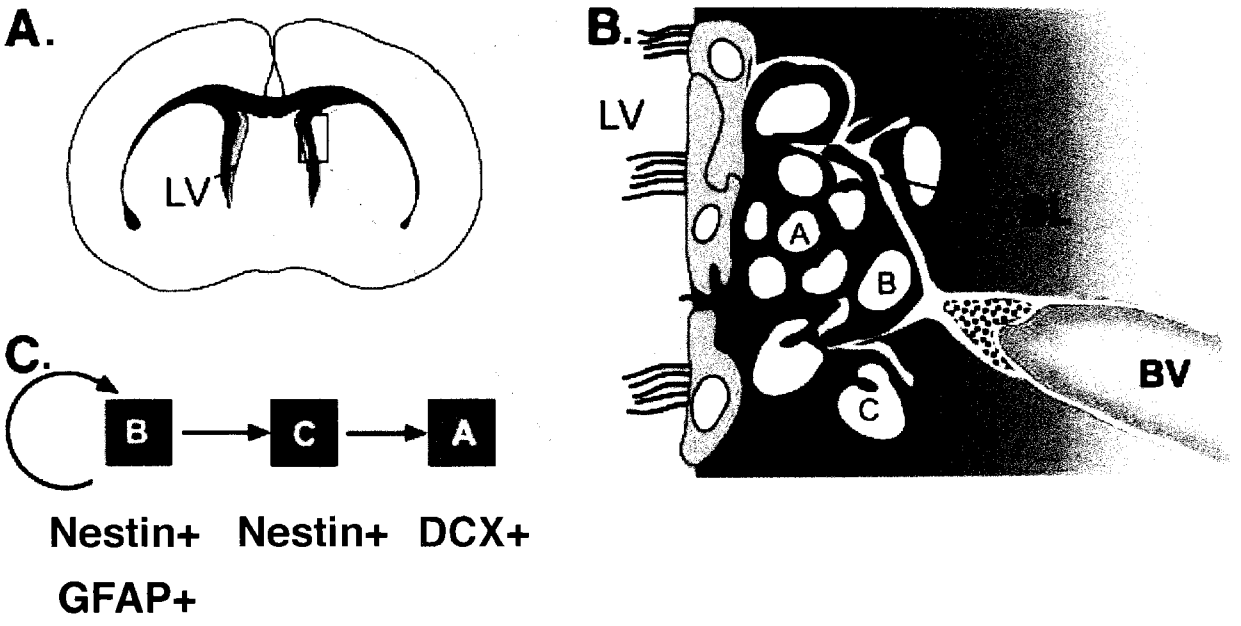


**Figure 1.4**

A similar model is presented for the adult SVZ using a different nomenclature. Here, definitive evidence for a multipotential stem cell population with astrocytic properties denoted as Type B cells based on their nestin and GFAP expression has been demonstrated (Alvarez-Buylla and Lim, 2004). Type B cells differentiate further into transit amplifying Type C cells that solely express nestin. These Type C cells differentiate into Type A migratory neuroblasts that express DCX. Finally, these early neuronal Type A $DCX^+$ progenitor cells migrate along the RMS to become mature interneurons in the OB (Figure 1.4) (Doetsch et al., 1999).

The *in vitro* study of postnatal neurogenesis involves isolating and culturing NPCs from neonatal or adult SGZ and SVZ. Neonatal cultures are primarily used, as yield is much greater than adult sources. Cells are dissociated into a single cell suspension and grown in the presence of epidermal growth factor (EGF) and basic fibroblast growth factor (FGF2) wherein only mitogen-responsive cells proliferate and form free floating spherical clusters of cells termed NSPs. Upon removal of mitogen factors and plated on an adhesive support, NSPs can differentiate into all CNS cell types (Figure 1.5) (Reynolds and Weiss, 1992). The mitogen- responsive cells that generate NSPs are thought to be derived from Type 1 or Type B stem-like cells found in the SGZ and SVZ, respectively, however, some cells may be derived from their transit amplifying daughter cells (Type 2 or Type C cells, respectively) (Doetsch et al., 1999; Kempermann et al., 2004). If NSPs are dissociated and resuspended in medium with growth factors, a minority of these cells will form secondary and tertiary NSPs that, along with the ability to differentiate into all CNS cell types, indicating that these cells exhibit a multipotential neural stem cell-like phenotype (Doetsch, 2003; Song et al., 2002). This NSP assay provides a simple *in vitro* model of CNS NPC differentiation that can be

used to test the effect of distinct external micro-environmental influences that can affect the fate of these cells (*i.e.,* communication with terminally differentiated "instructive" cell types). Thus, with the properties of this isolated *in vitro* NPC model, intrinsic and extrinsic factors for neural stem cell fate can be elucidated by varying paracrine growth factors, juxtracrine extracellular matrix components, or co-culture with other CNS cell types (Marshall et al., 2007).

### 1.1.3 Regulation of neurogenesis.

Determining the regulatory mechanisms of NPC proliferation and specification has only just begun. Intrinsic regulation such as epigenetic, transcriptional, and posttranscriptional control most likely involves molecular mechanisms such as silencing genes via DNA methylation when NPCs commit further into specific cell lineages and activation of genes that are sequentially turned on during NPC specification (Cameron et al., 1998; Cheng et al., 2005). While intrinsic factors remain to be fully elucidated, extrinsic cues such as steroids, growth factors, and other biochemical factors have been clearly implicated in the control of NPC proliferation and specification. For example, over the course of the female reproductive cycle, when estrogen levels are maximal, there is an increased proliferation of cells only in the SGZ, but not the SVZ (Tanapat et al., 1999). Conversely, the production of the peptide hormone prolactin during the first half of pregnancy enhances SVZ neurogenesis increasing OB neuronal integration and enhancing olfactory capabilities (Shingo et al., 2003). Diverse environmental factors, including an increase in regional serotonin levels, performing

**Figure 1.5 Model of postnatal *in vitro* neurogenesis: The neurosphere (NSP) approach.** Cells are extracted from the neurogenic regions (SVZ or SGZ) of newborn mice and dissociated into a serum-free single cell suspension bathed with EGF and FGF2 (A). Cultures are grown for 8 DIV under conditions where only mitogen-responsive cells are able to proliferate and form spherical clusters composed of clonal progeny termed NSPs (B). Primary NSPs can be dissociated again into a single cell suspension and passaged where only a minority of cells are capable of forming secondary NSPs indicative of sustained self renewal in a small proportion of NSP cells (C). The capacity to form tertiary NSPs is considered indicative of "unlimited" self-renewal characteristic of stem-like NPCs. When NSPs are plated under various differentiation conditions, they can differentiate into neurons, astrocytes, and/or oligodendrocytes indicative of multipotentiality (D). Adapted from (Reynolds and Rietze, 2005).

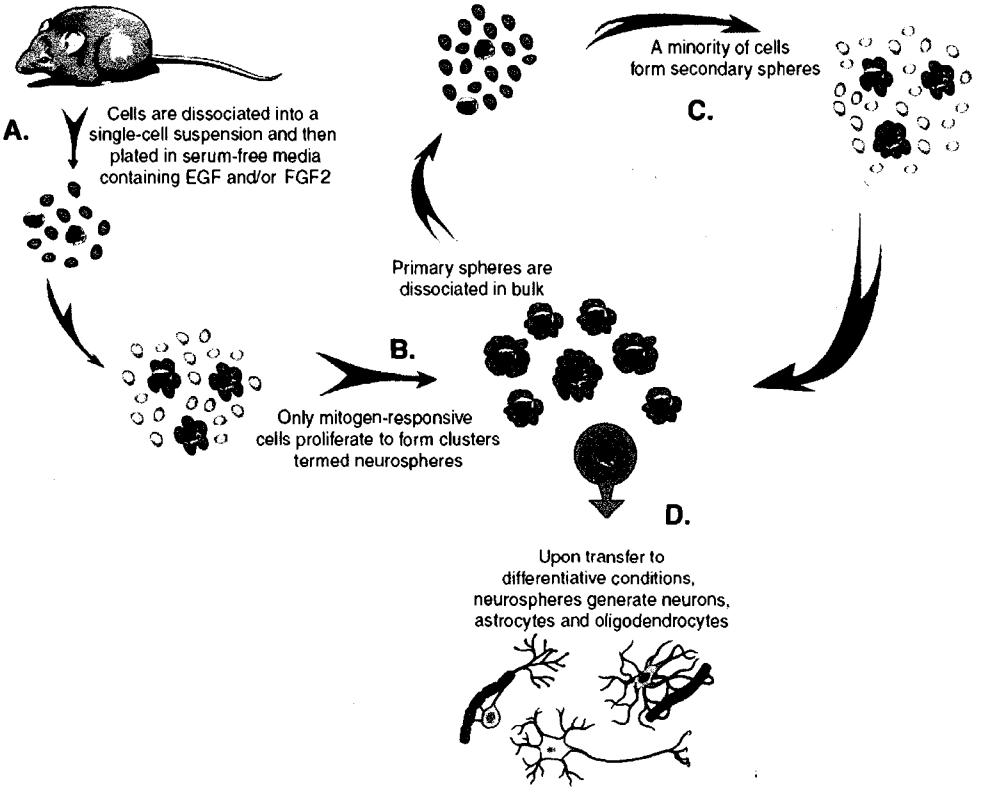
A.
Cells are dissociated into a single-cell suspension and then plated in serum-free media containing EGF and/or FGF2
B.
Only mitogen-responsive cells proliferate to form clusters termed neurospheres
Primary spheres are dissociated in bulk
C.
A minority of cells form secondary spheres
D.
Upon transfer to differentiative conditions, neurospheres generate neurons, astrocytes and oligodendrocytes

**Figure 1.5**

learning tasks, voluntary exercise, and an overall enriched environment, promotes mammalian neurogenesis while stress, stress-related steroids, and aging are associated with decreased NPC proliferation and/or specification (Brezun and Daszuta, 1999; Eriksson and Wallin, 2004; Gould et al., 1999; Kempermann et al., 1997; Kuhn et al., 1996). Notch, cytokine ciliary neurotrophic factor (CNTF), EGF, and FGF2 signalling have all been implicated in neural stem cell self renewal (Lennington et al., 2003). Bone morphogenetic protein (BMP) signalling plays a negative regulatory role in neurogenesis while noggin reverses the effect of BMP by preventing signal activation (Gross et al., 1996; Shou et al., 1999).

In addition to paracrine regulation, adult NPCs can also be "instructed" towards different CNS lineages by adjacent terminally differentiated cells. Song *et al*, have shown that direct contact between immortalized rat precursor cells and hippocampal astrocytes promotes neuronal commitment (Song et al., 2002). Wnt signalling pathways have been implicated, but additional pathways are likely involved (Lange et al., 2006; Muroyama et al., 2004); for instance, Lim and Alvarez-Buylla have demonstrated that direct cell-cell contact between SVZ-derived astrocytes and NPCs may be necessary for neuronal specification (Lim and Alvarez-Buylla, 1999). As such, this study will focus on elucidating the role of connexin-mediated communication between NPCs, between NPCs and astrocytes, and cell-autonomous communication mechanisms in the control of NPC proliferation and specification *in vivo* and *in vitro*.

## 1.2 Connexin-mediated communication.

### 1.2.1 Gap junctions: structure and function.

Gap junctions are formed when two transmembrane channels, elaborated in junctional membranes by adjacent cells, dock to form an intercellular channel. These transmembrane channels are also known as connexons or hemichannels (Figure 1.6). Collections of intercellular channels make up the morphologically defined gap junction. These intercellular channels provide a means for direct molecular signalling and ionic current exchange between connected cells. Each connexon-hemichannel is comprised of six protein subunits called connexins (Stout et al., 2004). Connexin proteins have a general structure that consists of a highly conserved four transmembrane spanning domain (M1,M2,M3,M4), a cytoplasmic N–terminal tail, one cytoplasmic loop, two extracellular loops with three conserved cysteine residues per loop that are thought to be involved in connexon docking and maintaining tertiary structure stability, and a variable cytoplasmic C-terminal tail essential for intracellular connexin-mediated signalling (Figure 1.6) (Sosinsky and Nicholson, 2005).

The connexin subunit nomenclature is complex. These proteins are named based on their molecular weight in kilodaltons (kDa) and origin of species; for example, murine connexin 30 (mCx30, Gjb6) has a molecular weight of 30 kDa whereas hCx30/ GJB6 represents the homologous 30 kDa connexin in humans. Connexins can also be divided into subgroups ($\alpha$, $\beta$, or $\gamma$) based on their sequence identity and length of cytoplasmic loop (Sohl and Willecke, 2003). Connexins are then abbreviated Gj (gap junction) and numbered based

**Figure 1.6 Gap junction structure: Connexins, connexons, and intercellular channels.** Closely (3.5 nm) apposed connexon-hemichannels from adjacent cells can dock and form functional gap junctional intercellular channels (A). Depending on their molecular composition, gap junctions can be either homomeric/homotypic (1), heteromeric (2), or heterotypic (3). Homotypic or heterotypic channels are composed of two identical connexon-hemichannels or two different connexon-hemichannels, respectively. Homomeric or heterotypic connexon-hemichannels are comprised of identical connexin subunits or different isoforms (possibly pannexins), respectively. Heteromeric channels are formed by docking of heterotypic connexons with any other partner. Each connexon-hemichannel is composed of six connexin subunits. Connexin protein subunits have four transmembrane spanning domains, two extracellular loops with three conserved cysteine residues per loop, a small N-terminal tail, a cytoplasmic loop, and a variable intracellular C-terminal tail involved in intracellular signalling (B). Adapted from (Sohl et al., 2005).

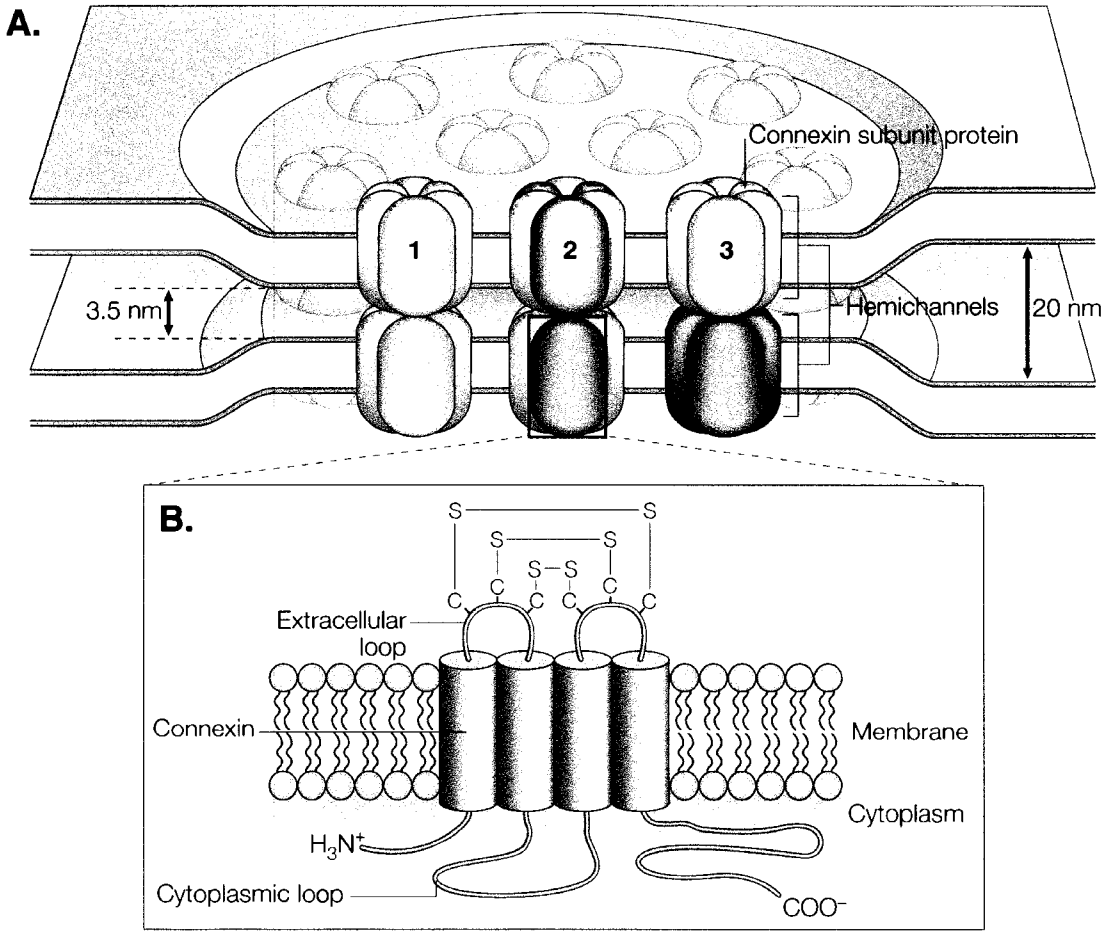
A.
Connexin subunit protein
1
2
3
3.5 nm
Hemichannels
20 nm
B.
S
S
S
S
S
S
C
C
C
C
C
C
Extracellular loop
Connexin
Membrane
Cytoplasm
$H_3N^+$
Cytoplasmic loop
$COO^-$

**Figure 1.6**

on the order of their discovery; for instance, mCx43 was the first connexin found in the α group (Gja1) while mCx30 was the sixth connexin found in the β group (Gjb6) (Sohl and Willecke, 2003). Connexin genes tend to be clustered together in their single copy form when orthologous connexin genes are compared between human and mice; for example, mouse Cx26, Cx30, and Cx46 are found on chromosome 14 while the same human connexin genes are also clustered together but on human chromosome 13 (Sohl and Willecke, 2003). The general genomic structure of connexin genes include exon 1 with a 5' untranslated region separated by an intron with variable length then followed by exon 2 that contains the complete coding region and a 3' untranslated region (Sohl and Willecke, 2003).

To date, the connexin family consists of 20 members in the mouse and 21 in the human (Sohl and Willecke, 2004). The specificity of molecular passage for each connexon-hemichannel is governed by the variable individual composition and the diverse combination of intercellular junction formation. When a connexon-hemichannel contains the same six connexin subunits it is denoted as homomeric, while heteromeric connexon-hemichannels are composed of different types of connexin subunits. Intercellular channels can be composed of homotypic channels (docking of identical connexon-hemichannels) or heterotypic channels (docking of different homomeric or heteromeric connexon-hemichannels) (Figure 1.6, A) (Bruzzone et al., 1996). With this in mind, gap junctions can display a vast combinatorial connexin complexity along with several interesting functional consequences (Valiunas et al., 2000).

Functionally, gap junctions provide cellular signalling and ionic conductance between adjacent cells by the bidirectional passive diffusion of small molecules < 1000 Daltons that include second messengers (lipid and peptide), metabolites, and ions (Sohl and

Willecke, 2004). Gap junction-mediated communication permits the passage of electrical, metabolic, and immunological information (*i.e.*, cross-presenting peptides) that can direct cell processes like development, muscle cell synchronization, cell death, and neuronal signalling (Neijssen et al., 2007). For example, cardiac myocytes synchronize their contractions by communicating electrically through gap junctions found dispersed in intercalated discs; the summation of these electrically coupled cardiomyocytes accounts for the rhythmic beating heart (Beyer et al., 1987). Also, neuronal gap junctions, often synonymous with electrical synapses, play a critical role in modulating synchronous activity between neurons and mediating oscillations that are important for functional specialization (Galarreta and Hestrin, 1999; Gibson et al., 1999; Landisman et al., 2002; Mann-Metzer and Yarom, 1999).

### 1.2.2 Gap junctional and non-junctional communication.

Most mammalian cells are capable of forming low resistance intercellular channels with their neighbours representing the electrophysiological signature of gap junctional intercellular communication (GJIC) (Sohl and Willecke, 2004). GJIC mediates cell to cell communication by electrical signalling via the regulated exchange of intracellular ions ($Ca^{+2}$, $K^{+}$. $Na^{+}$, and $Cl^{-}$) or by biochemical coupling through the exchange of small metabolites like adenosine triphosphate (ATP), cyclic adenosine monophosphate (cAMP), glucose, or inositol 1,4,5-triphosphate (IP3) (Bruzzone, 2001; Goldberg et al., 2004; Montoro and Yuste, 2004). In the CNS, GJIC accounts for the synchronization and electrotonic coupling observed between neurons in many areas including the neocortex, hippocampus, inferior olive, striatum, and retina (Connors et al., 1983; Cook and Becker,

1995). Although connexins were thought to be the only proteins able to form and function through intercellular channels between adjacent cells, emerging evidence suggests that connexins may also function through alternative ways and that a new family of channel forming proteins, pannexins, may share some of these functions (Barbe et al., 2006; Stout et al., 2004).

In addition to intercellular communication, connexins can also signal through functional connexon-hemichannels in non-junctional membranes. For several decades, connexon hemichannels were thought to be in a closed state until mobilized as intercellular channels since open porous channels to the extracellular milieu could result in cell death (for a review see (Stout et al., 2004)). Recent work has demonstrated that connexon-hemichannels can either be found in an open or closed state under physiological or pathophysiological conditions; for example, under normal conditions, Cx43 hemichannels are believed to be involved in the release of small molecules like ATP from astrocytes which elicits glial calcium waves (Guthrie et al., 1999; Verderio et al., 2001). Channel opening can be provoked by various stimuli including a reduction in extracellular [$Ca^{+2}$], membrane depolarization, intracellular kinase activity, and mechanical stress (Sohl et al., 2004). Unlike that of GJIC, the mechanistic basis for hemichannel gating has not been fully understood.

In addition to GJIC and hemichannel activity, connexins can also participate in channel-independent processes that are thought to be mediated by protein-protein interactions with the intracellular C-terminal domain (Giepmans, 2004). For example, Cx43 is able to inhibit tumor cell growth independently of gap junctional communication (Moorby and Patel, 2001; Olbina and Eckhart, 2003). This growth inhibition is achieved by transfecting Cx43 mutants that cannot form functional channels or by expressing solely the C-terminal tail, suggesting

the existence of a channel-independent mechanism for growth control (Zhang et al., 2003). Finally, connexin-mediated adhesion resulting from the docking of connexons elaborated by adjacent cells has also been shown to impact upon the migration of embryonic neuronal progenitors and immature neurons along radial glia over the course of cortical development. This adhesive property occurs independently of any requirement for functional channel opening between "gapped" NPCs and radial glia (Elias et al., 2007).

### 1.3 Connexin expression in the developing and adult CNS.

The large repertoire of connexins, their sequential expression, and specific cell type expression pattern in the developing CNS defines, in part, their functional role. Functional channel formation and connexin expression has been observed in several different cell types including astrocytes, neurons, oligodendrocytes, ependymal cells, and microglia (Dermietzel and Spray, 1993; Rouach et al., 2002; Rozental et al., 2000). Out of the 20 plus identified mammalian connexins, at least half of these connexin members are expressed in the CNS with Cx26, Cx29, Cx30, Cx32, Cx36, Cx43, Cx45, and Cx47 being clearly identified in gap junctions of neurons and glia while Cx31, Cx37, Cx46, and Cx57 expressed by other cell types in the brain including cerebral endothelial cells (Nagy et al., 2004; Rouach et al., 2002; Rozental et al., 2000). Connexin-mediated communication and GJIC in the mammalian brain have been implicated in several functional roles including buffering ionic or regulatory biochemical concentrations, and propagating electrical signals required for neuronal circuit synchronization (Connors and Long, 2004; Wallraff et al., 2006). GJIC is also involved in regulating the development of the neocortex by the spatial-temporal expression of specific connexin genes resulting in the construction of specialized compartmental domains that are

involved in inductive interactions (Lo, 1996; Naus and Bani-Yaghoub, 1998). For instance, Cx32 expression is found to be predominantly postnatal corresponding with myelination, while Cx43 is expressed prenatally and thought to be involved in neocortical lamination and functional neuronal organization (Belliveau et al., 1991; Matsumoto et al., 1991; Nadarajah et al., 1997). Thus, manipulation of gap junctional expression at the cellular level will clarify their specific roles in the CNS and is an approach employed in this thesis.

### 1.3.1 Connexin expression in neurons, oligodendrocytes, and astrocytes.

Neurons are the fundamental cellular units of the nervous system having structural properties that allow them to conduct electrical impulses from one neuron to the next thereby generating a large selection of physiologically relevant actions. The mechanisms of neuronal impulse signalling come in two main forms: chemical and electrical synapses. Gap junctions are the structural units of these primitive electrical synapses which have been extensively studied and verified both *in vivo* and *in vitro* (Furshpan and Potter, 1959; Meier and Dermietzel, 2006; Mollgard and Moller, 1975; Nadarajah et al., 1997; Rozental et al., 1998). Electrotonic coupling between neurons and their role in neuronal synchronization has been observed in many areas of the mammalian brain including the hippocampus, developing neocortex, locus coeruleus, hypothalamus, inferior olive, striatum, and retina (Cook and Becker, 1995; Dermietzel and Spray, 1993). During early development, this GJIC-mediated coupling occurs throughout all neocortical layers and progressively decreases as neuroblasts undergo their final divisions, begin to migrate, and differentiate into mature neurons (Connors et al., 1983). Developing neurons have been shown to express

Cx43 and Cx40, while mature neurons express Cx36, Cx45, and Cx57 although expression patterns and timing are regionally specific (Hombach et al., 2004; Maxeiner et al., 2003; Sohl et al., 2005; Venance et al., 2000). Cx32 was previously thought to be expressed by neurons, but is now known to be restricted to immature and mature oligodendrocytes (Dermietzel et al., 1989; Melanson-Drapeau et al., 2003; Sohl et al., 2005).

The myelinating cells of the CNS, oligodendrocytes, function to insulate axons and enhance neuronal conduction. Several groups have shown that Cx32 is expressed by oligodendrocytes and that the Cx32 spatio-temporal expression pattern coincides with oligodendrogenesis (Belliveau et al., 1991; Dermietzel et al., 1989; Menichella et al., 2003). Other connexins expressed by oligodendrocytes include Cx29 and Cx47 (Dermietzel et al., 1997; Odermatt et al., 2003). The proposed role of GJIC in oligodendrocytes is likely to be metabolic, where reflexive channels permeate ions and nutrients from their soma to all of their myelin layers thereby reducing the path length of nutrient or trophic factor distance (Naus and Bani-Yaghoub, 1998; Paul, 1995). Based on genetic neuropathies seen with Charcot-Marie-Tooth disease, a peripheral demyelinating disease, and its association with mutations of the human Cx32 gene, connexins are proposed to play a critical role in the transduction of signals between Schwann cell and axon (Nagy et al., 2003a; Paul, 1995). However, when the oligodendrocyte connexin gene Cx32 is deleted via the generation of $Cx32^{(-/-)}$ mice or when Cx47 is deleted, these mice show little CNS demyelination and abnormalities while the Cx32-Cx47 double null-mutant phenotype mice shows fatal demyelination (Odermatt et al., 2003). This suggests that oligodendrocyte connexins and to a greater extent all CNS connexin genes may have some overlapping roles capable of compensating for development deletion.

Astrocytes have multiple roles in the CNS including metabolic support, extracellular ionic concentration regulation, transmitter uptake and release, structural support, maintenance of the blood brain barrier, modulation of synaptic transmission, nervous system repair, regulating neuronal development, and architectural control of the adult brain (Bennett et al., 2003; Nedergaard et al., 2003; Slezak and Pfrieger, 2003). Being the main cell type in the CNS coupled by gap junctions, there is no surprise that connexin-mediated signalling underlies the fundamental mechanism in carrying out several functions mentioned above (Giaume and McCarthy, 1996; Rouach et al., 2002). Astrocytic gap junctions and hemichannels are chiefly composed of Cx43, but Cx26, Cx30, Cx40, Cx45, and Cx46 have also been detected (Dahl et al., 1996; Dermietzel et al., 1991; Kunzelmann et al., 1997). All these gap junctions are thought to contribute to the formation of a functional astrocytic syncytium (Dermietzel et al., 1991). Several cellular functions have been attributed to this gap junction coupled glial syncytium including extracellular $K^+$ buffering after excessive neuronal firing, propagating $Ca^{+2}$ waves thereby influencing neuronal activity, mediating metabolic cooperation in the uptake of neurotransmitters released by neighbouring neurons, and releasing energy-producing compounds like glucose for neuronal nourishment (Dani et al., 1992; Enkvist and McCarthy, 1994; Giaume et al., 1997; Sohl et al., 2004). The level of GJIC activity in astrocytes has been shown to be regulated by several factors including astrocyte maturation, neurotransmitters, neuromodulators, extracellular ion concentrations, and pharmacological agents that promote gap junction coupling or uncoupling (Enkvist and McCarthy, 1994; Giaume and Venance, 1995; Mantz et al., 1993). Also, astrocytic GJIC has been proposed as a mechanism in the control of glial cell proliferation wherein inhibition of GJIC by uncoupling agents leads to an increase in the proliferation rate of cultured

astrocytes (Rouach et al., 2004; Tabernero et al., 2001). However, conflicting evidence demonstrates reduced proliferation rate of primary cultured astroctytes from $Cx43^{(-/-)}$ mice. This could be explained by the cellular expression of other compensatory connexins (Naus et al., 1997).

Although astrocytes are involved in several supportive roles in the CNS, emerging evidence proposes a more instructive and active function (Horner and Palmer, 2003). In the developing CNS, radial glial cells provide signals mediated by GJIC to developing neuroblasts as they migrate and mature during neocorticogenesis (Bittman et al., 1997; Connors et al., 1983; Naus and Bani-Yaghoub, 1998). Surprisingly, not only do radial glial gap junctions mediate neuronal migration in the classical GJIC manner, but also provide dynamic adhesive contacts that interact with the internal cytoskeleton of immature neuroblasts thereby providing the contacts necessary for neuronal migration in the developing neocortex (Elias et al., 2007). Co-culture experiments where adult hippocampal-derived NPCs were plated with hippocampal astrocytes, demonstrated that astroglia were capable of instructing these precursor cells to adopt a neuronal fate (Song et al., 2002). Further supporting a direct cell-cell contact system, neurogenesis was enhanced when SVZ-derived precursors were plated on astrocytic monolayers thereby raising the possibility of intercellular channel signalling as an underlying mechanism (Lim and Alvarez-Buylla, 1999).

## 1.4 Connexin-mediated control of NPC fate

During embryonic development, the variable spatio-temporal gap junctional expression pattern has been implicated in the control of cell differentiation and growth (Caveney, 1985). Commonly, increased intercellular coupling between cells is observed during development and begins to diminish as cells become terminally differentiated like that seen in the CNS (Naus and Bani-Yaghoub, 1998; Peinado et al., 1993). Restricted GJIC has been shown to delineate cells into specific compartmental domains by defining borders, and that cells in these explicit developmental fields can collectively adopt the same fate (Kalimi and Lo, 1989; Lo, 1996). This restricted design is constructed by the changing connexin expression pattern over the course of development with borders constructed by cells expressing incompatible connexin partners (Fraser et al., 1987; Guthrie and Gilula, 1989). Connexin-mediated communication via GJIC or connexon-hemichannels has also been implicated in controlling NPC differentiation, proliferation, migration, axonal growth and guidance, and synaptogenesis in the developing and mature CNS (Guthrie and Gilula, 1989; Melanson-Drapeau et al., 2003; Warner et al., 1984; Weissman et al., 2004).

Throughout CNS development, numerous connexins (Cx26, Cx29, Cx30, Cx32, Cx36, Cx43, and Cx47) have been shown to be dynamically expressed and involved with several developmental time points (Dermietzel et al., 1989; Nadarajah et al., 1997; Sohl et al., 2001). Cx43 and Cx26 are expressed prenatally and remain present throughout development (Nadarajah et al., 1997). Since $Cx43^{(-/-)}$ mice show defects in neuronal migration and laminar organization of the neocortical layers and have been shown to localize to both radial glial cells and NPCs, Cx43-mediated communication may well

provide the appropriate signals for embryonic neurogenesis (Bittman and LoTurco, 1999; Bruzzone and Dermietzel, 2006). On the other hand, Cx32 and Cx36 are predominately expressed during the first postnatal week of life while Cx30 and Cx29 are primarily expressed during the second postnatal week (Belluardo et al., 2000; Dermietzel et al., 1989; Kunzelmann et al., 1999; Nadarajah et al., 1997). The main function of postnatal CNS connexin expression has not yet been completely resolved. Cx36 and Cx26 expression are primarily involved in neuronal GJIC while Cx32 expression is thought to partake in postnatal myelination and oligodendrogenesis (Belluardo et al., 2000; Matsumoto et al., 1991; Melanson-Drapeau et al., 2003). Due to a similar temporal expression pattern, Cx30 may contribute to postnatal myelination development via astrocyte-oligodendrocyte gap junctional interactions (Nagy et al., 2003b; Nagy et al., 1997). Thus, although several astrocyte connexins have been implicated in regulating CNS development, the impact on adult and postnatal progenitor cell fate has yet been determined.

### 1.5 Cx30 expression profile in the CNS.

In addition to Cx43, the highly coupled mammalian astrocyte expresses other connexins that could yield great functional diversity; for instance, Cx30 has been recently co-localized to gray matter astrocytes in the rodent and human brain and due to its late temporal expression pattern it is believed to be involved in several late developmental events including the formation of the blood-brain barrier, promoting myelination, and maturation of brain energy metabolism (Leong and Clark, 1984; Nagy et al., 1999). Although Cx43, being expressed prenatally and found in radial glial cells, has been extensively implicated in neocorticogenesis, the possible role of Cx30, being expressed by postnatal astrocytes, in

adult neurogenesis remains to be elucidated (Bittman et al., 1997). In the rodent brain, Cx30 mRNA levels increase after the second postnatal week while other astrocyte connexin genes (Cx26 and Cx43) are expressed prenatally (Dahl et al., 1996; Nagy et al., 1999). This suggests that Cx30 gap junctions appear to be a feature of the adult mouse brain. Cx30 channels have the ability to form homotypic (Cx30-Cx30) channels between astrocytes and to form heterotypic channels (Cx30-Cx43, Cx30-Cx47, Cx30-Cx32) with other astrocytes or oligodendrocytes (Altevogt and Paul, 2004; Nagy et al., 2003a; Nagy et al., 1999). Although Cx30 is closely related to Cx26 in primary amino acid sequence (77%), evidence demonstrates that unique intercellular channel composition partly regulates the passage of signalling molecules because different homotypic channel gating properties against different dyes with various molecular weights and charges is observed (Dahl et al., 1996; Manthey et al., 2001). Based on evidence described previously with respect to Cx30 spatio-temporal and cell type expression, I hypothesize that Cx30-mediated signalling may be involved in the regulation of NPCs in the postnatal mammalian brain.

### 1.6 The role of Cx30 in NPC fate.

To test this hypothesis, I propose to use $Cx30^{(-/-)}$ mice to ascertain whether there are any alterations in NPC specification, proliferation, and migration. The phenotype of $Cx30^{(-/-)}$ mice has been previously determined and defined as severe hearing impairment due to lack of endocochlear potential, increased emotionality, and reduced exploratory activity possibly due to the associated neurochemical changes in the knockout (KO) mouse brain (Dere et al., 2004; Teubner et al., 2003). However, no previous studies have investigated the effect of Cx30 null-mutation on adult NPC fate and function. Since astrocytes are the dominant cell

type expressing functional connexins, they have the capacity to "instruct" adult NPCs as previously demonstrated albeit without examination of connexin-mediated control prior to this thesis (Lim and Alvarez-Buylla, 1999; Song et al., 2002). Understanding the role of astrocyte-specific connexin proteins like Cx30 in NPC specification, migration, and proliferation will be critical for future NPC related neuroregenerative therapies. Taken together, *I hypothesize that Cx30-mediated signalling between astrocytes and NPCs directs these progenitor cells toward a neuronal fate.* Therefore, the studies presented in this thesis are directed to comprehending the effect of Cx30 null-mutation on NPC fate. The overall objectives of this thesis include:

(1) To identify cells that express Cx30 and/or have the potential to participate in Cx30-mediated signalling with astrocytes *in vivo* and *in vitro*.

(2) To establish the impact of Cx30 null-mutation on NPC proliferation, survival, migration, and specification in the neurogenic niches of adult mouse brain.

(3) To determine whether Cx30-mediated signalling between postnatal astrocytes and NPCs is required for neurogenesis *in vitro*.

## Chapter 2: Expression of Cx30 in astrocytes and NPCs in postnatal mouse brain *in vivo* and *in vitro.*

### 2.1 Introduction

Connexins are expressed in many different tissues with variable cellular distributions attributing to their functional diversity (Naus and Bani-Yaghoub, 1998). Over half of the known mammalian connexin genes have been found to be expressed in the mammalian brain (Nagy et al., 2004; Rouach et al., 2002; Rozental et al., 2000). Connexin expression is cell type-specific (Sohl et al., 2004); for instance, the cell type primarily coupled by gap junctions in the CNS, astrocytes, are known to express Cx26, Cx30, and Cx43 (Dahl et al., 1996; Nagy et al., 2004; Rash et al., 2001). While Cx43 expression is highest prenatally when neocortical development occurs, Cx30 is first expressed postnatally suggesting a role in late developmental events (Leong and Clark, 1984; Nagy et al., 1999). Subsequently, investigating the possible functional roles of Cx30 in adult mammalian neurogenesis will provide further insight in the field of adult neural stem cell therapies. The objective in this chapter was to determine whether NPCs express Cx30 in the adult mouse brain and/or other connexins compatible with Cx30 that would allow NPCs to form functional intracellular channels with Cx30-expressing astrocytes.

### 2.2 Materials and methods.

#### 2.2.1 Animals.

Breeding pairs of Cx30 $^{(-/-)}$ mice, in which the Cx30 coding region was replaced with the E. coli β-galactosidase reporter gene containing a nuclear localization sequence (Teubner

et al., 2003), were kindly donated by Dr. Klaus Willecke (Universitat Bonn, Germany). Cx30 $^{(-/-)}$ mice were then backcrossed to C57BL/6 WT mice for three generations, thereby generating N3 Cx30 $^{(-/-)}$ mice. Congenic WT mice were then derived in our laboratory through heterozygote matings. All WT mice used in this study were N3 generation with identical genetic background as their Cx30 $^{(-/-)}$ littermates. All animals used in this study were between two and four months of age at time of sacrifice.

### 2.2.2 Brain tissue preparation.

Mice were lethally anesthetized with euthansol and transcardially perfused with 10 mM phosphate buffered saline (PBS, 10 mM NaPhosphate, 154 mM NaCl) solution followed by 3.7% formaldehyde in 10 mM PBS. Brains were removed and post-fixed for 24 hours in the same fixative. After a 24 to 48 h post-fix, brains were cryoprotected in a 20% sucrose solution in 10 mM PBS containing 0.001% sodium azide. For sectioning, brains were mounted with TissueTek (Sakura, Torrance, CA) and flash frozen with $CO_2$. Serial coronal or sagittal (10 μm) sections were cut on a Leica CM1900 cryostat (Leica Microsystems Inc., Richmond Hill, Ontario). Sections were collected in the following regions for SVZ analysis (Coronal: Bregma 1.10 mm to 0.5 mm; Sagittal: interaural lateral 1.0 mm to 1.40 mm) and SGZ analysis (Coronal: Bregma -1.68 mm to -2.08 mm; Sagittal: interaural lateral 1.0 mm to 1.40 mm).

### 2.2.3 Immunofluorescence.

Sections were hydrated in 10 mM PBS solution for 5 min at room temperature followed by overnight incubation at 4°C with primary antibodies diluted in Antibody Buffer (Ab buffer: 10 mM PBS, 3% bovine serum albumin, 0.3% triton-X). Sections were then

rinsed three times for 5 minutes in 10 mM PBS solution. Secondary antibodies diluted in Ab buffer were incubated for one hour at room temperature in a humidified chamber. Slides were once again rinsed three times for 5 minutes with 10 mM PBS solution. Vectashield (Vector Laboratories Inc., Burlingame, CA) or Antifade (4.6 mM p-phenylenediamine in 100 mM PBS, 0.5 M NaHCO3 buffered at pH 8.0) was used as the immunofluorescence mounting medium and a sealed glass coverslip was placed on top of sections to maintain integrity. Primary and secondary antibodies along with their respective dilutions or final concentrations are listed in Table 1 and Table 2 in Appendix I. Fluorescence microscopy was performed on a Leica DMXRA2 microscope equipped with epifluorescence or on a LSM 510 confocal laser scanning microscope (Carl Zeiss Canada Ltd., Toronto).

**2.2.4 NSP culture and analysis.**

WT neonates (P0-P3) were sacrificed by lethal injection with sodium pentobarbital and their brains were rapidly removed and placed in ice cold artificial cereberospinal fluid (aCSF; 26 mM $NaHCO_3$, 124 mM NaCl, 5 mM KCl, 2 mM $CaCl_2$-$2H_2O$, 1.3 mM $MgCl_2$-$6H_2O$, 10 mM D-glucose, 1% penicillin/ streptomycin). The cerebellum was removed and the brain was blocked rostral-side up and cut on a vibrating microtome (Leica VT1000 S, Leica Microsystems Inc., Richmond Hill, Ontario, Canada) into 500 μm coronal sections in ice cold aCSF. Under a dissecting microscope, sections of interest were cleared free of meninges and the hippocampus containing the SGZ or ventricular zone containing the SVZ were precisely dissected with fine surgical instruments. Tissue was minced with a scalpel and then enzymatically dissociated in dissociation media (26 mM NaHCO3, 124 mM NaCl, 5 mM KCl, 0.1 mM $CaCl_2$-$2H_2O$, 3.2 mM $MgCl_2$-$6H_2O$, 10 mM D-glucose, 1%

penicillin/streptomycin, 0.1% neural protease, 0.01% papain, 0.01% DNAse I) for 45 min at 37 °C on a clinical rotator. A series of trituration and soft centrifugation steps were performed to remove enzymes and disperse cells prior to resuspension in maintenance medium (Dulbecco's modified Eagle's medium F12 (DMEM)/F12 containing 2 mM L-glutamine, 1% penicillin/ streptomycin, 2% B27 supplement, 20 ng/ml human EGF, and 10 ng/ml FGF2). Cell suspensions were plated in 6 cm low adherence plates (Corning Inc., Corning, NY) at a concentration of 2.5 X $10^5$ viable cells per plate as determined by hemocytometer counts of trypan blue-excluding cells. Cells were cultured in suspension at 37 °C in a 5% $CO_2$/ 95% atmosphere incubator with fresh EGF and FGF2 added every two days over the first 8 *in vitro* (DIV) to promote the clonal expansion of NSP cultures.

For immunocytochemistry, NSPs were grown for 12 DIV. Cells were fixed in 3.7% formaldehyde in 10 mM PBS for 10 min. Following extensive washes in PBS, NSPs were cryoprotected for 24 h in a 15% sucrose solution (15% weight/volume sucrose in 10 mM PBS + 0.001% sodium azide), flash-frozen, and serially sectioned (10 µm thickness) on a Leica CM1900 cryostat. Cultures and serial sections were processed for immunocytochemistry as described above (Methods 2.2.3).

**2.2.5 Flow cytometry.**

NSP cultures were expanded for 12-14 DIV before being suspended in 4 mL 2% formaldehyde in 10 mM PBS and titurated (glass pasteur pipette) for 1-5 min until single cell suspension was achieved by visual inspection using a hemocytometer with trypan blue. The single cell suspension was incubated in 2% formaldehyde for a further 20 min on ice followed by two washes and gentle centrifugation at 2000 rpm for 5 min in 5 ml PFN (2%

fetal bovine serum, 0.1% $NaN_3$ in 10 mM PBS). Cell membranes were then permeabilized in PFN containing 0.18% saponin. Cell suspensions were separated into 1.5 ml ependorf tubes at a concentration of 1 x $10^6$ cells per tube. Primary antibodies were added directly to cell suspensions at appropriate concentrations followed by incubation at room temperature for 30 min on a shaker. Each sample was washed twice by the addition of 0.8 ml of PFN and spun down at room temperature for 5 min at 2200 rpm. Secondary antibodies were added to cell suspensions at appropriate concentrations followed by incubation at room temperature for 30 min on a shaker and washed as described above. Cells were resuspended in 0.5 ml of PFN and analyzed using a Beckman Coulter FC500 Flow Cytometer (Beckman Coulter Canada Inc., Mississauga, ON) and Beckman Coulter CXP software. Antibody concentrations for flow cytometry are provided in Table 3 in Appendix I.

## 2.3 Results

### 2.3.1 Cx30 is expressed by GFAP$^+$ astrocytes, GFAP$^+$/ nestin$^+$ Type 1 NPCs, and nestin$^+$/GFAP$^-$/DCX$^-$ Type 2a NPCs in the SGZ of adult mouse brain.

To determine whether Cx30 is expressed by astrocyte-like NPCs in adult SGZ, Cx30 protein was localized to discrete cell types by immunofluorescence using both epifluorescence and confocal microscopy. Double- and triple-labelling for the following antigenic markers with Cx30 were used to distinguish between astrocytes, neurons, oligodendrocytes, and various NPC populations. GFAP was used to detect reactive astrocytes (Bachoo et al., 2004; Lu et al., 2001). Expression of chondroitin sulfate proteoglycan NG2 and the platelet derived growth factor α receptor (PDGFαR) were used to

identify glial and early oligodendrocyte progenitors (Penderis et al., 2003). Nestin immunoreactivity was used to distinguish between astrocytes and Type 1 NPCs and identify Type 2a intermediate progeny (Ernst and Christie, 2006; Lendahl et al., 1990). DCX, a microtubule-associated protein, was used to label Type 2b and Type 3 early neuronal progenitor cells (Engelhardt et al., 2005). The mature neuronal nuclear antigen, NeuN, was used to label terminally differentiated neurons (Weyer and Schilling, 2003).

Extensive Cx30 labeling was detected in the DG of the hippocampal formation (Figure 2.1). Similar to other connexin staining, Cx30 immunoreactivity exhibited a punctate staining pattern throughout the SGZ, and the polymorphonuclear layer of the dentate gyrus (PMNL) (Figure 2.1 A,B,E). In the granule cell layer, little to no Cx30 protein expression was detected (Figure 2.1 A,B,E). Consistent with previous reports (Nagy et al., 2004; Nagy et al., 1999), Cx30 localized to a subset of $GFAP^+$ astrocytes in the DG (Figure 2.1B,D,F, arrows). We also show, for the first time, that discrete $nestin^+$ cells are $Cx30^+$ (Figure 2.1, C, arrows). Since Cx30 was found to be expressed by $GFAP^+$ cells and $nestin^+$ cells in the SGZ, triple labelling was performed to determine whether Cx30 localized to Type 1 $GFAP^+$/ $nestin^+$ NPCs (Figure 2.1,D,F, arrows). Confocal imaging revealed co-localization of Cx30 with nestin and GFAP in several focal planes along the Z-axis (Figure 2.1, F, dotted lines). Cx30 was also detected in $nestin^+/GFAP^-$ cells (Figure 2.1, D, F). To distinguish between Type 2b and Type 3 NPCs, Cx30 expression in $DCX^+$ cells was also investigated but showed no co-localization (data not shown). Moreover, proliferating $BrdU^+$ cells labelled over three days were found to be in close proximity to Cx30 expressing cells but no $Cx30^+$/ $BrdU^+$ co-labelled cells were identified. These data are consistent with antigenic indications that Cx30 localizes to slowly dividing Type 1 and Type 2a NPCs, but not transit amplifying

**Figure 2.1 Cx30 is expressed by NPCs and astrocytes in the SGZ of the DG.** Schematic of the hippocampal formation with a red box representing region presented in photomicrographs (A). Cx30 is expressed in GFAP$^+$ astrocytes (B), nestin$^+$ Type 2a NPCs (C), nestin$^+$ / GFAP$^+$ Type 1 NPCs (D) but not mature NeuN+ neurons (E) in SGZ coronal sections of the WT adult mouse brain. Epifluourescent results were confirmed using confocal microscopy. Cx30 is expressed in a subset of Type 1 nestin$^+$ / GFAP$^+$ NPCs (F). Dotted lines indicate region of Z-axis sectioning that illustrate co-labelling of Cx30 with nestin and GFAP in several focal planes. Sections derived from Cx30$^{(-/-)}$ mice served as negative controls demonstrating the specificity of labelling (G). Arrows indicate co-labelling of punctate Cx30 staining with other cell markers. Scale bars, 50 μm. Abbreviations: CA1, CA3, CA3a-b, CA pyramidal cell field of the hippocampus; GrDG, granule cell layer of the dentate gyrus; SGZ, subgranular zone of the DG.

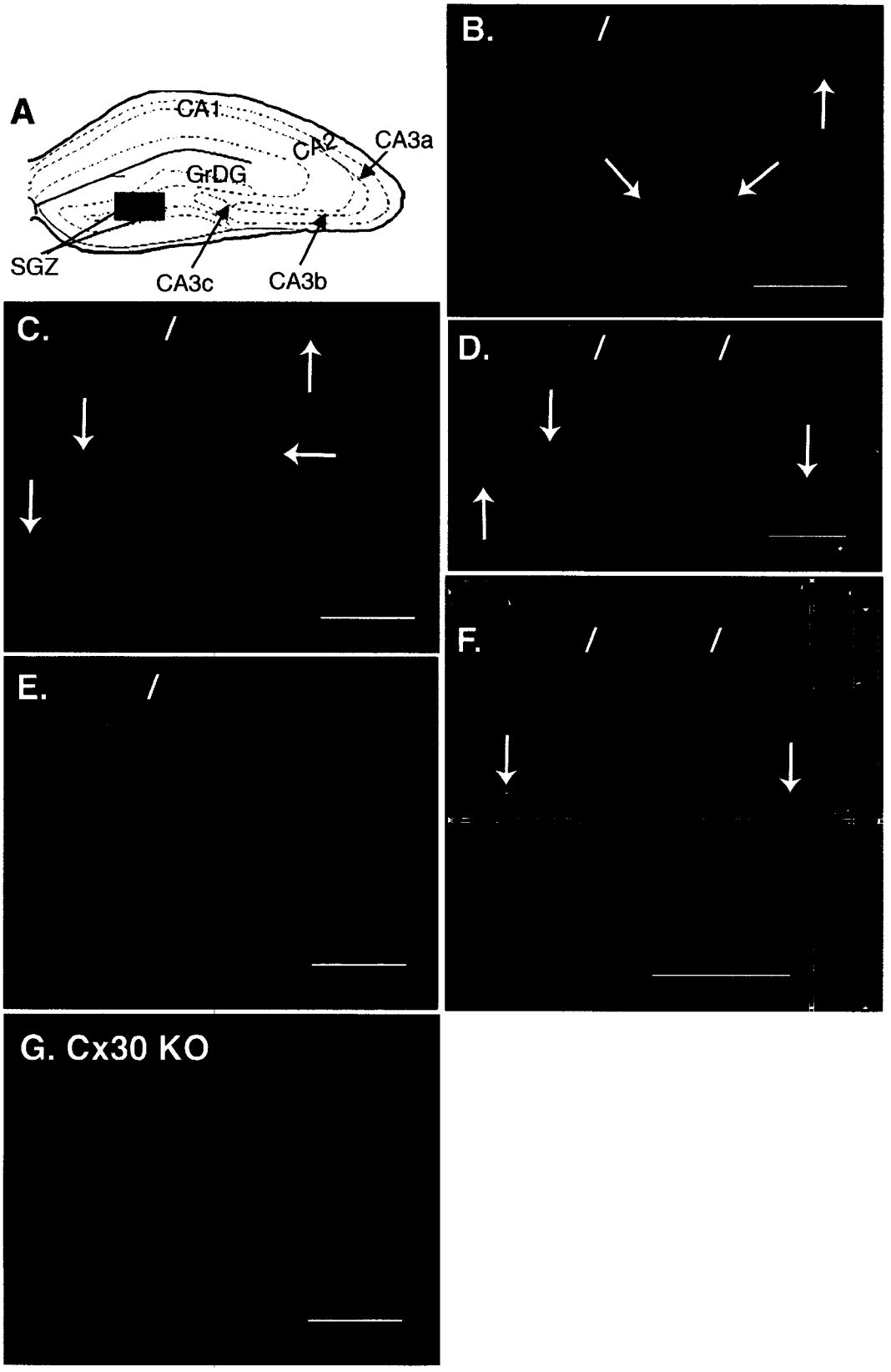


**Figure 2.1**

Type 3 cells. Cx30 was not detected in $NeuN^+$ neurons or $NG2^+$/ $PDGF\alpha R^+$ glial and early oligodendrocyte progenitor (Figure 2.1, E). Specificity was confirmed using sections from Cx30 null-mutant mice to control for artifactual labelling (Figure 2.1,G) and incubation of secondary antibodies in the absence of primary antibodies to control for non-specific labelling (data not shown). No signal was detected in either negative control.

### 2.3.2 Cx30 is expressed in $GFAP^+$ astrocytes, $nestin^+$/ $GFAP^+$ Type B NPCs, and $nestin^+$/$GFAP^-$/$DCX^-$ Type C NPCs in the SVZ of adult mouse brain.

Comparable analyses were performed in the SVZ of adult mice. Expression of Cx30 was assessed by epifluorescence (Figure 2.2) and confocal microscopy (Figure 2.3) in the SVZ region and the dorso-lateral aspect (DLA) of the LV where the RMS emerges. In the SVZ, Cx30 was detected with the expected punctate staining characteristic of gap junction proteins and a heterogeneous distribution pattern from the dorsal to ventral SVZ region with some ectopic expression in the adjacent striatal region (Figure 2.2). In the DLA of the LV, Cx30 staining was also punctate, but more uniform. As in the SGZ, Cx30 was found to be expressed in a subset of $GFAP^+$ cells (Figure 2.2, B, arrows), consistent with previous findings (Dahl et al., 1996). In addition, Cx30 localized to $nestin^+$ NPCs (Figure 2.2, C, arrows). Confocal imaging of Cx30, GFAP, and nestin triple staining confirmed the expression of Cx30 by $nestin^+$/ $GFAP^+$ Type B NPCs (Figure 2.3). Immunolabelling of various antigenic lineage markers demonstrated Cx30 expression in $GFAP^+$ astrocytes, Type C $nestin^+$/ $GFAP^-$ NPCs, and Type B $nestin^+$/ $GFAP^+$ NPCs in the DLA of the LV (Figure 2.3, C, arrows and dotted lines), RMS (Figure 2.3,E, arrows and dotted lines), and SVZ in

**Figure 2.2 Cx30 is expressed by NPCs and astrocytes in the SVZ of the LV.** Schematic of the murine forebrain with SVZ indicated in red and a black box represents region presented in photomicrographs (A). Cx30 is expressed by $GFAP^+$ astrocytes (B), $nestin^+$ type B/C NPCs (C) but not mature $NeuN^+$ neurons (D). Sections derived from Cx30 $^{(-/-)}$ mice served as negative controls demonstrating the specificity of labelling (E). Arrows indicate co-labelling of Cx30 with other cell markers. Scale bars, 50 μm. Abbreviations: LV, lateral ventricle; SVZ, subventricular zone.

**Figure 2.2**

**Figure 2.3 Cx30 is expressed by Type B "stem-like" NPCs in the SVZ, the DLA of the SVZ, and the RMS**. Saggital (A) and coronal (B) schematics indicating location of photomicrographs. Confocal imaging of triple immunolabelling confirmed many nestin$^{+}$/ GFAP$^{+}$ Type B NPCs that express Cx30 in the DLA of the LV (C) the SVZ (D), and in the RMS (E). Arrows indicate cells co-expressing Cx30 in nestin$^{+}$ and/or GFAP$^{+}$ cells. Dotted lines localize Z-axis sectioning in several focal planes. Abbreviations are as defined in Figure 2.1 and 2.2: and NC, neocortex; RMS, rostral migratory stream; CB, cerebellum; CC, corpus callosum; and DLA, dorso-lateral aspect of the SVZ. Scale bars, 25 μm.

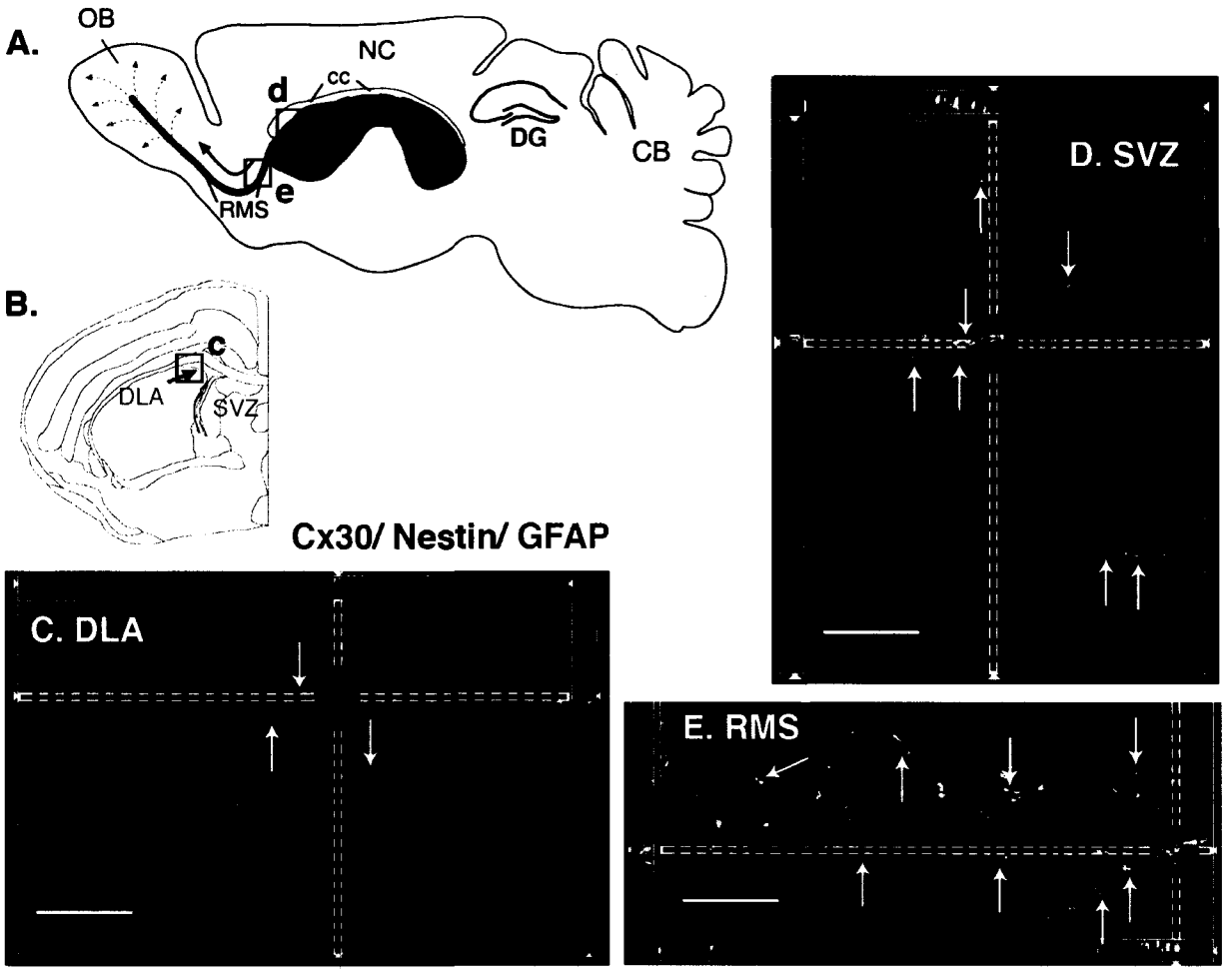
A.
OB
NC
cc
d
DG
CB
RMS
e
B.
c
DLA
SVZ
Cx30/ Nestin/ GFAP
C. DLA
D. SVZ
E. RMS

**Figure 2.3**

both coronal and sagittal sections (Figure 2.3, D, arrows and dotted lines). Confocal imaging confirmed Cx30 expression in nestin$^+$/GFAP$^+$ Type B NPCs in several focal planes along the Z-axis (Figure 2.3, C, D, E, dotted lines). Cx30 was not detected in NG2$^+$ glial progenitor cells, PDGFαR$^+$ oligodendrocyte progenitors, DCX$^+$ Type C neuroblasts, or NeuN$^+$ mature neurons (Figure 2.2,D). Negative controls included immunoreaction for Cx30 in Cx30 null-mutant mice to control for artifactual labelling (Figure 2.2,E) and incubation of secondary antibodies in the absence of primary antibodies to control for non-specific labelling (data not shown).

### 2.3.3 Confirmation of Cx30 expression by astrocytes, Type 1/B NPCs, and Type 2a/C NPCs *in vitro*.

To validate these findings, NPCs isolated from the SGZ or SVZ of from P0-P3 old neonates were cultured as NSPs. Previous attempts to generate a sufficient yield of NSP cultures from adult mice by other members of the Bennett laboratory were unsuccessful so neonatal cultures were employed for both immunocytochemical and flow cytometry analyses. Consistent with our *in vivo* analysis of adult mice in both SGZ and SVZ-derived NSPs, double immunolabelling for various antigenic lineage markers and Cx30 revealed Cx30 co-localization with GFAP-expressing cells (Figure 2.4, A) and nestin-expressing cells (Figure 2.4, B) but not other NPC markers (data not shown). Again, triple labelling and confocal imaging was performed to determine whether Cx30 is expressed by Type B GFAP$^+$/ nestin$^+$ NPCs in SVZ-derived NSPs. Analysis of several focal planes along the Z-axis confirmed Cx30 expression in Type B nestin$^+$/ GFAP$^+$ NPCs (Figure 2.4, C).

**Figure 2.4 Cx30 is expressed by proliferating hippocampal and SVZ-derived NSPs cultured *in vitro*.** Cx30 localizes to $GFAP^+$ cells (A) and $nestin^+$ NPCs (B) in hippocampal-derived NSPs. Insets depict higher magnification of individual cells. Confocal imaging confirmed triple immunolabelling for Cx30, nestin, and GFAP, in a subset of Type B NPCs in SVZ-derived NSPs (C). Arrows point to cells co-labelled with Cx30, nestin and/or GFAP. Dotted lines indicate region of Z-axis sectioning confirming co-labelling in several focal planes. Scale bars, 50 μm.

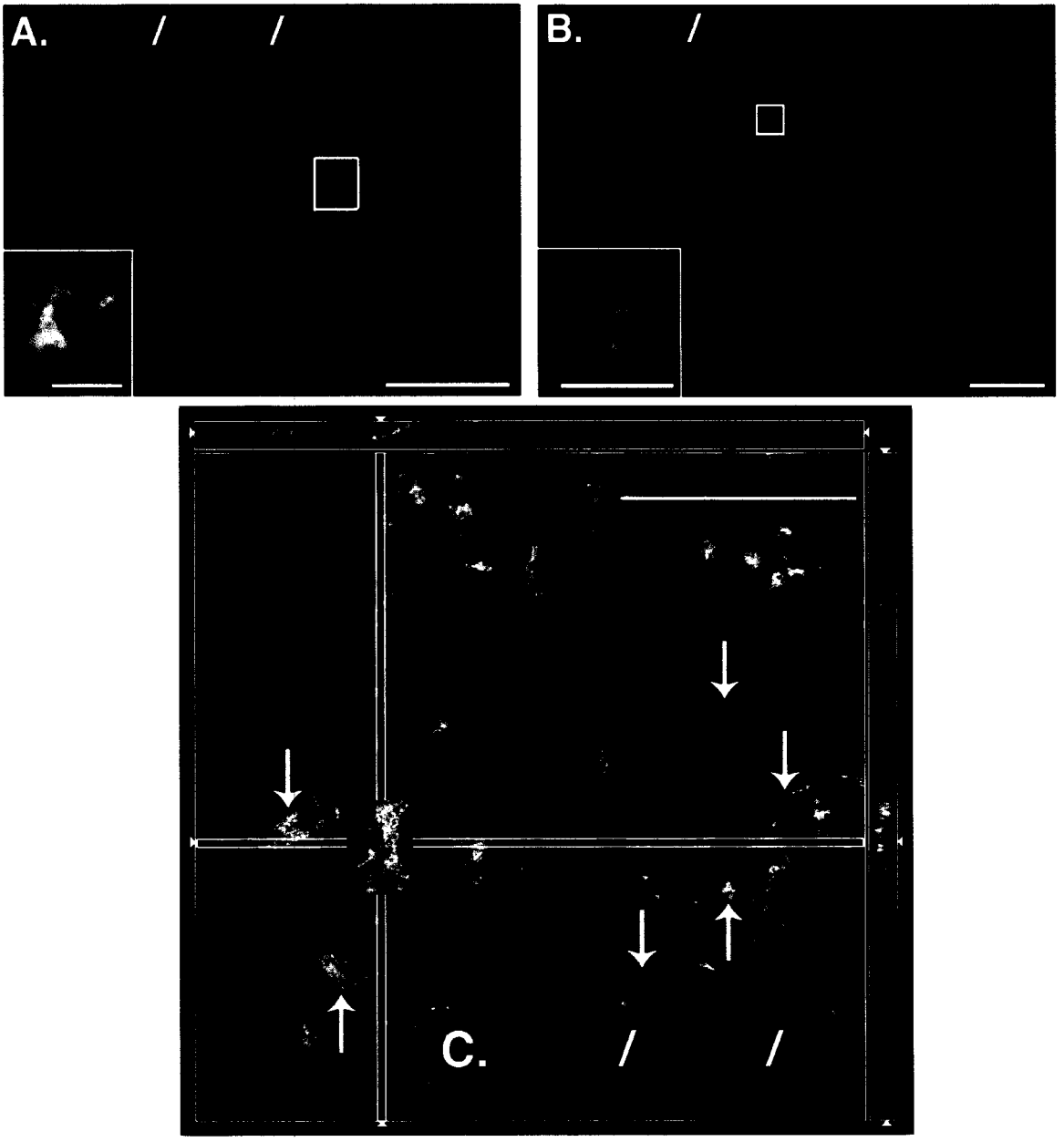


**Figure 2.4**

### 2.3.4 Quantification of $Cx30^+$ NPCs.

To quantify $Cx30^+$ NPC subsets, a flow cytometric approach was employed. NSPs were dissociated and subjected in antigenic analysis. Quantitative analysis required several essential controls. Once viable cell populations were determined based on forward scatter (FS), a parameter that indicates the relative size of cells, and side scatter (SS), a parameter that denotes the granularity and inner complexity of cells, these cells were gated for further analysis. Secondary antibodies used in these experiments were coupled to fluorescein (FITC), R-phycoerythrin (R-PE), or cyanine 5 (Cy5). Samples incubated without primary antibodies, secondary antibodies alone, or isotypic and mismatch, primary and secondary antibodies were used to assess autofluorescence and non-specific labelling. These controls were carried out in order to effectively analyze the percentage of cell types expressing specific antigenic markers and the proportion of cell types expressing Cx30.

Next, hippocampal and SVZ-derived NSPs were labelled for nestin, Cx30, and/or GFAP, and the relative percentage of cells expressing these cell markers were measured. Triple-labelling flow cytometry experiments with their corresponding quadrant percentage s in two dimensional histogram plots are illustrated in Figure 2.5 and Figure 2.7 for hippocampal and SVZ-derived NSPs, respectively.

In hippocampal-derived NSPs, the relative percentage of NSP-derived cells quantitated in replicate or triplicate experiments are presented in Figure 2.6. To further analyzes discrete subsets, we determined the percentage of $GFAP^+$ and/or $nestin^+$ cells that expressed Cx30. These data are presented in Figure 2.6, B. Note that the majority of Type 1 $nestin^+$/ $GFAP^+$ subpopulations, 93.44 +/- 3.33% (n=2) co-expressed Cx30 (Figure 2.6, B).

The relative percentage of Cx30 expression in these subpopulations is represented in a schematic diagram where $Cx30^+$ expression is labelled blue for $GFAP^+$ or $nestin^+$ populations ($Cx30^-$ expression in white), while $Cx30^+$ expression is labelled red for $nestin^+$ / $GFAP^+$ subpopulations ($Cx30^-$ expression in green) (Figure 2.6, C).

Similar results were observed in SVZ-derived NSPs (Figure 2.8, A, B). In the Type B $nestin^+$ / $GFAP^+$ NPC subpopulation, 91.59 +/- 2.96% (n=2) co-expressed Cx30 (Figure 2.6, B). As for the SGZ (Figure 2.6), the relative percentage of Cx30 expression in these subpopulations is represented in a schematic diagram where $Cx30^+$ expression is labelled blue for $GFAP^+$ or $nestin^+$ populations ($Cx30^-$ expression in white), while $Cx30^+$ expression is labelled red for $nestin^+$ / $GFAP^+$ subpopulations ($Cx30^-$ expression in green) (Figure 2.6, C).

**Figure 2.5 Flow cytometry of Cx30 expression by hippocampal-derived NSPs confirming immunocytochemical analyses.** Two and three dimensional histogram analyses demonstrating methodology and controls employed and representative data generated in each flow cytometry experiment with hippocampal-derived NSP cells alone, and cells along with appropriate primary and secondary antibodies (cells alone with secondary antibodies, data not shown). Specific quadrant percent numbers represent the percentage of gated NSP cells expressing corresponding cell markers. Fluorophore abbreviations include: FITC, fluorescein; and RPE, R-phycoerythrin; and Cy5, cyanine 5.

## Hippocampal-Derived NSPs

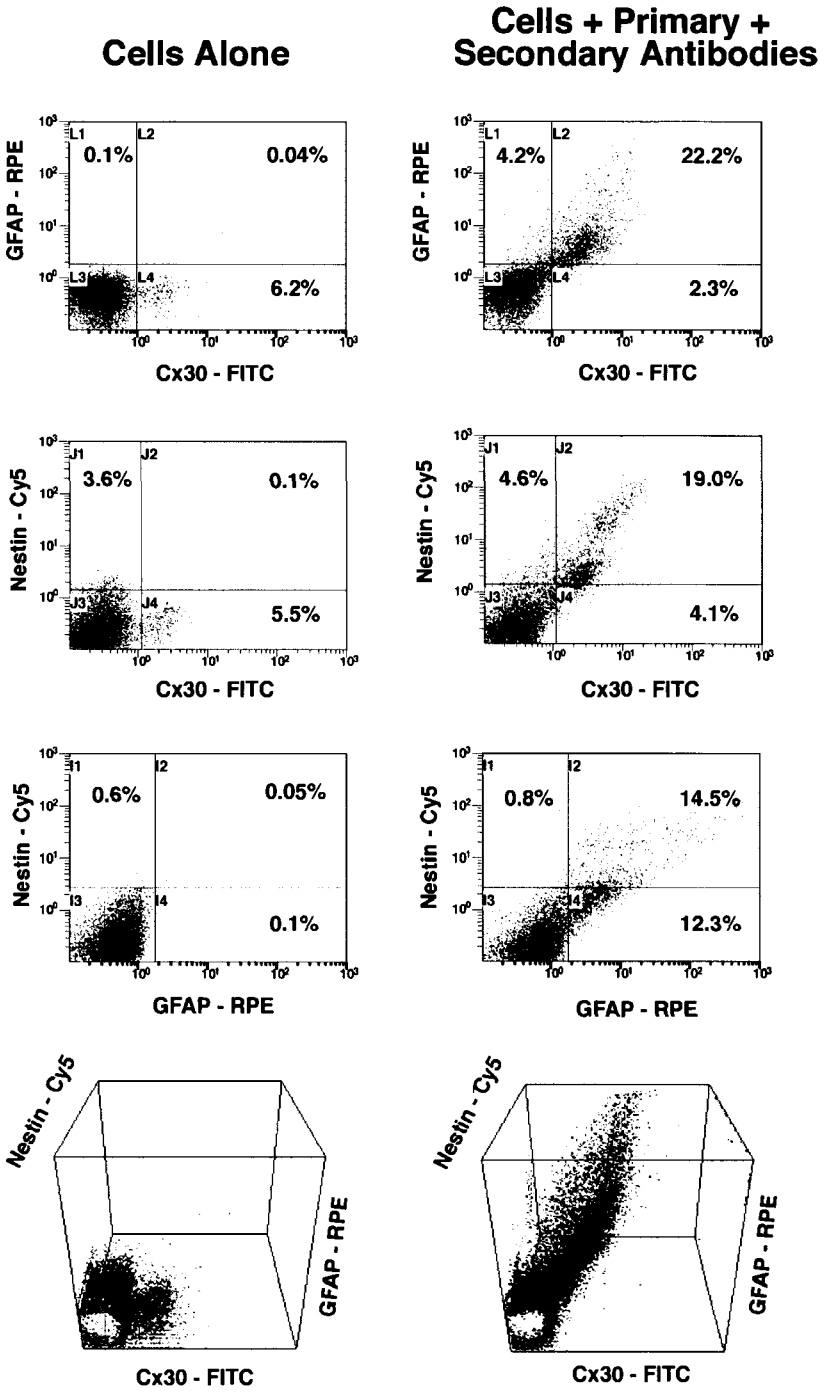


Figure 2.5

**Figure 2.6 Quantitation of $Cx30^+$ cells and antigenic lineage analysis of hippocampal-derived NSPs.** The percentage of hippocampal-derived NSPs expressing Cx30, GFAP, nestin, or co-expressing Cx30 and nestin or GFAP (A). The percentage of $GFAP^+$, $nestin^+$, or $nestin^+$/ $GFAP^+$ cells that express Cx30 (B). Data represent mean plus standard error of measurement (SEM) of experiments conducted in replicate or triplicate. These data are summarized in (C). The percentage of $GFAP^+$ or $nestin^+$ cells in NSPs expressing $Cx30^+$ depicted in blue. $GFAP^+$ or $nestin^+$ cells that are not $Cx30^+$ is depicted in white. The percentage of $nestin^+$/ $GFAP^+$ cells that express Cx30 is indicated in red while those cells that lack Cx30 expression are indicated in green.

Hippocampal-Derived NSPs

A.

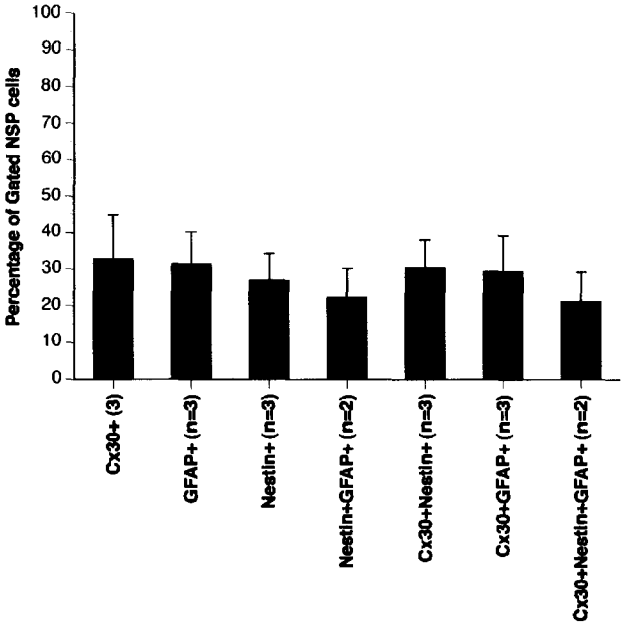


B.

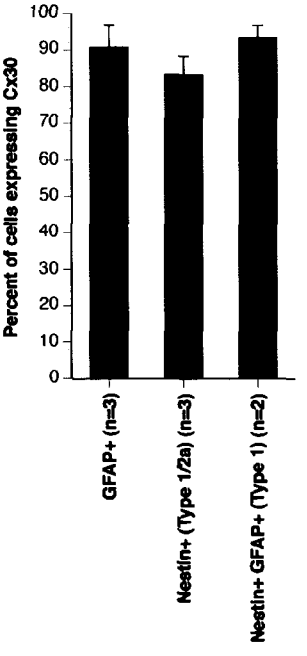


C.

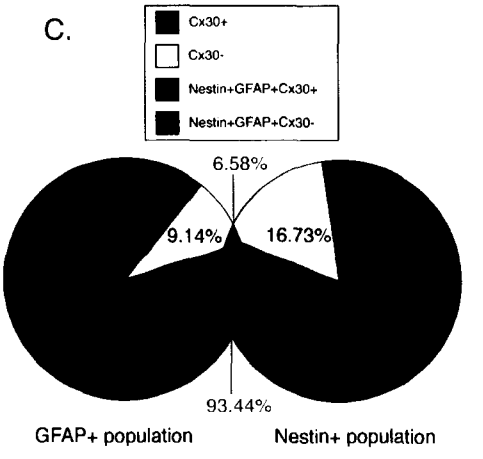


Figure 2.6

**Figure 2.7 Flow cytometry of Cx30 expression by SVZ-derived NSPs confirming immunocytochemical analyses.** Two and three dimensional histogram analyses demonstrating methodology and controls employed and representative data generated in each flow cytometry experiment of SVZ-derived NSP cells alone, and cells along with appropriate primary and secondary antibodies (cells alone with secondary antibodies, data not shown). Specific quadrant percent numbers represent the percentage of gated NSP cells expressing corresponding cell markers. Abbreviations are as defined in Figure 2.5.

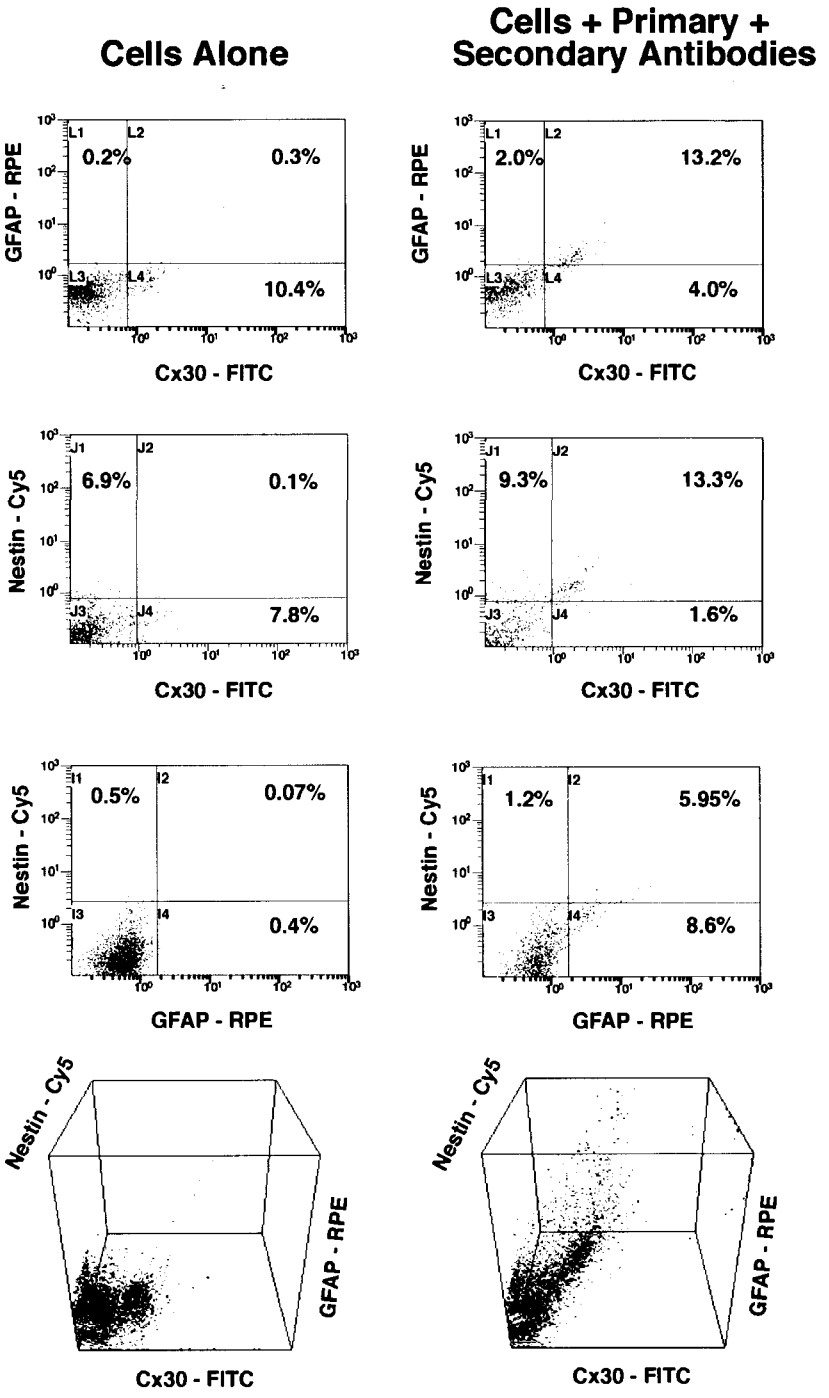
Cells Alone
Cells + Primary + Secondary Antibodies
GFAP - RPE
Cx30 - FITC
L1
L2
L3
L4
0.2%
0.3%
10.4%
2.0%
13.2%
4.0%
Nestin - Cy5
J1
J2
J3
J4
6.9%
0.1%
7.8%
9.3%
13.3%
1.6%
I1
I2
I3
I4
0.5%
0.07%
0.4%
1.2%
5.95%
8.6%

**Figure 2.7**

**Figure 2.8 Quantitation of Cx30$^+$ cells and antigenic lineage analysis of SVZ-derived NSPs.** The percentage of SVZ-derived NSPs expressing Cx30, GFAP, nestin, or co-expressing Cx30 and nestin or GFAP (A). The percentage of GFAP$^+$, nestin$^+$, or nestin$^+$/ GFAP$^+$ cells that express Cx30 (B). Data represent mean plus SEM of experiments conducted in replicate or triplicate. These data are summarized in (C). The percentage of GFAP$^+$ or nestin$^+$ cells in NSPs expressing Cx30 is depicted in blue. GFAP$^+$ or nestin$^+$ cells that are not Cx30$^+$ is depicted in white. The percentage of nestin$^+$/GFAP$^+$ cells that express Cx30 is indicated in red while those cells that lack Cx30 expression are indicated in green.

SVZ-Derived NSPs

A.

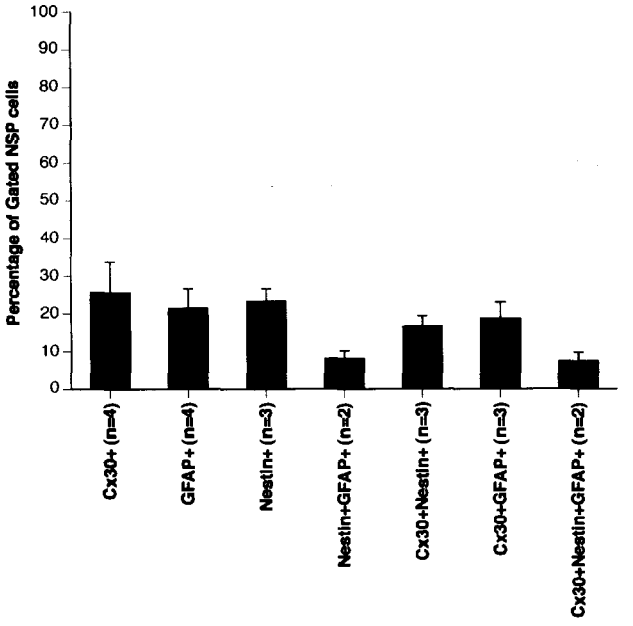


B.

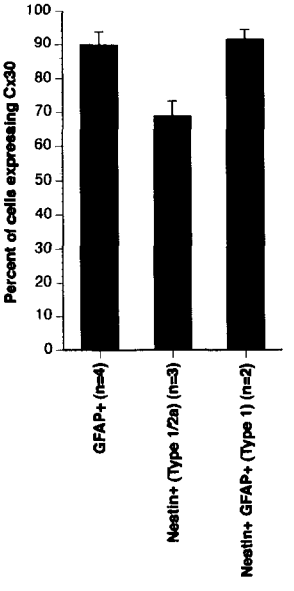


C.

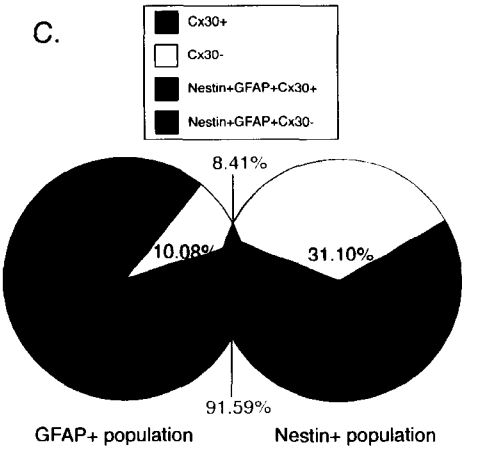


**Figure 2.8**

## 2.4 Discussion

Although connexin-mediated communication has been implicated in providing the necessary intercellular signals for mammalian brain development (Sutor and Hagerty, 2005), few studies have determined whether this control may be recapitulated in adult brain. The functionality of each individual connexin varies due to their distinctive spatio-temporal expression pattern, cell type expression, and molecular structure (Sohl et al., 2004). Here, we show for the first time that Cx30 is expressed by nestin$^+$ NPCs in adult brain within the neurogenic niches of SGZ and the SVZ. Further, Cx30 was localized to a subset of nestin$^+$/ GFAP$^+$ astrocytes that themselves have been characterized as multipotential Type 1/B progenitors with similar characteristics to neural stem cells (Doetsch, 2003; Kempermann et al., 2004). Cx30 was not identified in mature NeuN$^+$ neurons, PDGFαR$^+$ early oligodendrocyte progenitors, NG2$^+$ glial progenitors, or DCX$^+$ early neuronal progenitors. Finally, Cx30 was not expressed in actively proliferating (BrdU$^+$) NPCs, but in quiescent or slowly proliferating populations not labelled over our 3 day BrdU injection protocol. These data are consistent with a Type 1/B phenotype (Doetsch, 2003; Kempermann et al., 2004) and congruent with most literature pertaining to Cx30 expression in GFAP$^+$ cells in the adult rodent brain (Altevogt and Paul, 2004; Dahl et al., 1996; Dani et al., 1992; Nagy et al., 2004; Nagy et al., 2003b; Nagy et al., 1999; Rash et al., 2001); however, one study observed Cx30 mRNA expression in dying neurons after kainite-induced seizures suggesting a possible involvement in the neuronal apoptotic process (Condorelli et al., 2002). Moreover, Cx30 expression was confined to subsets of NPCs and astrocytes and was not ubiquitously expressed by each population. Confocal imaging of Cx30 expression in SVZ-derived NSPs demonstrated co-localization with a small proportion of nestin$^+$ Type C NPCs, GFAP$^+$

astrocytes, and GFAP$^+$ / nestin$^+$ type B NPCs. This evidence was further supported by additional *in vitro* studies performed by Lianne Gauvin, a M.Sc. student in the Bennett laboratory, where GFAP$^+$ and nestin$^+$ NPCs cultured *in vitro* as SGZ-derived NSPs were also found to express Cx30 (Gauvin, M.Sc. thesis).

To quantitate expression in these subsets of NPCs, flow cytometric analyses were performed. Localization of Cx30 to GFAP$^+$ and/or nestin$^+$ cell populations and not other NPCs or terminally differentiated CNS cell types was confirmed. The percentage of Cx30$^+$ expressing cells within NSPs was low with 32.88% and 25.57% in hippocampal and SVZ-derived NSPs, respectively with Cx30 expression restricted to 90.85% and 89.92% GFAP$^+$ cells and 93.44% and 91.59% nestin$^+$/ GFAP$^+$ NPCs. Expression was more divergent in the nestin$^+$ populations including more committed Type 2a/C NPCs. In hippocampal-derived NSPs, 83.27% expressed Cx30 while 68.89% expressed Cx30 in SVZ-derived NSPs. These data suggest that Cx30 expression in more committed nestin$^+$ NPCs may vary due to their environmental niche.

Cx30-mediated gap junctions have been previously implicated in astrocyte-astrocyte intercellular networks (Nagy et al., 2003b). The finding that most Type 1/B cells also expressed Cx30 suggests a possible functional role for Cx30-meditated communication between these multipotential Type 1/B progenitor cells and the potential for astrocytes to communicate directly with this stem-like subset of NPCs in adult brain. Several regulatory cell-cell communication scenarios are possible. In 2002, Gage's group demonstrated that astrocytes derived from the hippocampal formation actively "instruct" adjacent NPCs to adopt a neuronal lineage and that this communication required direct cell-cell contact in

addition to paracrine release of neurogenic factors (Song et al., 2002). Enhanced neurogenesis was reported previously by the Alvarez-Buylla team when SVZ-derived NPCs were plated in direct contact with astrocytes (Lim and Alvarez-Buylla, 1999). The data presented in this thesis identify a possible signalling mechanism through which $GFAP^+$ astrocytes may communicate with Type 1/B and some Type 2a/C NPCs through Cx30 homotypic gap junctional coupling. This hypothesis was tested further by loss of function studies *in vivo* and NSP differentiation experiments *in vitro* in the next chapters.

Altogether, we propose that Type 1/B NPCs can communicate with the extracellular milieu, can synchronize their activity, and/or themselves can couple to terminally differentiated astrocytes via channels composed of Cx30 and compatible connexin partners.

## Chapter 3: Diminished neuronal specification in Cx30 KO mice.

### 3.1 Introduction.

To determine whether Cx30-mediated communication regulates NPC fate in adult brain, we used a loss of function approach evaluating NPC proliferation, survival, specification, and migration in Cx30 $^{(-/-)}$ mice. Phenotypically, these mice have severe hearing impairment due to lack of endocochlear potential required for proper audition, and increased emotionality with reduced exploratory activity (Dere et al., 2004; Teubner et al., 2003). This phenotype provides an animal model for human genetic hearing impairment diseases resulting from mutations in the human Cx30 and Cx26 gene (Evirgen et al., 2008; Zhao et al., 2006). No study, however, has examined whether loss of Cx30 impacts upon adult neurogenesis.

### 3.2 Materials and Methods.

#### 3.2.1 Animals.

Cx30 $^{(-/-)}$ mice were kindly donated from Dr. Klaus Willecke. Please refer to Methods 2.2.1 for detailed information pertaining to the generation and genetic background of the Cx30 $^{(-/-)}$ mice and WT animals used in this study.

#### 3.2.2 BrdU labelling.

BrdU (50 μg/g in sterile 10 mM PBS, pH 7.0) was administered intraperitoneally. Animals received two daily injections (4-5 hours apart) over two consecutive days followed by one injection on the third day. Animals were sacrificed 24 hours after last BrdU injection

and their brains were processed as described in Methods 2.2.2. Coronal and sagittal adult WT and Cx30 $^{(-/-)}$ mouse brain sections encompassing the SGZ in dorsal hippocampus and the forebrain SVZ were incubated in 10 mM PBS for 5 min followed by incubation in 2 N HCl for one hour at 37 °C. Subsequently, three 5 min neutralization washes with 0.1 M borate buffer (pH 8.5) followed by three 5 min washes with 10 mM PBS were performed. Sections were incubated overnight at 4 °C inside a humidified chamber with monoclonal mouse anti-BrdU (6 μg/mL; Roche) diluted in Ab buffer. Sections were then washed with 10 mM PBS and incubated at room temperature (inside a humidified chamber) with a Cy3-conjugated anti mouse IgG (1:800; Jackson ImmunoResearch) in Ab buffer. Fluorescence digital micrographs were captured with OpenLab Software, version 3.5 (Improvision, Lexington, MA) on a Leica DMXRA2 microscope equipped with epifluoresence. $BrdU^+$ cells / 0.1 $mm^2$ were counted in the SVZ, DG, the CA1 pyramidal cell field, the OB, and the RMS.

**3.2.3 Lineage analysis.**

Double immunofluorescence was performed as outlined previously (Methods 2.2.3) to determine the percentage of proliferating cell types. Sections of interest (representative of the DG and SVZ) were incubated with antibodies against BrdU along with antibodies raised against antigenic lineage markers: nestin (NPCs), NG2 (glial progenitors and some NPCs), DCX (neuronal progenitors), or NeuN (mature neurons). The numbers of $BrdU^+$, $nestin^+$, $DCX^+$, and $NG2^+$ cells were counted per region along with the number cells dually expressing BrdU and one of the assessed lineage markers. The total number of $BrdU^+$ cells was averaged with corresponding genotype (*i.e.*, average total $BrdU^+$ cells for WT mice) and

the percent proliferating cell lineage progenitor (% double-labeling) was calculated by dividing the number of double-labeled cells (*i.e.*, nestin$^+$/BrdU$^+$ cells) over the average total of BrdU$^+$ cells.

### 3.2.4 Statistics.

Data were analyzed with GraphPad InStat statistics program (GraphPad Software Inc.) where a Student's *t* test was used to determine statistically significant differences between WT and Cx30$^{(-/-)}$ mice. Statistical significance was set at $p < 0.05$ (one asterisk or one pi ($\pi$) on the graph), $p < 0.01$ (two asterisks or two pis ($\pi$) on the graph), and $p < 0.001$ (three asterisks on the graph).

## 3.3 Results.

### 3.3.1 Cx30 null-mutation has no impact on the total number of proliferating BrdU$^+$ cells in both neurogenic regions of adult mouse brains.

In Chapter 2, we found that Cx30 is expressed by activated astrocytes, potential instructive cells in the SGZ and SVZ neurogenic niches, and by quiescent nestin$^+$ NPCs. To determine whether the loss of Cx30 alters the proliferative indices of these progenitor populations in the DG and SVZ, WT and KO mice received five intraperitoneal BrdU injections (50 μg/g) over three consecutive days and were perfused 24 hours after last injection. The number of BrdU$^+$ cells per 0.1 mm$^2$ was determined in the dorsal DG (bregma -1.68 mm to -2.08 mm). A total of 13 Cx30 KO mice in a mixed 129/SV/C57Bl/6

**Figure 3.1 The overall rate of cell proliferation is comparable in adult WT and Cx30$^{(-/-)}$ mice in both the SGZ and SVZ.** Schematic of the dorsal hippocampus (A). The location of the photomicrographs presented in D and E are indicated by the box. Abbreviations are as in Figure 2.1. There is no difference in total number of BrdU-labelled cells detected in adult Cx30 null-mutant mice in the SGZ (B), the CA1 region (used as a bioavailability control) (C), or the SVZ (F). Representative photomicrographs of WT and KO DG immunolabelled for NeuN (red) and BrdU (green) are presented in D and E. Arrows indicate BrdU$^{+}$ cells in the SGZ. Scale bars, 50 μm.

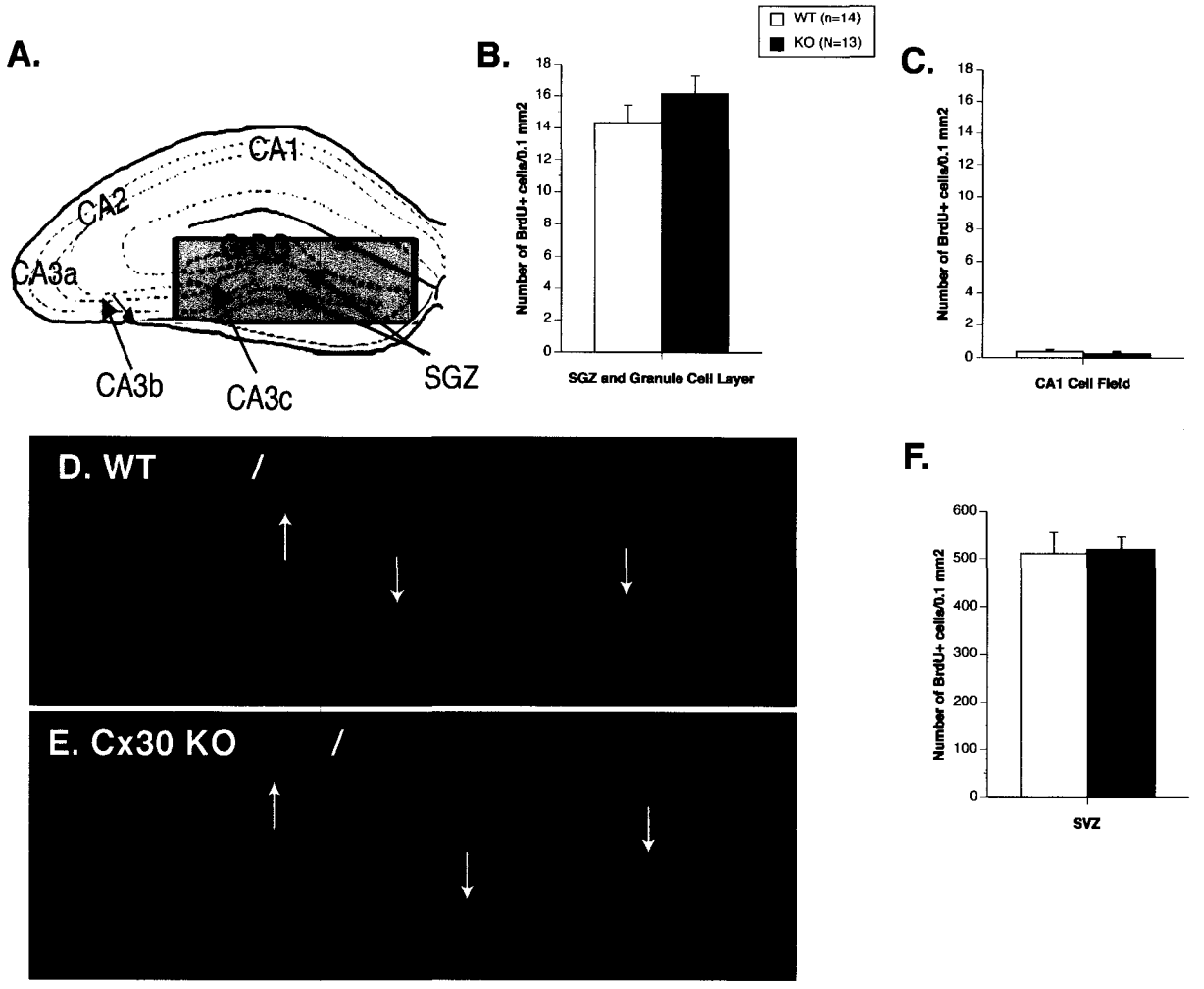
A.
CA1
CA2
CA3a
CA3b
CA3c
SGZ
B.
WT (n=14)
KO (N=13)
Number of BrdU+ cells/0.1 mm2
SGZ and Granule Cell Layer
C.
Number of BrdU+ cells/0.1 mm2
CA1 Cell Field
D. WT
E. Cx30 KO
F.
Number of BrdU+ cells/0.1 mm2
SVZ

**Figure 3.1**

**Figure 3.2 Cx30 null-mutant mice have a higher percentage of proliferating nestin$^+$ (Type C/2a) NPCs in the SVZ and the SGZ.** There is an increase in the percentage of proliferating nestin$^+$ Type 2a/ C cells in both neurogenic regions of the adult Cx30 null-mutant mouse brain reaching statistical significance in the SVZ (B), with a similar trend in the SGZ (A). (Student's *t*-test,*$p < 0.05$). Schematic of the forebrain is presented localizing the SVZ (red) with the box representing location of photomicrographs in F and G (C). Representative photomicrographs of the DG (D,E) and SVZ (F,G) with corresponding cell marker expression are presented. Arrows indicate nestin$^+$ BrdU$^+$ cells. Scale bars, 50 μm. Inset scale bars, 25 μm. Schematic of the hippocampal formation with the box representing the location of the photomicrographs in D and E (H). All abbreviations are as in Figure 2.1 and 2.2.

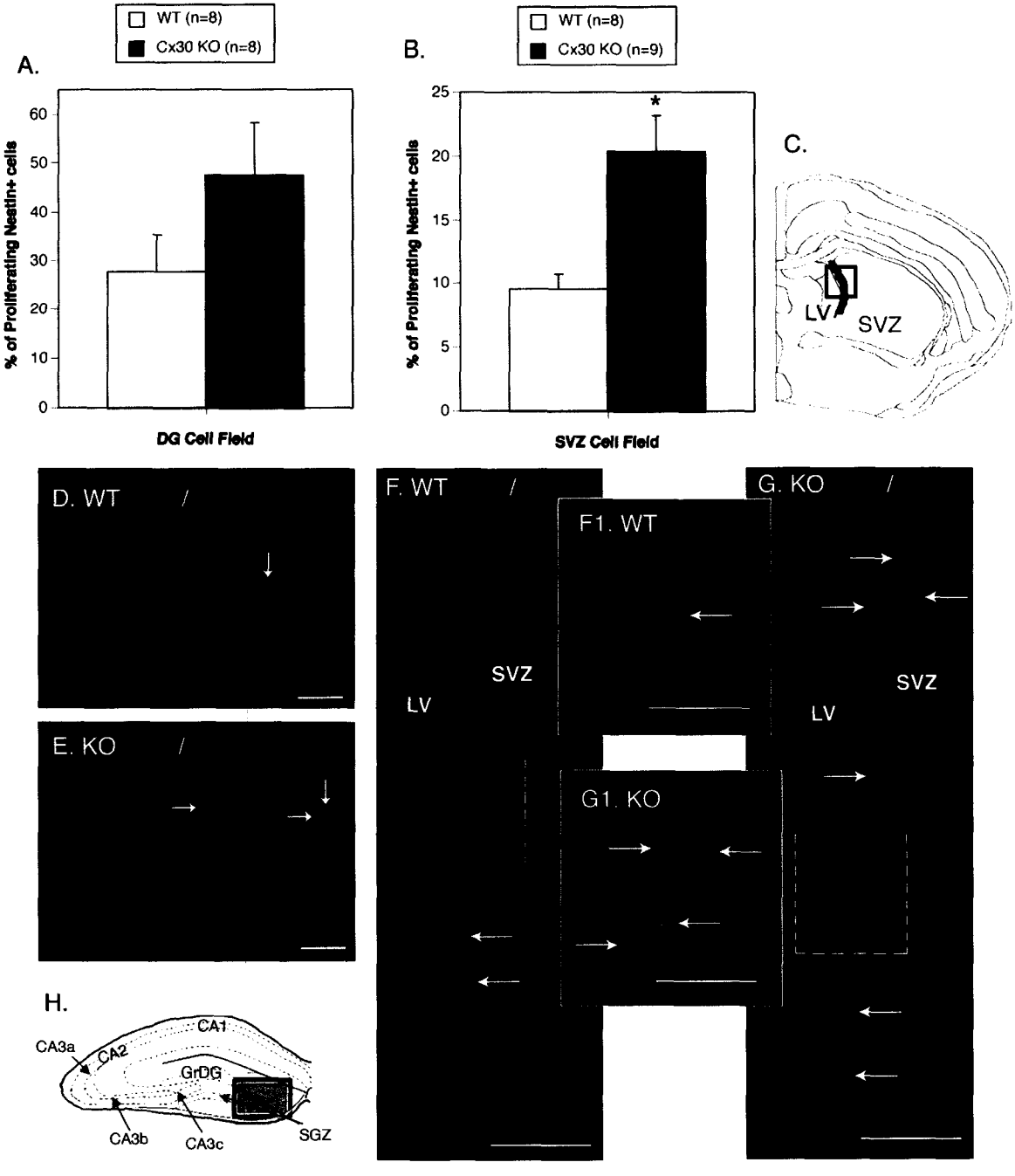
A.
WT (n=8)
Cx30 KO (n=8)
% of Proliferating Nestin+ cells
DG Cell Field
B.
WT (n=8)
Cx30 KO (n=9)
% of Proliferating Nestin+ cells
SVZ Cell Field
C.
LV
SVZ
D. WT
E. KO
F. WT
F1. WT
SVZ
LV
G. KO
G1. KO
SVZ
LV
H.
CA1
CA3a
CA2
GrDG
CA3b
CA3c
SGZ

**Figure 3.2**

47.7 % +/- 10.4 % while WT mice had 27.7% +/- 7.4 % (Figure 3.2, A). Similarly in the SVZ, the percentage of proliferating NPCs in the KO mice was 20.4 % +/- 2.8 % which is significantly greater than WT mice with 9.5 % +/- 1.2 % (Student *t*-test, $p<0.05$) (Figure 3.2, B). Representative digital photomicrographs of this increase in nestin$^+$ BrdU$^+$ double-labelled cells in the DG and SVZ of Cx30 KO mice are depicted in Figure 3.2.

### 3.3.3 Cx30 null-mutant mice have a lower percentage of proliferating DCX$^+$ (type A/2b and 3) early neuronal progenitor cells in the SVZ and the SGZ.

The percentage of proliferating early neuronal (DCX$^+$) progenitors was measured in both brain regions in 10 WT and 10 Cx30 KO mice. The number of DCX$^+$ cells per cell field was comparable in both the DG and SVZ for both the WT and KO mice (data not shown). However, a significant decrease in the percentage of proliferating early neuronal progenitors (DCX$^+$BrdU$^+$ cells) in the DG and SVZ of Cx30 null-mutant mice was detected (Figure 3.3). In WT DG, 21.9 % +/- 5.1% of DCX$^+$ progenitor cells were actively proliferating as compared to 10.2 % +/- 3.1 % in KO mice (Student's *t*-test, $p<0.05$) (Figure 3.3, B). Similarly in the SVZ, more DCX$^+$ progenitors were actively proliferating in WT mice compared to KO mice with WT mice having 32.1 % +/- 3.1 % versus KO mice with 16.6 % +/- 7.6 %. (Student's *t*-test, $p < 0.05$) (Figure 3.3, C). Representative photomicrographs illustrate the significant reduction of DCX$^+$BrdU$^+$ cells in Cx30 null-mutant mice in both regions (Figure 3.3, E, F, G, H ).

background (N3 generation) were compared to 14 WT littermates (N3 generation). WT mouse had 14.35 +/- 1.09 $BrdU^+$ cells per 0.1 $mm^2$ while Cx30 KO mice had 16.15 +/- 1.12 $BrdU^+$ cells per 0.1 $mm^2$. Thus, no statistically significant difference was observed in the number of $BrdU^+$ cells found in the dorsal DG (Figure 3.1, B). There was also no difference in BrdU incorporation in the CA1 pyramidal cell field (bioavailability control) (Figure 3.1, C), indicating that the BrdU bioavailability in the hippocampus is equivalent between WT and KO mice. BrdU cell proliferation was comparable in the SVZ (bregma 1.10 mm to 0.5 mm). WT mice had 510.71 +/- 44 $BrdU^+$ cells per 0.1 $mm^2$ in the SVZ which is comparable to the KO mice with 519.94 +/- 26 $BrdU^+$ cells per 0.1 $mm^2$ (Figure 3.1, F).

### 3.3.2 Cx30 null-mutant mice have a higher percentage of proliferating $Nestin^+$ (type B and C/1 and 2a) NPCs in the SVZ and the SGZ.

Although total cell proliferation in WT and KO mice was found to be the same, the identity of these proliferating cells was not known. Hence, the percentage of proliferating $nestin^+$ NPCs was assessed in the DG and SVZ of both WT and KO mice. Double-labelling for BrdU and nestin was performed to identify Type B and C/ 1 and 2a NPC subsets. The number of cells dually expressing nestin and BrdU was measured and divided by the total number of $BrdU^+$ cells in each brain region and for each genotype. We found that Cx30 null-mutation did not alter the total number of $nestin^+$ NPCs in both the DG and SVZ (data not shown). However, in both the DG and SVZ, the percentage of proliferating NPCs ($nestin^+/BrdU^+$ co-labeled cells) increased in Cx30 KO mice as compared to WT mice (Figure 3.2, A, B). In the DG, the percentage of proliferating NPCs for Cx30 KO mice was

**Figure 3.3 Cx30 null-mutant mice have a lower percentage of proliferating $DCX^+$ (Type A/3) early neuronal progenitor cells in the SVZ and the SGZ.** Schematic of the hippocampal formation with the box representing the location of the photomicrographs in E and F (A). There is a decrease in the percentage of proliferating $DCX^+$ Type 2b and 3/ A early neuronal progenitor cells in both neurogenic regions in adult Cx30 null-mutant mouse brain, SGZ (B) and SVZ (C). Schematic of the forebrain is presented localizing the SVZ (red) with the box representing location of photomicrographs in G and H (D). Representative photomicrographs of each neurogenic region and genotype with DCX and BrdU immunolabelling (E-H). Arrows indicate $DCX^+BrdU^+$ cells. Scale bars (E, E1, F), 50 μm. Inset scale bars (G1, H1), 25 μm. (Student's *t*-test,*$p < 0.05$). All abbreviations are as in Figure 2.1 and 2.2.

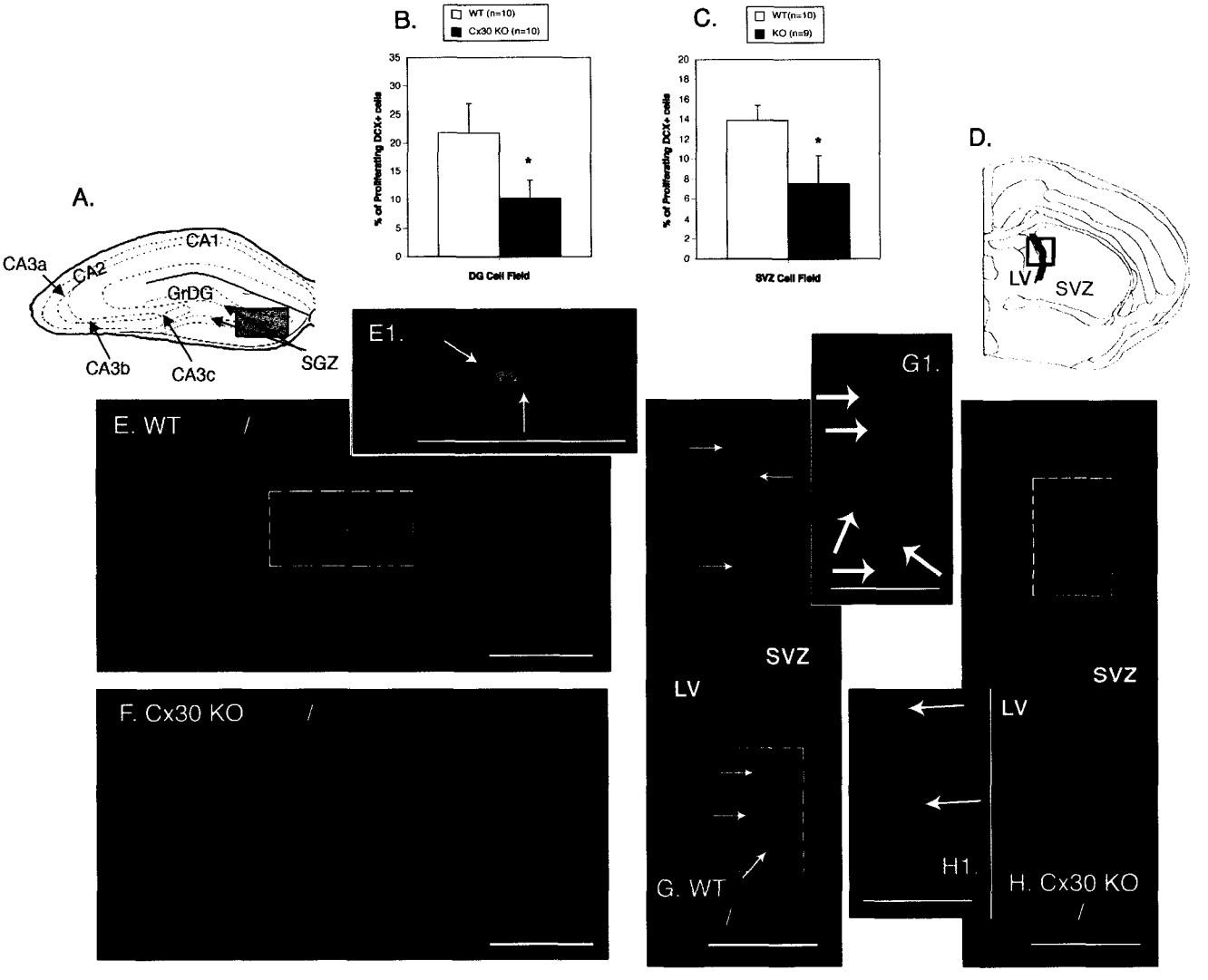
A.
CA1
CA3a
CA2
GrDG
CA3b
CA3c
SGZ
B.
WT (n=10)
Cx30 KO (n=10)
% of Proliferating DCX+ cells
DG Cell Field
C.
WT(n=10)
KO (n=9)
% of Proliferating DCX+ cells
SVZ Cell Field
D.
LV
SVZ
E1.
E. WT
F. Cx30 KO
G1.
SVZ
LV
G. WT
H1.
LV
SVZ
H. Cx30 KO

**Figure 3.3**

### 3.3.4 There is no change in the percentage of proliferating $NG2^+$ glial progenitor cells in the SGZ and SVZ between Cx30 null-mutant mice and WT mice.

The percentage of proliferating glial progenitors was also assessed and detected by the surface proteoglycan marker, NG2. The number of $NG2^+$ cells per cell field was comparable in both brain regions between WT and KO mice (data not shown). In the DG, the percentage of proliferating glial progenitors ($NG2^+BrdU^+$ cells) was 3.5 % +/- 2.1 % in Cx30 KO mice statistically comparable to the percentage in WT mice with 4.0 % +/- 2.0% (Figure 3.4, B). In the SVZ, the percentages of proliferating glial progenitors was also similar with KO mice at 0.9 % +/- 0.9 % and WT mice at 1.2 % +/- 0.8% (Figure 3.4, C). Since there was no difference in the percentage of proliferating glial progenitor cells, proliferative indices for astrocytes ($GFAP^+$), oligodendrocyte progenitors ($PDGF\alpha R^+$), and mature oligodendrocytes ($RIP^+$, $CNPase^+$) were not investigated further.

### 3.3.5 No significant difference was observed in the survival of $BrdU^+$ proliferating cells, 14 days and 28 days post BrdU injection retained in the SVZ or present throughout the granule cell layer of the SGZ.

The number of BrdU labelled cells in both neurogenic regions was assessed 1, 14, and 28 days after the last BrdU injection. In the DG of both WT and KO mice, total $BrdU^+$ cell number declined significantly over the 14 and 28 day timepoint. WT mice was found to have 14.3 $BrdU^+$ cells per 0.1 $mm^2$ one day post-BrdU injection which dropped considerably 14 days post BrdU injection and 28 days post-BrdU injection with 4.8 and 2.7 $BrdU^+$ cells per 0.1 $mm^2$, respectively (Figure 3.5, A). Cx30 KO mice show a similar trend with 16.2 $BrdU^+$

**Figure 3.4 There is no difference in the percentage of proliferating $NG2^+$ glial progenitor cells in the SGZ and SVZ between Cx30 null-mutant mice and WT mice.** Schematic of the hippocampal formation with the box representing the location of the photomicrographs in E and F (A). There is no change in the percentage of proliferating $NG2^+$ glial progenitor cells in both neurogenic regions in adult Cx30 null-mutant mouse brain, SGZ (B) and SVZ (C). Schematic of the forebrain is presented localizing the SVZ (red) with the box representing location of photomicrographs in G and H (D). Representative photomicrographs of each neurogenic region and genotype with NG2 and BrdU immunolabeling (E-H). Arrows indicate $NG2^+BrdU^+$ cells. Scale bars, 50 μm. Inset scale bars, 25 μm. All abbreviations are as in Figure 2.1 and 2.2.

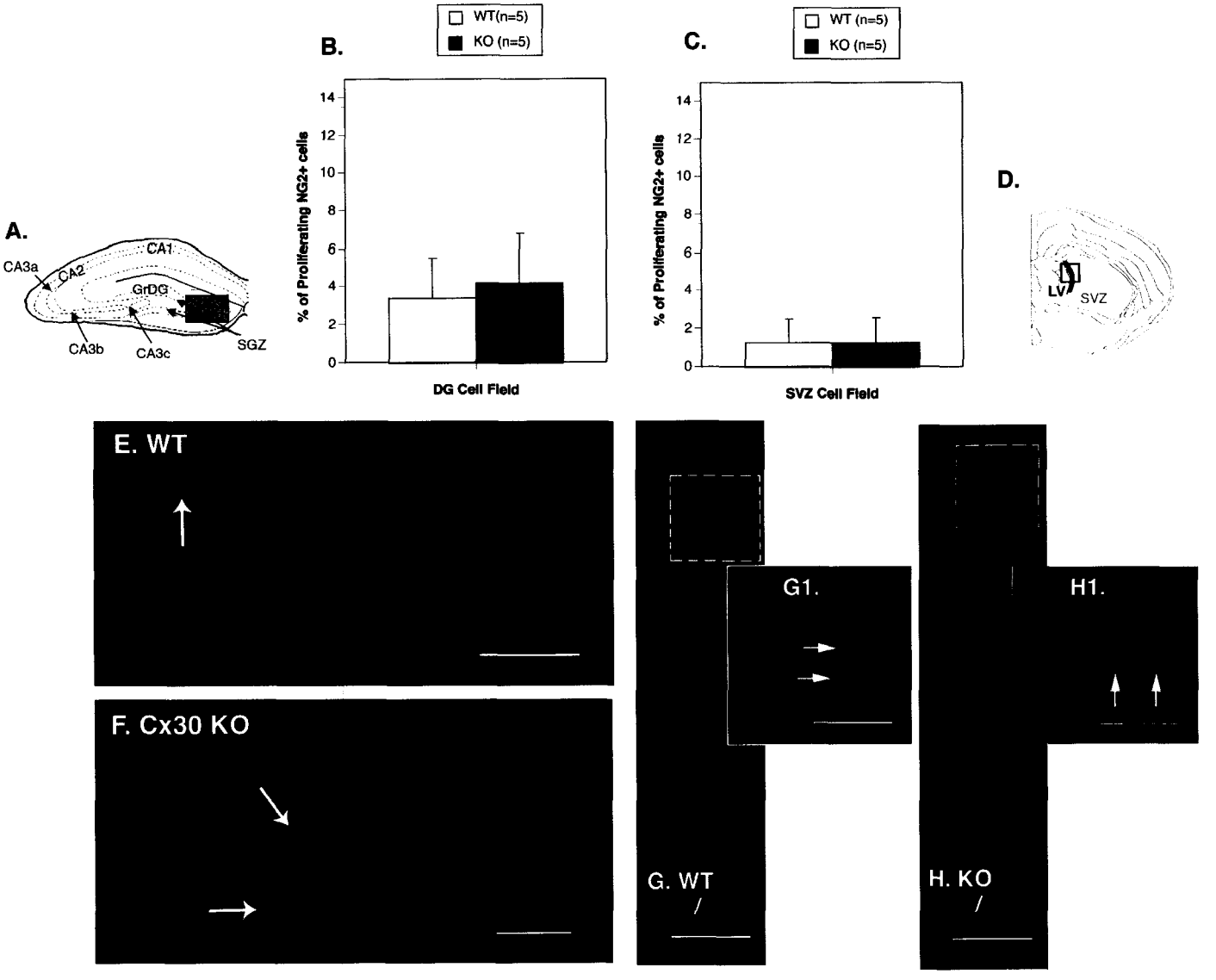
A.
CA1
CA3a
CA2
GrDG
CA3b
CA3c
SGZ
B.
WT(n=5)
KO (n=5)
% of Proliferating NG2+ cells
DG Cell Field
C.
WT (n=5)
KO (n=5)
% of Proliferating NG2+ cells
SVZ Cell Field
D.
LV
SVZ
E. WT
F. Cx30 KO
G1.
H1.
G. WT
H. KO

**Figure 3.4**

cells per 0.1 $mm^2$ and a decrease in cell number to 7.7 and 2.9 $BrdU^+$ cells over 14 days and 28 days post BrdU injection, respectively. Over the 28 day survival period, both WT and KO mice showed an 81% reduction in BrdU numbers.

While investigating the SVZ over the course of 1, 14, and 28 day(s) post BrdU injection, similar trends found in the DG were observed. Both WT and KO mice showed a significant reduction in the number of $BrdU^+$ proliferating cells 14 and 28 days post BrdU injection when compared to the 1 day time point. After one day, WT and KO mice had comparable values for the number of $BrdU^+$ cells per 0.1 $mm^2$ in the SVZ with 510.7 and 519.9 BrdU+ cells, respectively (Figure 3.1, F). At the day 14 timepoint, WT and KO mice also had comparable BrdU numbers with 47.9 and 45.4, respectively. This shows a reduction in 14 day survival by 90% for WT and 91% for KO mice. When the BrdU cell number was determined 28 days post BrdU injection, KO mice showed a slight increase in the number of $BrdU^+$ cells per 0.1 $mm^2$ in the SVZ with 21.1 +/- 5.3 compared to WT mice with 12.9 +/- 4.0 albeit not significant (Figure 3.5, B). However, the percent survival for 28 days demonstrates similar proportions with 2.5% for WT and 4.1% for KO mice. Together, these data suggest that Cx30 null-mutation does not impact upon the retention or survival of Type B and C cells generated in the SVZ.

### 3.3.6 Cx30 null-mutant mice have more $BrdU^+$ cells in the RMS and the OB over the course of 1, 14, and 28 day(s) post BrdU injection.

Because Cx30 null-mutation enhances the proliferative index of Type B and C NPCs (Figure 3.2) but expansion of this pool does not impact on the total number of proliferating

**Figure 3.5 Survival of $BrdU^+$ cells, 1, 14, and 28 day(s) post BrdU injection.** Labelled cell number was quantified 1, 14, and 28 days after the last BrdU injection in coronal sections as described in Materials and Methods. The number of surviving $BrdU^+$ cells per 0.1 $mm^2$ markedly decreased within 14 days and 28 days after last BrdU injection in the SGZ (A), and the SVZ (B) region in WT and $Cx30^{(-/-)}$ adult mouse brain. When Cx30 null-mutant mice are compared to time course matched WT mice, there is no statistical difference in the number of $BrdU^+$ cells surviving in either the SGZ, or the SVZ between genotypes.

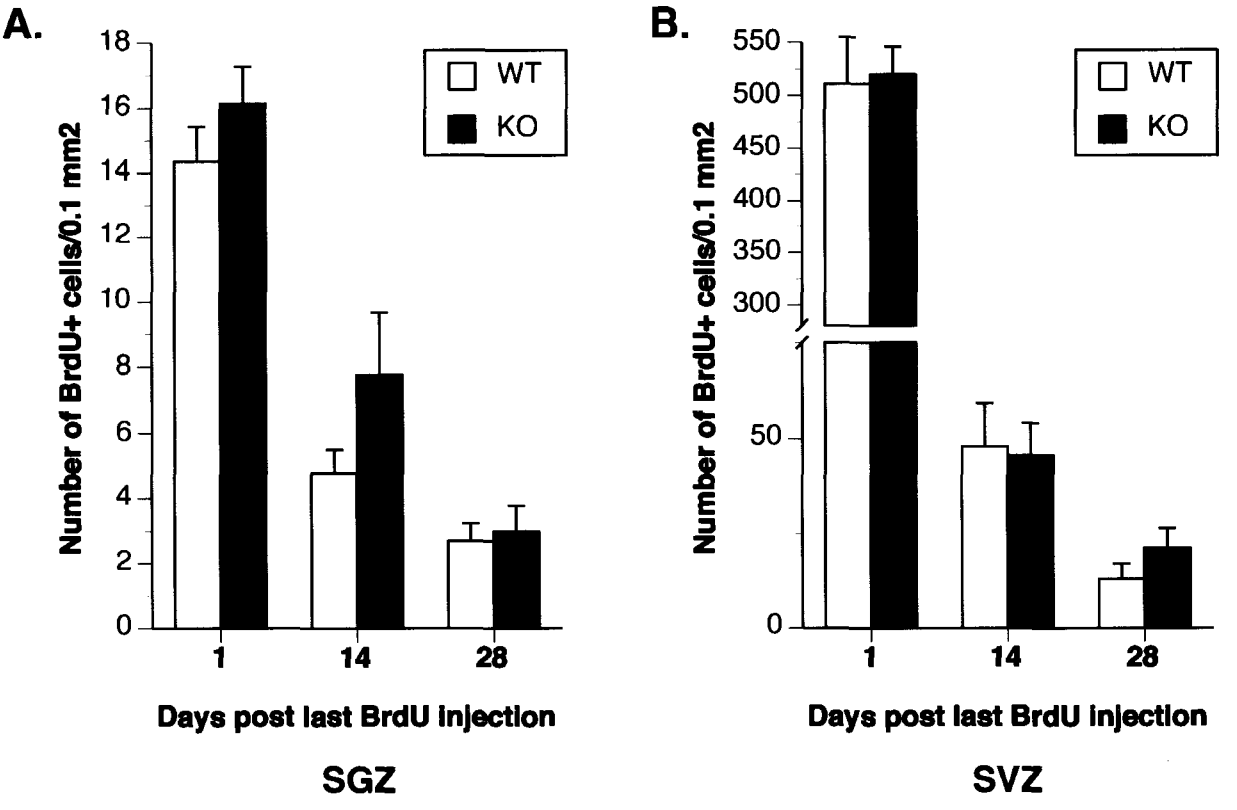
A.
Number of BrdU+ cells/0.1 mm2
18
16
14
12
10
8
6
4
2
0
WT
KO
1
14
28
Days post last BrdU injection
SGZ
B.
Number of BrdU+ cells/0.1 mm2
550
500
450
400
350
300
50
0
WT
KO
1
14
28
Days post last BrdU injection
SVZ

Figure 3.5

cells retained in the SVZ (Figure 3.1 and 3.5), labelled progeny have likely either migrated from their origin or are deleted soon after birth. To distinguish between these possibilities, we followed the fate of BrdU-labelled cells throughout the SVZ, RMS, and OB in sagittal sections. The number of $BrdU^+$ cells per 0.1 $mm^2$ was measured in each region at 1, 14, and 28 day(s) after last BrdU injection. One day after a series of 5 BrdU injections, Cx30 null-mutant mice exhibited a statistically significant increase in $BrdU^+$ cells per 0.1 $mm^2$ in the RMS with 476.35 +/- 64.74 compared to WT mice with 219.43 +/- 27.21 (Student's t test, ** $p < 0.01$; Figure 3.6, A). Similarly for the 14 and 28 day post BrdU injection time points, KO mice had an augmented $BrdU^+$ cell number per 0.1 $mm^2$ in the RMS: KO mice had 145.99 +/- 49.54 compared to WT mice with 24.43 +/- 10.95 after 14 days while KO mice had 27.63 +/- 2.65 $BrdU^+$ cells compared to WT mice with 11.72 +/- 1.98 after 28 days (Mann-Whitney test, + $p < 0.05$; Figure 3.6, A). Together, these data suggest that the expanded pool of Type B and C BrdU-labelled cells (Figure 3.2) rapidly migrated into the RMS (Figure 3.6). Since BrdU is not readily detected once cells have undergone three sequential divisions due to dilution of the label in progeny, it is less likely, (although still possible), that loss of Cx30 accelerates cell division over the course of migration as label would likely be below limits of detection in rapidly dividing cells over the course of the 28 day observation period.

To further test this hypothesis, the number of $BrdU^+$ cells per field in the OB was measured in both WT and Cx30 null-mutant mice. In appropriate sagittal sections, Cx30 null-mutant mice exhibited more $BrdU^+$ cells per OB field then WT mice at both the 14 and 28 day time points (few $BrdU^+$ cells were detected one day after last BrdU injection, data not shown) suggesting the progeny of proliferating Type B and C cells in the SVZ migrated

to the OB and survived more effectively in the absence of Cx30. After 14 days post BrdU injection, Cx30 null-mutant mice had more $BrdU^+$ cells with 53.06 +/- 9.19 compared to WT mice with 20.50 +/- 1.75 (Mann-Whitney test, + $p < 0.05$; Figure 3.6, B). Likewise after 28 days post BrdU injection, the number of $BrdU^+$ cells per OB field was enhanced in Cx30 null-mutant mice with 44.98 +/- 6.96 compared to WT mice with 20.85 +/- 2.18 (Mann-Whitney test, + $p < 0.05$; Figure 3.6, B). Representative photomicrographs of increased $BrdU^+$ cells per area in the RMS are illustrated in Figure 3.6, C, D.

### 3.3.7 The percentage of neurogenesis in the OB is equivalent between WT and Cx30 null-mutant mice.

To determine the extent of terminal neuronal fate of NPCs in the SVZ-RMS-OB neurogenic tract, sagittal sections of both WT and Cx30 null-mutant mice were double immunolabelled with NeuN and BrdU, and the percentage of neurogenesis (the percentage of $NeuN^+$ $BrdU^+$ cells relative to total $BrdU^+$ cells) was calculated per OB field. Interestingly, after 14 days post BrdU injection, the percentage of neurogenesis, as defined above, was equivalent between WT and Cx30 null-mutant mice with 49.58 +/- 3.06% and 45.66 +/- 1.05%, respectively (Figure 3.6, E). Likewise, at the 28 day time point, the percentage of neurogenesis was the same for both WT and Cx30 null-mutant mice OB fields with 45.79 +/- 4.23% and 45.77 +/- 0.39% , respectively (Figure 3.6, E).

**Figure 3.6 Impact of Cx30 null-mutation on NPC migration to, and percent neurogenesis in, the OB 14 and 28 days post BrdU injection.** The extent of NPC migration was assessed by measuring the number of $BrdU^+$ cells per 0.1 $mm^2$ in the RMS in sagittal sections from the appropriate interaural region (A). There is a statistically significant increase in the number of $BrdU^+$ cells observed in the RMS of Cx30 null-mutant mice in all time points (1 d, 14 d, 28 d post BrdU injection). Representative photomicrographs of sagittal RMS regions (outlined in white) in both WT and KO mice illustrating the increase in $BrdU^+$ cell number in KO mice (C, D). $BrdU^+$ cells are green and indicated with arrows while $NeuN^+$ cells are labelled red. The number of $BrdU^+$ cells per field in the OB was significantly augmented in Cx30 null-mutant mice both 14 d, and 28 d after the last BrdU injection (1 day time point, data not shown) (B). The neurogenic fate of $BrdU^+$ cells in the OB, measured as the percentage of $NeuN^+$ $BrdU^+$ cells, was found to be similar between WT and Cx30 null-mutant mice (E) (Mann-Whitney test; +, $p < 0.05$). Scale bars, 500 μm.

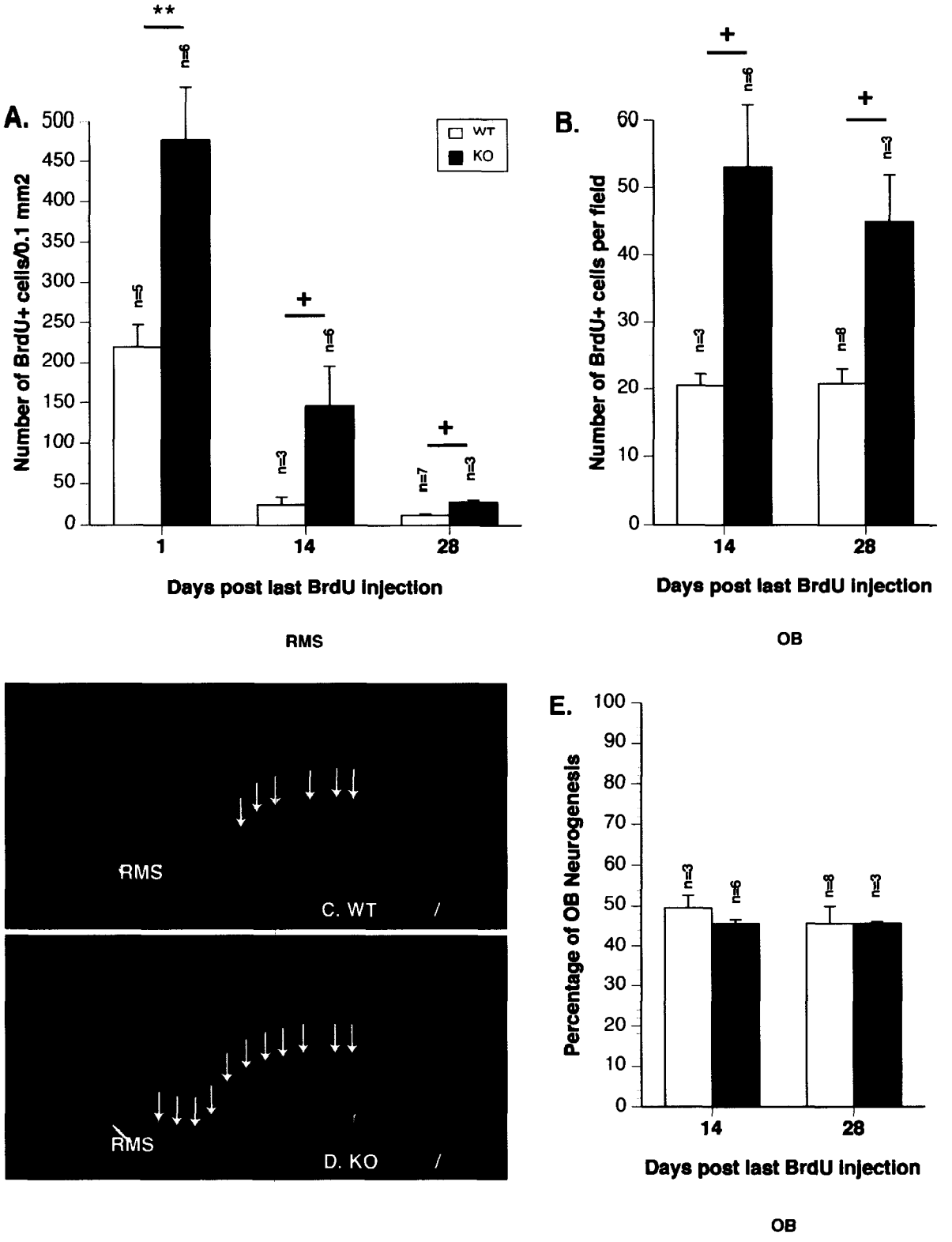
A.
Number of BrdU+ cells/0.1 mm2
WT
KO
**
+
+
n=5
n=6
n=3
n=6
n=7
n=3
1
14
28
Days post last BrdU injection
RMS
B.
Number of BrdU+ cells per field
+
+
n=3
n=6
n=8
n=3
14
28
Days post last BrdU injection
OB
RMS
C. WT
RMS
D. KO
E.
Percentage of OB Neurogenesis
n=3
n=6
n=8
n=3
14
28
Days post last BrdU injection
OB

Figure 3.6

### 3.4 Discussion

Here, evidence is presented for the first time demonstrating that early NPCs (Type 1 and 2a in the SGZ and Type B and C in the SVZ) express Cx30. Using a loss of function approach, we show that null-mutation enhances proliferation of Type B and C NPCs in both the SGZ and SVZ, but does not result in an expansion of this pool at this origin. Rather, in the SVZ, labelled progeny migrate through RMS reaching the OB yet fail to terminally differentiate to neurons. Although survival of NPC progeny is enhanced in the absence of Cx30, these cells do not generate new neurons. Moreover, because adult neurogenesis is comparable between WT and Cx30 $^{(-/-)}$ mice in the OB, these data further suggest that the Cx30 is required for some, but not all, early NPCs to commit to a neuronal lineage and may be more important to ensure the deletion of excess progeny who have not achieved appropriate lineage throughout the migration process than the specification of developing neurons.

To ensure that the increase in proliferating Type 1, 2a, B, and C NPCs was not due to enhanced BrdU bioavailability in Cx30 null-mutant mice, a number of controls were performed. BrdU was used to identify proliferating cells in adult male N3 Cx30 null-mutant and N3 congenically matched WT mice. Congenicity is essential as strain difference in vasculature unrelated to the gene of interest could impact upon BrdU passage through the blood brain barrier. BrdU is a thymidine analog that has been used extensively as a proliferating cell marker in adult neurogenesis. The standard method consists of pulse injection of BrdU in the intraperitoneal cavity and immunohistochemistry to detect the fate of dividing cells and their progeny (Kee et al., 2002). The number of cells labelled with

BrdU is dependent on its bioavailability (half life 2 hours) and its specific characteristic to label cells only entering S phase (Gilbert et al., 2005). Using this technique, we found no difference in the number of actively proliferating cells in the Cx30 null-mutant mice as compared to WT mice in the DG along with no significant change in the SVZ. The bioavailability control showed no difference in BrdU incorporation in the essentially post-mitotic CA1 pyramidal cell field demonstrating that comparable amounts of BrdU passed the blood brain barrier in both genotypes (Melanson-Drapeau et al., 2003).

The DG is reported to contain NPCs with a finite proliferative potential albeit with some controversy while the SVZ contains NPCs and putative neural stem cells with unlimited proliferative potential (Doetsch, 2003; Gage, 2000; Seaberg et al., 2005). It is likely, even probable, that different niche signals are paramount in the DG and SVZ. Furthermore, anatomical differences between the two niches are likely manifested in the different combination of connexins that form channels and receive correct proliferative signals. We have yet to identify the repertoire of connexins expressed in the SVZ and have only begun to do so in the DG to test this hypothesis. It would be of great interest to establish whether other astrocytic connexins are differentially expressed (Cx26, Cx30, Cx43) (Dahl et al., 1996; Rash et al., 2001) in these two areas that may, in part, provide further insight into underlying mechanisms with respect to instructive cell populations responsible for the observed NPC phenotype following Cx30 null-mutation.

Although both areas measured coronally showed no difference in the number of $BrdU^+$ cells, both areas exhibited an increase in the percentage of BrdU-labelled $nestin^+$ cells and a decrease in the number of BrdU-labelled $DCX^+$ cells. No change in glial progenitor

cell proliferative ($NG2^+BrdU^+$ cells) response was observed. Thus, while the total number of $nestin^+$ and $DCX^+$ NPCs remains constant, loss of Cx30 increases the percentage of $nestin^+$ NPCs that are actively proliferating and decreases the number of neuronally committed intermediate progeny actively expanding. The percentage of proliferating $DCX^+$ cells in the adult WT mouse hippocampus has been previously measured at 20 % which is comparable to 22 % observed in this study (Plumpe et al., 2006). When congenically matched Cx30 null-mutant mice are compared, this percentage is nearly halved in both neurogenic niches. Conversely, there is enhanced percentage of proliferating $nestin^+$ cells in Cx30 null-mutant mice. Taken together, these data suggest that in the absence of Cx30, $nestin^+$ NPCs remain in a hyperproliferative state and fail to specify further towards a neuronal lineage. Yet we did not detect an increase in the total number of progenitor cells within the neurogenic niches. To address this disconnect, we evaluated migrating cell number from the originating niche. In SVZ-derived cells, we found that the excess Type B and C progeny migrated successfully to the OB, but failed to generate mature neurons. We have yet to establish the identity of these cells retained in the OB 28 days after the last BrdU injection.

These data lead me to speculate on several potential mechanisms. Cx30 expressed by astrocytes could be required to form functional gap junctions with $DCX^+$ neuronal progenitors. Consequently, loss of Cx30 inhibits the expansion of $DCX^+$ cells while $nestin^+$ progenitors hyperproliferate or stay longer in a proliferative phase to overcome this defect. Also, Cx30-mediated communication may be required for proliferating $nestin^+$ NPCs to transiently step out of the cell cycle in order for progeny to specify to a subset of proliferating $DCX^+$ progenitors and thus fail to progress through the developmental checkpoints required to complete neurogenesis.

Surprisingly, loss of Cx30 did not impair upon migration and may have even enhanced RMS NPC migration. Based on previous studies indicating that other astrocyte specific connexin subunits , Cx26, and Cx43, are required for proper neuronal migration during prenatal neocortical development (Elias et al., 2007), we had predicted that migration towards the OB might be impaired. Since Cx30 is only expressed postnatally, it may have a prominent role in regulating adult neurogenesis by providing the appropriate contact points for NPC migration (Dahl et al., 1996; Nagy et al., 1999). However, this hypothesis was not supported by our analysis of BrdU-labelled cell number along the RMS and in OB 14 and 28 days after last BrdU injection.

We have yet to determine the fate of these excess BrdU-labelled SVZ cells that migrate along the RMS. When the number and fate of $BrdU^+$ cells in the OB was measured after 14 days post BrdU injection, the number of $BrdU^+$ cells was enhanced in KO mice, but the percentage of neurogenesis ($BrdU^+$ $NeuN^+$ cells) was similar at 49.58 % for WT mice and 45.66 % for Cx30 null-mutant mice. These data suggest that while Cx30-mediated communication impacts upon early NPC proliferation and may promote transition to the next developmental stage of a subset of these cells, it is not necessary for migration or proper neuronal specification of cells that have achieved the appropriate lineage by the time they reach the OB. Looking at the 28 day post BrdU injection time point, similar results like those seen in the 14 day time point were observed. This further supports the notion that Cx30 may play a role forming early adhesive contacts needed for proper initial specification, but does not play a significant role in end stage specification at the level of the OB wherein cells, primarily Type A, are adopting a neuronal lineage. Moreover, Cx30 appears to refine neurogenesis within the originating niche (SVZ) but is not necessary or sufficient *in vivo* to

abrogate neurogenesis indicated by comparable neuronal replacement in the OB of WT and null-mutant animals. This proposes a possible mechanism of action whereby the loss of Cx30 and the decreased specification at the early section of the RMS (proximal to the SVZ region) is compensated by the increased number of NPCs migrating along the RMS thereby increasing the number of $BrdU^+$ cells at the OB. The increased migration of $BrdU^+$ NPCs seen in Cx30 KO mice coupled with equivalent percentages of neurogenesis at the level of the OB may functionally counteract early diminished neuronal specification observed in the SVZ. The reasoning for variable region specific roles for Cx30 may be attributed to its spatial expression, altered cell type expression, and/or different gap junction composition. It will be essential to identify the lineage of the excess cells in the OB, their connexin profile, and the impact of their presence on OB function.

## Chapter 4: SVZ-derived astrocytes expressing Cx30 direct postnatal NPCs toward a neuronal lineage *in vitro.*

### 4.1 Introduction.

There is growing evidence indicating that the passage of ions, metabolites, and secondary messengers between cells via connexin-mediated gap junctions alters NPC fate (Bittman and LoTurco, 1999; Nadarajah et al., 1998; Rozental et al., 1998). Astrocyte specific Cx43 has been extensively investigated and shown to be involved in prenatal neocorticogenesis by providing both intercellular signals and adhesive contacts to migrating progenitor cells (Belliveau et al., 1991; Elias et al., 2007; Matsumoto et al., 1991). In the postnatal mouse, two different research groups have shown that astrocytes grown from either neurogenic region can direct co-cultured NPCs toward a neuronal fate (Lim and Alvarez-Buylla, 1999; Song et al., 2002). Taken together, the highly coupled astrocyte appears to play a part in directing NPC fate both prenatally and postnatally. Thus, based on the postnatal expression pattern of Cx30 and its localization to both astrocytes and NPCs, Cx30 may play a significant role in postnatal neurogenic regulation. To assess whether astrocytic Cx30 is involved in NPC fate, the *in vitro* NSP model of neurogenesis was utilized to determine the intrinsic and extrinsic potential of NPCs. Here, we tested whether gap junction uncoupling impacts upon the capacity of astrocytes to "instruct" NSP-derived NPCs to adopt a neuronal lineage.

### 4.2 Materials and Methods.

#### 4.2.1 Differentiation of NSPs.

NSPs were isolated and grown in suspension for 8 DIV as described previously in Methods 2.2.4. On day 8, growth factors were removed from the NSP medium by gentle centrifugation and washes with 10 mM PBS. Free floating NSPs in suspension were transferred to 10 cm Petri dishes and plated on laminin (15 μg/ml)-coated glass coverslips. After one day of plating, the NSP media was replaced with maintenance media (DMEM/F12 containing 1 mM sodium pyruvate, 200 mM D-glucose, 1% penicillin/streptomycin, 2% N2 supplement). Half of the media was replaced every two days. After 6 DIV, plated NSPs were fixed in 4% formaldehyde for 15 min, washed with 10 mM PBS and immediately processed for immunocytochemistry.

### 4.2.2 Extraction and growth of astrocytes.

WT mice at the age of P7-P9 were sacrificed by lethal injection with sodium pentobarbital. Whole brains were dissected out and mounted for coronal sectioning. A Leica VT1000S vibratome was used to cut 500 μm coronal sections which were collected at the appropriate Bregma regions. With the use of a dissecting microscope and fine surgical instruments, the SVZ and DG were isolated. Tissue was minced with a scalpel and placed in dissociation media (26 mM $NaHCO_3$, 124 mM NaCl, 5 mM KCl, 0.1 mM $CaCl_2$-$2H_2O$, 3.2 mM $MgCl_2$-$6H_2O$, 10 mM D-glucose, 1% penicillin/streptomycin, 0.1% neural protease, 0.01% papain, 0.01% DNAse I) for 45 min at 37 °C on a clinical rotator. 10 mM PBS was added to mixture followed by mild tituration and gentle centrifugation for 5 min at 1500 rpm. Supernatant was removed, and washed again with 10 mM PBS. After the last PBS wash, cells were dispersed in astrocyte maintenance media (DMEM/F12, 10% FBS, 1% penicillin/streptomycin) and cell counts were determined with a trypan blue solution and a

hemacytometer. Cell suspensions were plated at 5.0 X $10^5$ cells per plate in a 10 cm Petri dish on poly-L-lysine (0.1 mg/ml poly-L-lysine in $ddH_2O$)-coated glass coverslips. Half of the media was replaced every three days until > 85% confluency was achieved 21 days after initial plating.

### 4.2.3 RT-PCR for Cx30 expression.

Astrocytes from specific neurogenic regions were grown for 21 DIV and total RNA was obtained via TRIzol extraction (Invitrogen, Carlsbad, California). SVZ and SGZ-derived NSPs were grown for 12 DIV as denoted earlier (Methods 2.2.2) and total RNA was also obtained via TRIzol extraction method. Total RNA solution was pre-treated with RQ1 DNAseI (Promega, Madison, WI) to remove residual genomic DNA. First-strand cDNA synthesis was performed using random hexamers (Promega) and Superscript II reverse transcriptase (RT) according to manufacturer's recommendations. The resulting random-primed cDNA template was used to perform polymerase chain reaction (PCR) with primers specific for the Cx30 (sense: 5'-GCCAGGGTGCAAGAACGTCTGC – 3', antisense: 5' – GGCATGGTTGGGTGGTTTCTC – 3') transcript and glyceraldehyde 3-phosphate dehydrogenase (GAPDH; sense: 5' - TGGTGCTGAGTATGTCGTGGAGT – 3' , antisense: 5' – AGTCTTCTGAGTGGCAGTGATGG – 3') transcript for standard control. The expected Cx30 transcript size is 535 base pair (bp) and the expected GAPDH transcript size is 292 bp. The following reagents were added to each PCR sample: 25 pmoles forward primer, 25 pmoles reverse primer, 5 µl of 10X PCR buffer, 4 µl of 10 mM deoxynucleotide triphosphates (dNTPs; Promega), 1 µl of Taq advantage DNA polymerase, and 2 µl of corresponding cDNA product (RT product). The PCR samples were brought up to a final

volume of 50 µl with nuclease free water and amplified in the Biometra T gradient PCR machine (Montreal Biotech Inc., Kirkland, PQ) using cycling protocol: 94°C for 5 min, 35 cycles of 94°C for 30 sec, 59°C for 60 sec, and 72°C for 1 min, and a final incubation at 72°C for 7 min.

### 4.2.4 Co-culture preparation and conditions.

NSPs were prepared, expanded and differentiated as described in Methods 4.2.1. Several differentiating conditions were analyzed. To assess spontaneous intrinsic NSP differentiation, NSPs were expanded in suspension for 8 DIV and then plated on laminin-coated glass coverslips in co-culture media (DMEM/F12 containing 1 mM sodium pyruvate, 200 mM D-glucose, 1% penicillin/streptomycin, 2% N2 supplement) for 6 days. Neuronal driving conditions were used as a control to determine the neurogenic potential of WT NSPs. These conditions entailed replacing media 24 h after plating with Neural basal media (Gibco, Invitrogen corporation) containing 0.5 µM retinoic acid (RA) and 20 ng/ml brain derived neurotrophic factor (BDNF) on laminin (15 µg/ml)-coated glass coverslips adhered to the bottom. The fate of NSPs in the presence of astrocytes was carried out by plating NSPs in 10 cm Petri dishes that contained confluent astrocytes on glass coverslips. The media was replaced with co-culture media after the first day of plating. To determine whether gap junctional mediated communication between astrocytes and NSPs played a significant role in NPC fate, cultures were incubated with the gap junction blocker 18 α-glycyrrhetinic acid (GRA, 100 µM) or its inactive analog glycyrrhizic acid (GZA, 100 µM ; GRA negative control).

### 4.2.5 BrdU labelling, immunocytochemistry, and NSP analysis.

To determine the fate of plated NSPs under various conditions, BrdU labelling was utilized to mark proliferating cells found in NSPs and to distinguish between NSP cells and co-cultured astrocytes. One day prior to NSP plating as described above in Methods 4.2.1, NSPs were incubated with BrdU (Roche Diagnostics, Laval, PQ; 20 μg/ml) for 24 hours at 37 °C. On the day of plating, the thymidine analog was removed by several 10 mM PBS washes and gentle centrifugation steps followed by a final dispersal of NSP pellet with appropriate co-culture media. Cells were placed in corresponding plating conditions (*i.e.* astrocyte monolayer) for 6 DIV before being processed for immunocytochemistry. Co-culture media (or neural basal media containing neurogenic factors) was removed and washed with 10 mM PBS followed by fixation with 4% formaldehyde in 10 mM PBS for 10 min. Samples were then washed for 15 min in 10 mM PBS and individual round glass coverslips were removed and placed in single plate wells (24 well plate). PBS solution was carefully removed followed by an hour incubation with 2 N HCl at 37°C. Subsequently, three 5 min washes with neutralization buffer (0.1 M borate buffer at pH 8.5) and three 5 min PBS washes were performed followed by overnight incubation at 4 °C with primary antibodies including either nestin (Chemicon, Temecula, CA; 1:25), tuj1 (1:100), GFAP (1:200), NG2 (Chemicon, Temecula, CA; 1:100), or RIP (1:50) and BrdU-Fitc (Cedarlane Laboratories Limited, Hornby, ON ; 1:50) diluted in Ab buffer. Samples were again washed three times for 5 min with 10 mM PBS followed by incubation with secondary antibodies at room temperature for one hour with Cy3-conjugated anti-mouse IgG (Jackson Immunoresearch; 1:400), or Cy3-conjugated anti-rabbit IgG (Jackson Immunoresearch; 1:200). Three 5 min PBS washes were performed. This was followed by the addition of

antifade for coverslipping. Samples were analyzed with epifluorescence on a Leica DMXRA2 microscope.

A total of three round glass coverslips were used for each antigenic marker-BrdU co-label per condition to increase the yield of plated and labelled NSPs. Since it was difficult to resolve individual cells in the NSP core, the fate of BrdU labelled cells was measured in the periphery of the NSP by the following procedure: the NSP core was determined initially under phase microscopy and then five random 40 X magnified microshots were taken 15 μm away from the defined core. Each microshot was used as an n=1 yielding an n=5 per NSP. The percentage of co-labelled antigenic marker$^+$ /BrdU$^+$ cells was measured and used to establish the fate of NSPs proliferating on the first day of plating under various conditions. For statistical analyses, data was analyzed using the GraphPad InStat statistics (GraphPad Software Inc.) program by an analysis of variance (ANOVA) followed by Tukey *post hoc* tests to identify conditions that were significantly different where applicable.

## 4.3 Results

### 4.3.1 Cx30 expression in SVZ derived-astrocytes and NSPs.

To determine whether SVZ and SGZ-derived NSPs and astrocytes expressed Cx30 capable of forming gap junctions, RT-PCR and immunocytochemistry were performed. RNA was isolated from cultured SVZ and SGZ-derived astrocytes after >85% confluency was achieved (21 DIV). Total RNA was also extracted from SGZ and SVZ-derived NSPs after 12 DIV. Total RNA was converted to cDNA via RT reaction outlined in Methods 4.2.3

**Figure 4.1 Cx30 expression in SVZ-derived astrocytes and NSPs.** RT-PCR demonstrating Cx30 expression in astrocytic cultures derived from the SVZ and SGZ (A), and SVZ-derived NSPs (A). Controls included reactions processed in the absence of template and reactions processed in the absence of RT product. Immunocytochemistry of SVZ-derived astrocytic cultures showing punctate Cx30 staining at the membrane of directly apposed cells and non-junctional membranes (B). Scale bar, 50 μm.

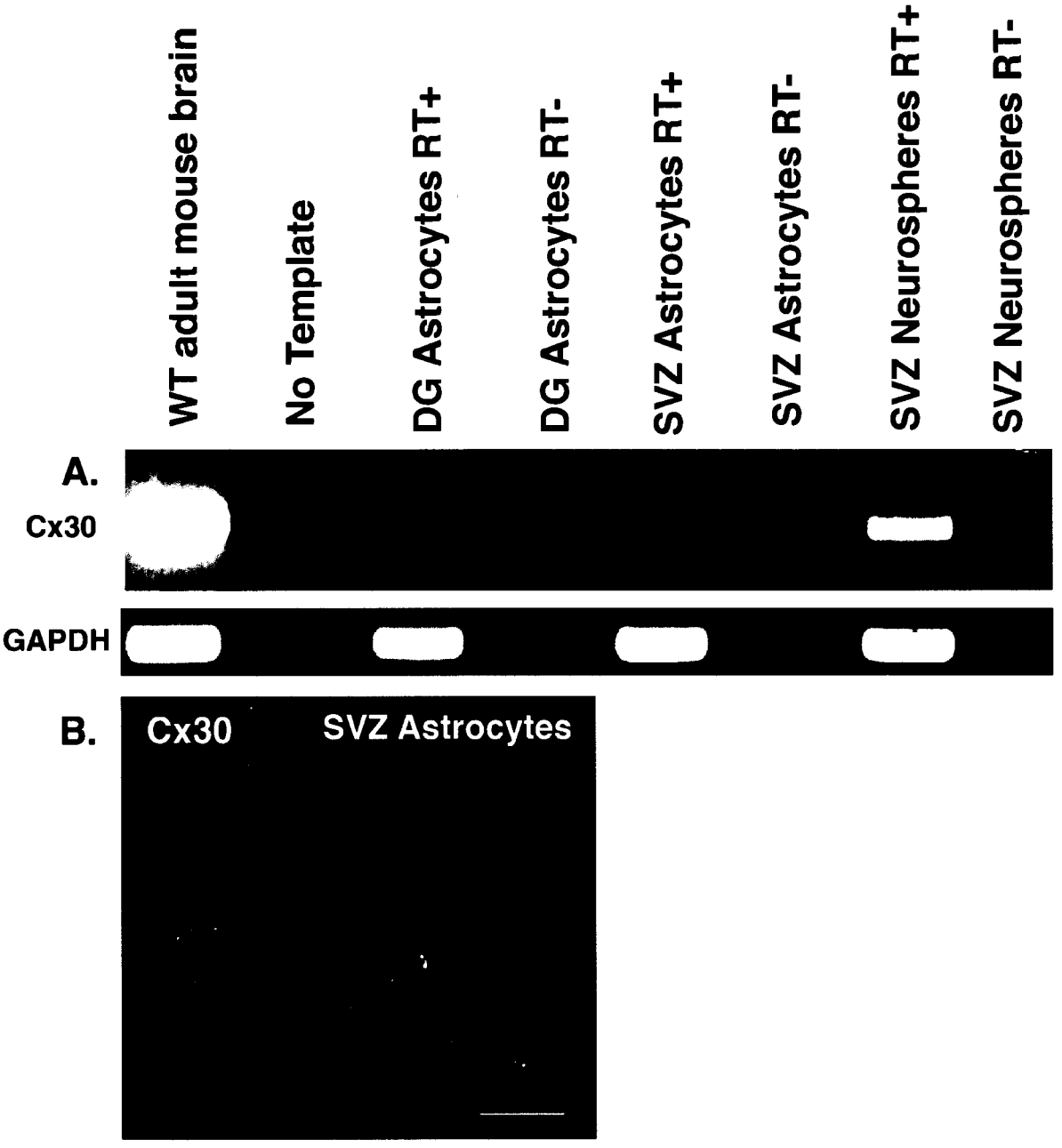
WT adult mouse brain
No Template
DG Astrocytes RT+
DG Astrocytes RT-
SVZ Astrocytes RT+
SVZ Astrocytes RT-
SVZ Neurospheres RT+
SVZ Neurospheres RT-
A.
Cx30
GAPDH
B.
Cx30
SVZ Astrocytes

Figure 4.1

and used to amplify transcripts via PCR. Although semi-quantitative, SVZ NSPs demonstrated the greatest expression of Cx30 relative to GAPDH and with respect to postnatal cell cultures, while SVZ-derived astrocytes exhibited slightly lower Cx30 expression followed by SGZ-derived astrocytes with very little Cx30 mRNA expression. Cx30 mRNA expression in SVZ-derived astrocytes has already been documented in our laboratory (Lianne Gauvin, M.Sc. thesis) and confirmed in this thesis at the protein level in Figure 2.4. Figure 4.1 shows the relative expression of WT adult mouse brain compared to cell culture samples for the SGZ and SVZ-derived astrocytes and SVZ-derived NSPs with appropriate standard loading controls using GAPDH. For Cx30 protein expression, immunocytochmeistry was performed on SGZ and SVZ-derived astrocytes and NSPs. Figure 4.1 demonstrates punctate Cx30 staining in cultured SVZ-derived astrocytes while Cx30 protein expression in SGZ and SVZ-derived NSPs was demonstrated previously in chapter 2 (Figure 2.4).

### 4.3.2 Role of co-culture in directing NPC fate *in vitro.*

After NSPs are expanded for 8 DIV with growth factors, BrdU was incubated for 24 hours one day prior to plating in various differentiating conditions. BrdU was added to label actively proliferating cells and thus identify mitotic cells that had adopted an alternative lineage in response to paracrine instruction or cell-cell communication following a 6 day treatment regime. To establish the fate of NPCs after 6 days of plating (DIV 14), immunocytochemistry was performed to identify BrdU-labelled cells that had adopted (or remained) a nestin$^+$, NG2$^+$, Tuj1$^+$, GFAP$^+$, or RIP$^+$ fate. The percentage of double positive cells (antigenic marker $^+$ and BrdU$^+$) was determined per antigenic lineage and

differentiating condition so that the fate of these NPCs could be evaluated. Since the phenotype detected in Chapters 3 and 4 was more robust in SVZ-derived NPCs and given that Cx30 expression in SGZ-derived astrocytes was lower than SVZ-derived astrocytes, we concentrated our efforts on analysis of SVZ-derived NSPs and SVZ-derived astrocytes in co-culture conditions.

Under spontaneous conditions where SVZ-derived NSPs were plated on laminin-coated glass coverslips in co-culture media, NPCs primarily specified to $GFAP^+$ astrocytes with 27.8 +/- 3.0 % (Figure 4.2, B) with a small minority differentiating to $tuj1^+$ immature neurons (Figure 4.2 A), $nestin^+$ NPCs (Figure 4.2, C), and $NG2^+$ glial progenitor cells (Figure 4.2, D ) at 2.4 +/- 0.5 %, 1.9 +/- 1.4 %, and 2.38 +/- 1.7 %, respectively. Together, these data confirm that NPCs spontaneously adopt a glial lineage when cultured in the absence of mitogens *in vitro.* When NSPs were plated under conditions enriched with paracrine neurogenic factors dubbed neuronal driving conditions (Neural-basal media supplemented with 0.5 μM RA and 20 ng/ml BDNF), a significant change in neuronal and astroglial fate was detected compared to spontaneous differentiation upon removal of mitogens. As expected, neuronal differentiation was enhanced and astroglial differentiation diminished with the percentage of tuj1 and BrdU labelled cells being 21.10 +/- 6.8 % compared to spontaneous control (2.35 +/- 0.5%) (**$p < 0.01$; ANOVA, *post hoc* Tukey test; Figure 4.2, A). On the other hand, astroglial cell fate was reduced to percentages of 6.80 +/- 1.5 % $BrdU^+$ cells labelled with GFAP (**$p < 0.01$; ANOVA, *post hoc* Tukey test; Figure 4.2, B). The percentage of $BrdU^+$ cells labelled for nestin or NG2 was very low with 0.3% +/- 0.3 and 0%, respectively (Figure 4.2, C, D).

Finally, the fate of NPC cultured in the presence of SVZ-derived astrocytes without neurogenic paracrine factors was determined. Cultures were maintained under conditions identical to the spontaneous specification paradigm except that NPC were plated on monolayers of WT SVZ-derived astrocytes. Similar to neuronal driving conditions, NSPs co-cultured with SVZ-derived astrocytes demonstrated significantly increased neuronal specification with 26.99 +/- 4.5 % of $BrdU^+$ cells labelled with tuj1, when compared to spontaneous control with 2.35 +/- 0.5 % (**p <0.01; ANOVA, *post hoc* Tukey test; Figure 4.2, A). The astroglial cell fate under astrocytic conditions was comparable to neuronal driving conditions where the percentage of $BrdU^+$ cells labelled GFAP was significantly reduced compared to intrinsic differentiation control (**p <0.01; ANOVA, *post hoc* Tukey test; Figure 4.2, B). $NG2^+$ glial progenitor cell fate when plated with astrocytes was comparable with spontaneous control while $nestin^+$ NPC fate was increased slightly compared to spontaneous control (Figure 4.2, C). These data confirm previous reports using immortalized rat hippocampal NPCs and murine SVZ-NPCs indicating that astrocytes from either neurogenic niche "instruct" NPCs to adopt a neuronal lineage (Lim and Alvarez-Buylla, 1999; Song et al., 2002).

**Figure 4.2 Astrocyte-NPC co-culture promotes neurogenesis *in vitro*.** NSP cultures were pulsed with BrdU at time of plating and differentiation assessed after 6 DIV following removal of mitogens (Laminin, spontaneous differentiation), treatment with paracrine neurogenic factors (Laminin + RA + BDNF, neuronal driving condition), or co-culture on astrocytic monolayers (Astrocyte layer). The number of neurons (A), astrocytes (B), undifferentiated NPCs (C), and glial progenitors (D) was assessed. Neurogenesis was enhanced by both paracrine factors and co-culture on astrocytic monolayers. (**$p < 0.01$ ANOVA, *post hoc* Dunnett's *t* test).

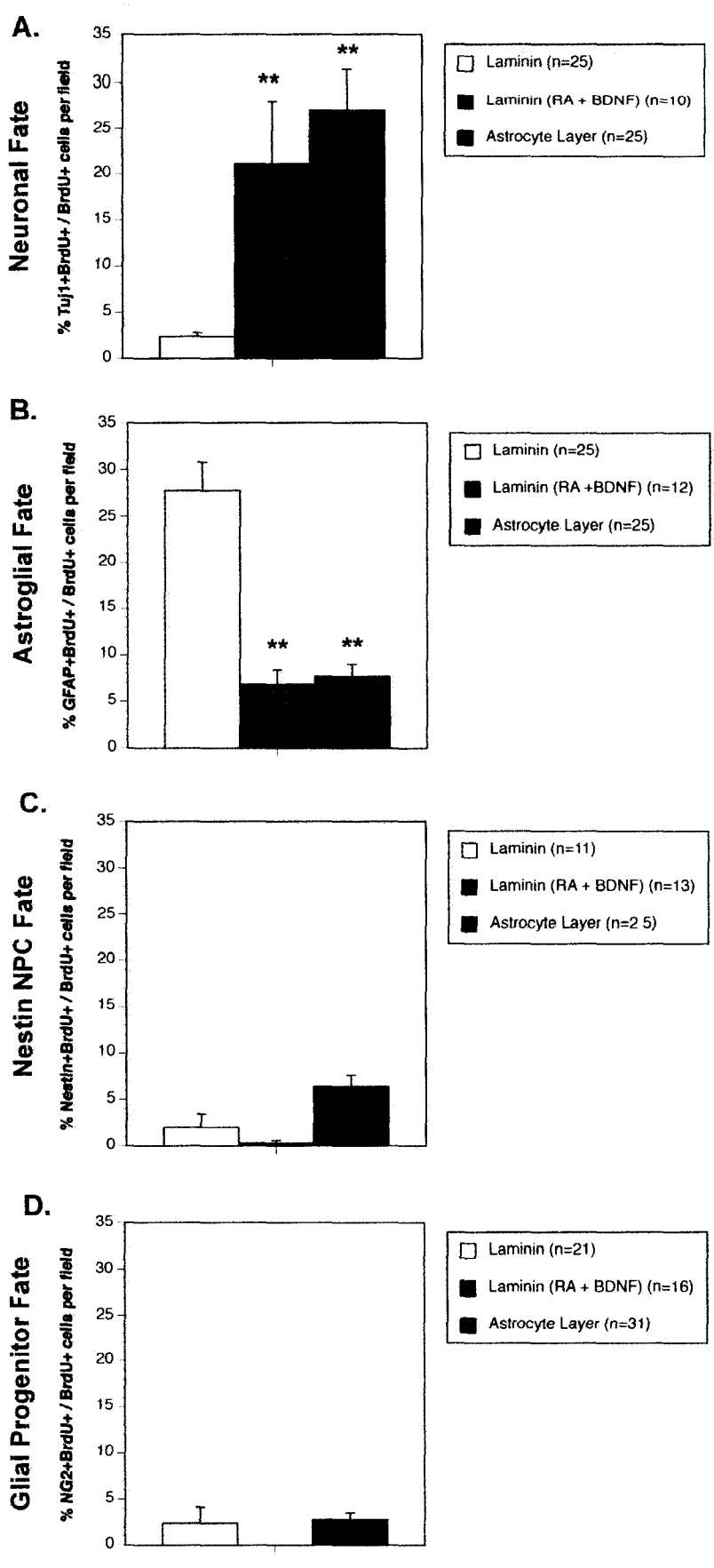
A.
Neuronal Fate
% Tuj1+BrdU+ / BrdU+ cells per field
35
30
25
20
15
10
5
0
**
**
Laminin (n=25)
Laminin (RA + BDNF) (n=10)
Astrocyte Layer (n=25)
B.
Astroglial Fate
% GFAP+BrdU+ / BrdU+ cells per field
35
30
25
20
15
10
5
0
**
**
Laminin (n=25)
Laminin (RA +BDNF) (n=12)
Astrocyte Layer (n=25)
C.
Nestin NPC Fate
% Nestin+BrdU+ / BrdU+ cells per field
35
30
25
20
15
10
5
0
Laminin (n=11)
Laminin (RA + BDNF) (n=13)
Astrocyte Layer (n=2 5)
D.
Glial Progenitor Fate
% NG2+BrdU+ / BrdU+ cells per field
35
30
25
20
15
10
5
0
Laminin (n=21)
Laminin (RA + BDNF) (n=16)
Astrocyte Layer (n=31)

**Figure 4.2**

### 4.3.3 Impact of gap junction blockers on neurogenesis in astrocytes-NPC co-cultures.

To determine whether connexin-mediated communication plays a role in mediating these "instructive" effects, co-cultures were performed in the presence of gap junction blockers and their respective inactive control analogs added at the time of plating. When the extent of neuronal fate was measured in astrocyte-NSP co-culture conditions with active gap junction blocker analog GRA present, the percentage of $BrdU^+$ cells labelled tuj1 substantially decreased to 5.0 +/- 1.3% compared to untreated astrocyte-NSP co-culture conditions (26.99 +/- 4.5%; $^{\pi\pi}$ $p < 0.01$, ANOVA, post hoc Tukey test)(Figure 4.3). To determine the specificity of gap junction blockade with GRA and rule out potential effects of the GRA vehicle, its inactive analog GZA was tested. The percentage of $BrdU^+$ cells identified as $tuj1^+$ cells was not significantly altered and was statistically comparable to cultures treated under neuronal driving conditions and untreated astrocyte-NSP co-cultures (Figure 4.3). These studies demonstrate the gap junction uncoupling agents inhibit neurogenesis *in vitro* mediated by direct contact with "instructive" astrocytes (Figure 4.3).

## 4.4 Discussion

Here, we demonstrate that astrocytes within the SVZ and SGZ neurogenic niches express Cx30 mRNA and protein. Since expression of Cx30 was higher in SVZ-derived astrocyte cultures, we focused our efforts on elucidating a role for Cx30-mediated communication in the SVZ *in vitro* model (Figure 4.1). Previously, we localized Cx30 expression to a subset of $nestin^+$ NPCs, GFAP astrocytes, and $nestin^+$/ $GFAP^+$ Type 1/B both *in vivo* and *in vitro*. This expression profile implicates Cx30-mediated communication in

**Figure 4.3 Gap junction blockade abrogates neurogenesis in astrocyte-NPC co-cultures.** Neurogenesis, measured as the percentage of $BrdU^+$ cells that differentiate to $tuj1^+$ immature neurons, is enhanced when SVZ-derived NSPs are plated in contact with SVZ-derived astrocytes with or without GZA (inactive gap junction blocker analog), or when NSPs are cultured with paracrine neuronal driving conditions (laminin + RA + BDNF) (A). When NSPs are plated in contact with astrocytes in the presence of active gap junction blocker, GRA, the extent of neuronal differentiation and is comparable to that observed under spontaneous differentiation conditions wherein NPCs adopt an astroglial fate (laminin alone, A) ($^{\pi}$ $p < 0.05$ ANOVA, *post hoc* Dunnett's t test, $^{**/\pi\pi}$ $p < 0.01$ ANOVA, *post hoc* Dunnett's t test, *** $p < 0.001$ ANOVA, *post hoc* Dunnett's t test). Representative digital photomicrographs of spontaneous differentiation conditions (B), neuronal driving conditions (C), astrocyte conditions (D), GZA-astrocyte conditions (E), and GRA-astrocyte conditions (F) are presented. Arrows point out tuj1 (red) and BrdU (green) double positive cells.

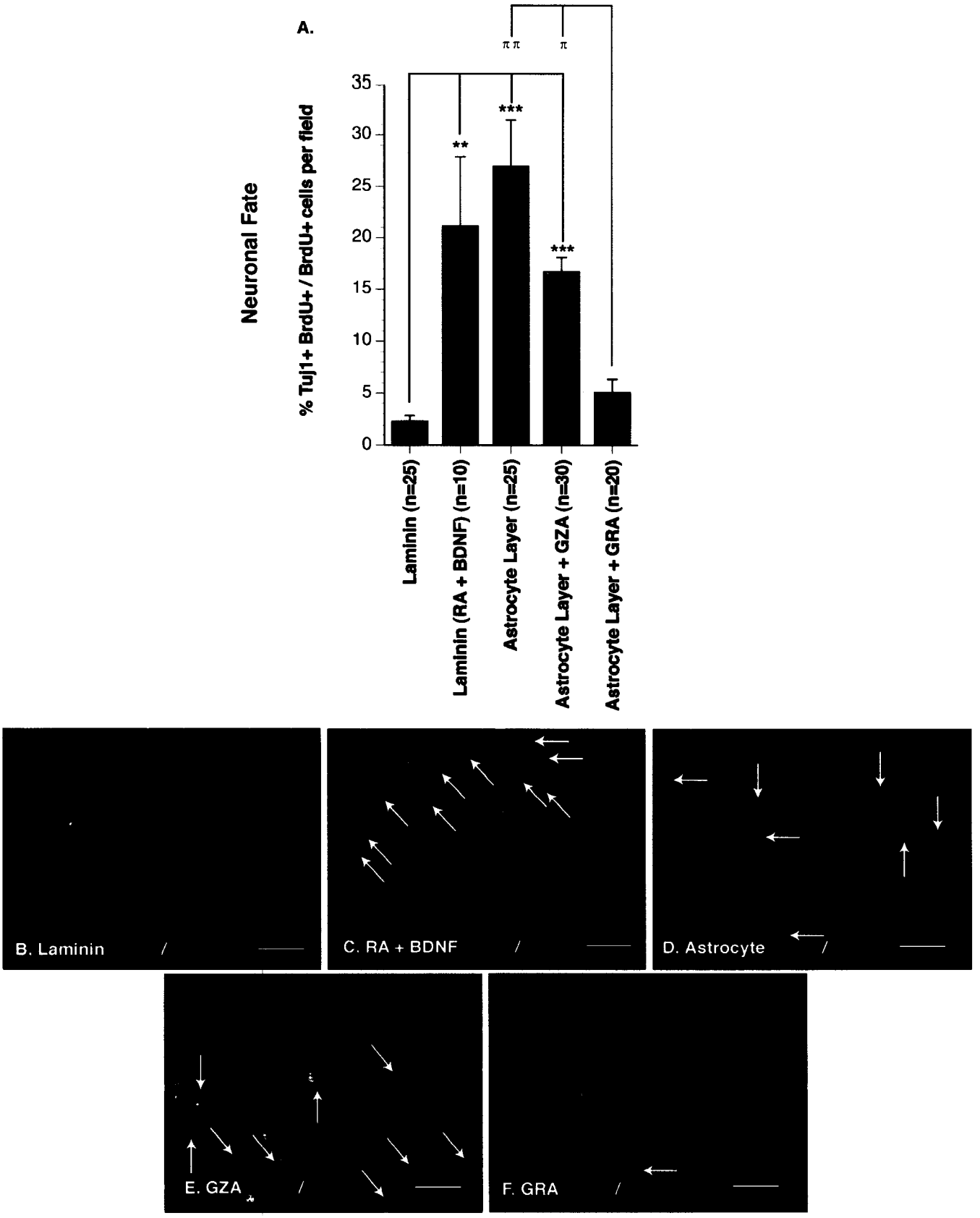
A.
Neuronal Fate
% Tuj1+ BrdU+ / BrdU+ cells per field
35
30
25
20
15
10
5
0
**
***
***
π π
π
Laminin (n=25)
Laminin (RA + BDNF) (n=10)
Astrocyte Layer (n=25)
Astrocyte Layer + GZA (n=30)
Astrocyte Layer + GRA (n=20)
B. Laminin
C. RA + BDNF
D. Astrocyte
E. GZA
F. GRA

**Figure 4.3**

regulation of NPC outcome via $GFAP^+$ instructive astrocytes through direct coupling with Type C and/or Type B progenitor cells underlying, in part, the effects of direct cell-cell contact on neurogenesis (Lim and Alvarez-Buylla, 1999; Song et al., 2002). Pharmacological results presented in this study demonstrate that cell-cell coupling through gap junctions are primarily involved in this instructive role. We show that, when NPCs are plated in the absence of extrinsic neurogenic factors, they are destined to become astrocytes. It is tempting to speculate that this fate possibly occurs to aid in finer regulating the fate of subsequent NPCs. These newly formed astrocytes may begin to form an endogenous astrocytic monolayer as to provide further signals in NPC specification. We further confirm that neurogenic paracrine overcome the intrinsic tendency towards an astroglial fate specification and promote neuronal differentiation and that co-culture with astrocytes is sufficient to induce this phenotype. These data clearly demonstrate an instructive role for astrocytes on NPC fate. Interestingly, while neuronal specification is enhanced under both astrocyte plating and neuronal driving conditions, the percentage of astroglial fate specification is diminished. This is likely due to the presence of several extrinsic factors that are capable of regulating NPC fate or that these extrinsic factors simultaneously increase neuronal and suppress astroglial differentiation. However, these data do not distinguish between the effects of direct NPC-astrocyte contact and release of neurogenic factors from astrocytes into the extracellular milieu. To identify a role for connexins in the control of NPC fate, SVZ-derived NSPs were plated with SVZ-derived astrocytes with either a gap junction blocker (GRA) or an inactive gap junction blocker analog (GZA). GRA completely inhibited the neurogenic influence of astrocyte co-culture on NPCs. These data clearly

implicate connexin-mediated communication in directing NPCs towards a neuronal differentiation.

We have yet to establish whether this control is Cx30-mediated and/or involves other connexins. Certainly, the NPC specific postnatal expression pattern of Cx30, coupled with observations of diminished neuronal specification in the SVZ of Cx30 $^{(-/-)}$ mice *in vivo,* along with enhanced neuronal specification when NPCs are plated with instructive astrocytes *in vitro* provides converging evidence that Cx30-mediated communication is involved in postnatal neurogenesis. These studies complement existing evidence that diffusible molecules produced by astrocytes in the SVZ also exert influences on NPC fate suggesting that direct cell contact via connexin-mediated communication may provide, in part, the contacts and medium needed for diffusion of the appropriate signals to achieve extrinsic control of NPC regulation. To make adult neurogenic regulation even more complex, other cells both locally and distally may exert some form of regulation; for example, ependymal cells that line the LV may promote self renewal of NPCs, factors released from blood vessels may have direct impact on NPC fate, and distal neurons may impact on NPC fate via altering ambient levels of neurotransmitters in the neurogenic niche, or possibly via synaptic contacts with NPCs (Alvarez-Buylla and Lim, 2004; Ramirez-Castillejo et al., 2006; Zhao et al., 2008). The connexin profile of ependymal cells has yet to be fully elucidated, but it is known that both Cx30 and Cx26 are expressed (Belliveau and Naus, 1995; Dere et al., 2004). Future studies will be necessary to directly assess whether this Cx30-mediated communication occurs via the classical GJIC, connexon hemichannel activity, or channel independent signalling. Also, the diffusible factors that cross through

channels or that bind to individual connexin subunits should be elucidated as to fully understand the molecular details of Cx30 mediated neuronal specification.

## Chapter 5: General Discussion

### 5.1 The role of Cx30 in dictating NPC fate *in vivo.*

The specific roles of connexin channels in the adult mammalian brain are somewhat unclear and remain as an unresolved research question. The experiments carried out in this thesis were employed to further understand the contribution of astrocyte specific Cx30 in postnatal and adult NPC fate. In the neurogenic niches of adult mouse brain, neurons and/or glial cells are thought to arise from NPCs/ NSCs via successive rounds of proliferation via intermediate transit amplifying progeny followed by terminal neuronal/ glial differentiation. The intrinsic control of NPC fate is defined by their epigenetic control, transcriptional, and post transcriptional regulation that has been shown during early brain development (Cheng et al., 2005); for instance, intrinsically regulated restricted GJIC has been shown to segregate cells into explicit developmental fields that prompts these cells to collectively adopt the same fate (Kalimi and Lo, 1989; Lo, 1996). NPC fate regulation is also controlled by extrinsic variables including direct cell contact by neighbouring cells or by the release of soluble paracrine factors from nearby or distal cells (Zhao et al., 2008). Several soluble extrinsic signals that can directly influence the fate of NPCs have been identified *in vivo* including FGF2 and EGF in promoting proliferation in the SVZ, BDNF in promoting adult neurogenesis, and prolactin in enhancing adult SVZ neurogenesis and neuronal integration (Henry et al., 2007; Kuhn et al., 1997; Shingo et al., 2003). One plausible extrinsic mechanism of direct cell contact is via connexin-mediated communication, for it has been previously implicated in NPC migration, differentiation, axonal growth and guidance, and synaptogenesis in the mature and developing CNS (Guthrie and Gilula, 1989; Melanson-

Drapeau et al., 2003; Warner, 1987; Weissman et al., 2004). To further support the notion of direct cell contact as system for regulating NPC fate, cultured NPCs in the presence of matured astrocytes can be instructed toward a neuronal product (Lim and Alvarez-Buylla, 1999; Song et al., 2002). Due to the localization of Cx30 in postnatal instructive astrocytes, Cx30 expression was hypothesized to play a role with regulating adult mammalian neurogenesis and this hypothesis was tested in the present thesis.

These data represent the first demonstration that postnatal NPCs express Cx30. The NPC types that co-localized with Cx30 in the SVZ, and SGZ were identified as a subset of $GFAP^+$, $nestin^+$, and $GFAP^+$ / $nestin^+$ cells. This expression pattern generated a possible hypothesis that Cx30-mediated communication between instructive $GFAP^+$ astrocytes with $GFAP^+$/ $nestin^+$ Type 1/B progenitors and/or $GFAP^-$/ $nestin^+$ NPCs is critical in the regulation of adult neurogenesis. To test this hypothesis, we investigated the effects of NPC fate when the Cx30 gene was deleted from the mouse genome. Overall indices of NPC proliferation were determined to be unaltered in Cx30 KO mice when compared to congenically matched WT mice. However, a shift in the identity of the proliferating NPC population was observed. Cx30 null-mutants exhibited an increase in the percentage of $BrdU^+$ cells labelled with nestin along with a decreased percentage of $BrdU^+$ cells labelled with DCX in both neurogenic regions of the adult brain. This implicates Cx30 in regulating NPC specification in the SVZ and SGZ of adult mice while Cx30 does not play a significant role in controlling proliferation.

To distinguish between these hypotheses, we measured the fate of BrdU-labelled cells 14 and 28 days post BrdU injection. The percentage of $BrdU^+$ cells that specified to

mature NeuN+ neurons was measured in the OB, the terminal site for neuron maturation and integration. At both time points, the percentage of neurogenesis was equivalent between mouse genotypes indicating the reduction in proliferating $DCX^+$ early neuronal progenitors did not impact upon the number of newly generated neurons. These data suggested that Cx30 may not play a significant role in the terminal regulation of NPC fate specification. Surprisingly, the total number of $BrdU^+$ cells per OB region was enhanced in Cx30 null-mutant mice. These observations suggested that 1) more site-specific proliferation is occurring in the OB in the absence of Cx30, 2) migration of intermediate progenitors is enhanced in Cx30 null-mutants, or 3) survival of intermediate progenitors is enhanced in the absence of Cx30 preventing deletion of excess progeny. The first hypothesis is unlikely given that the BrdU label is diluted below limits of detection after approximately three successive divisions (De Boer et al., 2003). Thus, the increase in BrdU-labelled cells in the OB 28 days after the last BrdU injection attributed to proliferation could only result if this expansion occurred specifically in the OB and not throughout the RMS predicted to dilute the label below the limits of detection. To test this possibility, the number of $BrdU^+$ cells in the OB was measured 1 day after the last BrdU injection and was determined to be equivalent in the OB suggesting the number of intermediate progenitors in the OB was not affected by the loss of Cx30. An increase in migration would likely manifest as an increase in BrdU-labelled number throughout the RMS and OB in Cx30 $^{(-/-)}$ compared to WT and increase in neuronal number in the OB. Although the number of $BrdU^+$ cells per 0.1 $mm^2$ in the RMS was increased in all timepoints (1, 14, 28 days post BrdU injection) in Cx30 null-mutant mice initially suggesting that BrdU labelled NPCs migrate faster along the RMS, terminal neurogenesis was not enhanced in the OB. Together, these observations suggest

that loss of Cx30 delays transition of Type B and C progenitors to the next developmental stage ($DCX^+$ Type A NPCs). Rather, the survival of actively proliferating Type B and C progeny that enter the RMS without successfully achieving the next developmental stage is enhanced. These aberrant progeny cease to proliferate in the RMS and thus retain BrdU label, migrate to the OB, yet fail to terminally differentiate likely because they have not passed the appropriate developmental checkpoints. Thus, the simplest explanation is that loss of Cx30 enhances the survival of immature progeny. Mechanistically, $GFAP^+$ instructive astrocytes located in the SVZ and SGZ may dictate the progression of NPCs to a neuronal linage via Cx30-mediated communication and provide adhesive contacts for further instructions along the RMS. At the terminal end of the RMS, NPCs may not need directive instructions from astrocytes, but rather respond to other external factors found in the OB microenvironment. Thus, these data implicate Cx30 in the proper transition of early NPCs to a neuronal lineage and in the deletion of progeny that fail to obtain the appropriate lineage.

**5.2 Postnatal 'instructive' astrocytes and their role in Cx30-mediated signalling.**

To provide direct evidence that Cx30 cell-cell communication between Type B and C NPCS and astrocytes directs the lineage progression of intermediate progeny, we utilized a well characterized simplified *in vitro* model of NPC differentiation, the NSP model. As described previously, NPCs from either neurogenic region are extracted from P0-P3 newborn WT mice and expanded as NSPs in a suspension containing growth factors. Initially, we looked at Cx30 expression in hippocampal and SVZ-derived NSPs by immunocytochemistry and RT-PCR (Figure 4.1). Lianne Gauvin, an alumni masters student

from the Bennett lab, had noticed the presence of Cx30 mRNA and localized Cx30 protein expression to a subset of $GFAP^+$ and $nestin^+$ NPCs found in hippocampal-derived NSPs. Here, these findings were expanded demonstrating that Cx30 mRNA is also expressed by SVZ-derived NSPs and that Cx30 protein localizes to a subset of $nestin^+$ (Type C NPCs), $GFAP^+$ (astrocytes), and $nestin^+$/ $GFAP^+$ (Type B NPCs) cells. For quantitative analyses, SGZ and SVZ-derived NSPs were expanded for 12-14 DIV and processed for flow cytometry. Various cell type markers were deployed to determine the relative proportion of Cx30 expression in the total NSP population and within specific NPC subpopulations. From the total NSP population, Cx30 was found to be expressed by approximately 30% of hippocampal and SVZ-derived NSP cells. In specific cell type subpopulations, Cx30 was found to be expressed in the majority of $GFAP^+$ astrocytes and Type 1/B cells in hippocampal and SVZ-derived NSPs, respectively. Further analysis localized Cx30 to 83.26% and 68.89% of $nestin^+$ cells in hippocampal and SVZ-derived NSPs.

Given this expression profile, we evaluated the possible role of connexin-mediated communication between astrocytes and Type B cells in directing early NPCs to adopt a neuronal lineage. After expansion as NSPs for 8 DIV, SVZ-derived cultures were pulsed with BrdU for 24 hours and then plated in various culture environments including spontaneous, neuronal driving, and astrocytic co-culture conditions. Each condition was used to explore intrinsic and extrinsic controls on NPC fate specification. We found that NSPs spontaneously differentiated to an astroglial lineage when plated on laminin-coated coverslips for 6 days in the absence of mitogens. Conversely, when exposed to paracrine neurogenic factors, the external factors found in this microenvironment directed NSPs away from their default astroglial program and promoted neuronal commitment. We found that

SVZ-derived astrocytes shown to express Cx30 and hypothesized to couple with SVZ-derived NSPs, enhanced neuronal NPC specification with neurogenesis comparable to that observed in neuronal driving conditions. This finding further supports the notion of Cx30's astrocytic expression and involvement in proper postnatal neurogenesis. The neurogenic impact of astrocyte-NPC contact was abrogated by the gap junction blocker GRA but not its inactive gap junction blocker analog, GZA. Together, these data demonstrate the need for direct cell contact signalling via gap junctional channels between NPCs and their instructive cells to alter NPC fate. Other groups have previously demonstrated similar results with respect to NSP-astrocyte co-culture experiments implying the need for direct cell contact in altering NPC fate specification (Lim and Alvarez-Buylla, 1999; Song et al., 2002). However, this is the first study to implicate GJIC in signalling these "instructive" actions.

Summarizing results from both *in vivo* and *in vitro* experiments, they implicate Cx30 in the control of NPC specification and/or migration in the SVZ and to a lesser extent the SGZ. Cx30-mediated communication may underlie, in part, the capacity of NPC populations to communicate with adjacent instructive astrocytes that regulate their specification into functional cell types and/or the survival of cells that achieve (or fail to) the appropriate developmental stage. Thus, the results presented in this study suggest a role for Cx30 in dictating adult and postnatal SVZ-derived NPC fate, by promoting neurogenesis.

**5.3 Significance of research.**

Neurodegenerative diseases such as Parkinson's, Alzheimer's disease and multiple sclerosis can cause severe physiological, emotional, and financial burden on the affected individual, their family, and the healthcare community. By understanding the

pathophysiological mechanisms behind these diseases coupled with ways to either prevent or end disease development is necessary to alleviate patient morbidity. Current therapies can temporary relieve symptoms and transiently improve the quality of life, but have little effect on preventing disease progression. With the recent discovery of the adult brain's capacity to regenerate, new neural stem cell replacement therapies are being considered as possible treatments. Determining the signalling mechanisms regulating NPC fate is essential to validate the promise of NPC mediated neuroregenerative therapies. This study presents relevant information pertaining to NPC regulation and its ability to respond to extrinsic factors by demonstrating the possible role of Cx30 in regulating NPC fate specification both *in vitro* and *in vivo*. Further analysis into the intracellular signals and pathways that are elicited by Cx30-mediated communication need to be determined and manipulated accordingly for proper use in brain stem cell replacement strategies.

## References.


Abematsu, M., Smith, I., and Nakashima, K. (2006). Mechanisms of neural stem cell fate determination: extracellular cues and intracellular programs. Curr Stem Cell Res Ther *1*, 267-277.

Altevogt, B.M., and Paul, D.L. (2004). Four classes of intercellular channels between glial cells in the CNS. J Neurosci *24*, 4313-4323.

Altman, J. (1969). Autoradiographic and histological studies of postnatal neurogenesis. IV. Cell proliferation and migration in the anterior forebrain, with special reference to persisting neurogenesis in the olfactory bulb. J Comp Neurol *137*, 433-457.

Altman, J., and Das, G.D. (1965). Autoradiographic and histological evidence of postnatal hippocampal neurogenesis in rats. J Comp Neurol *124*, 319-335.

Alvarez-Buylla, A., and Garcia-Verdugo, J.M. (2002). Neurogenesis in adult subventricular zone. J Neurosci *22*, 629-634.

Alvarez-Buylla, A., and Lim, D.A. (2004). For the long run: maintaining germinal niches in the adult brain. Neuron *41*, 683-686.

Bachoo, R.M., Kim, R.S., Ligon, K.L., Maher, E.A., Brennan, C., Billings, N., Chan, S., Li, C., Rowitch, D.H., Wong, W.H., *et al.* (2004). Molecular diversity of astrocytes with implications for neurological disorders. PNAS *101*, 8384-8389.

Barbe, M.T., Monyer, H., and Bruzzone, R. (2006). Cell-cell communication beyond connexins: the pannexin channels. Physiology (Bethesda) *21*, 103-114.

Belliveau, D.J., Kidder, G.M., and Naus, C.C. (1991). Expression of gap junction genes during postnatal neural development. Dev Genet *12*, 308-317.

Belliveau, D.J., and Naus, C.C. (1995). Cellular localization of gap junction mRNAs in developing rat brain. Dev Neurosci *17*, 81-96.

Belluardo, N., Mudo, G., Trovato-Salinaro, A., Le Gurun, S., Charollais, A., Serre-Beinier, V., Amato, G., Haefliger, J.A., Meda, P., and Condorelli, D.F. (2000). Expression of connexin36 in the adult and developing rat brain. Brain Res *865*, 121-138.

Bennett, M.V.L., Contreras, J.E., Bukauskas, F.F., and Saez, J.C. (2003). New roles for astrocytes: Gap junction hemichannels have something to communicate. Trends in Neurosciences *26*, 610-617.

Beyer, E.C., Paul, D.L., and Goodenough, D.A. (1987). Connexin43 - a Protein from Rat-Heart Homologous to a Gap Junction Protein from Liver. Journal of Cell Biology *105*, 2621-2629.

Bittman, K., Owens, D.F., Kriegstein, A.R., and LoTurco, J.J. (1997). Cell coupling and uncoupling in the ventricular zone of developing neocortex. Journal of Neuroscience *17*, 7037-7044.

Bittman, K.S., and LoTurco, J.J. (1999). Differential regulation of connexin 26 and 43 in murine neocortical precursors. Cerebral Cortex *9*, 188-195.

Brezun, J.M., and Daszuta, A. (1999). Depletion in serotonin decreases neurogenesis in the dentate gyrus and the subventricular zone of adult rats. Neuroscience *89*, 999-1002.

Bruzzone, R. (2001). Learning the language of cell-cell communication through connexin channels. Genome Biology *2*, 4027.

Bruzzone, R., and Dermietzel, R. (2006). Structure and function of gap junctions in the developing brain. Cell Tissue Res *326*, 239-248.

Bruzzone, R., White, T.W., and Paul, D.L. (1996). Connections with connexions: the molecular basis of direct intercellular signalling. Eur J Biochem *238*, 1-27.

Cameron, H.A., Hazel, T.G., and McKay, R.D. (1998). Regulation of neurogenesis by growth factors and neurotransmitters. J Neurobiol *36*, 287-306.

Caveney, S. (1985). The role of gap junctions in development. Annu Rev Physiol *47*, 319-335.

Cheng, L.C., Tavazoie, M., and Doetsch, F. (2005). Stem cells: from epigenetics to microRNAs. Neuron *46*, 363-367.

Condorelli, D.F., Mudo, G., Trovato-Salinaro, A., Mirone, M.B., Amato, G., and Belluardo, N. (2002). Connexin-30 mRNA is up-regulated in astrocytes and expressed in apoptotic neuronal cells of rat brain following kainate-induced seizures. Molecular and Cellular Neurosciences *21*, 94-113.

Connors, B.W., Benardo, L.S., and Prince, D.A. (1983). Coupling between neurons of the developing rat neocortex. Journal of Neuroscience *3*, 773-782.

Connors, B.W., and Long, M.A. (2004). Electrical synapses in the mammalian brain. Annu Rev Neurosci *27*, 393-418.

Cook, J.E., and Becker, D.L. (1995). Gap junctions in the vertebrate retina. Microsc Res Tech *31*, 408-419.

Dahl, E., Manthey, D., Chen, Y., Schwarz, H.J., Chang, Y.S., Lalley, P.A., Nicholson, B.J., and Willecke, K. (1996). Molecular cloning and functional expression of mouse connexin-30,a gap junction gene highly expressed in adult brain and skin. J Biol Chem *271*, 17903-17910.

Dani, J.W., Chernjavsky, A., and Smith, S.J. (1992). Neuronal activity triggers calcium waves in hippocampal astrocyte networks. Neuron *8*, 429-440.

De Boer, R.J., Mohri, H., Ho, D.D., and Perelson, A.S. (2003). Estimating average cellular turnover from 5-bromo-2'-deoxyuridine (BrdU) measurements. Proc Biol Sci *270*, 849-858.

Dere, E., De Souza-Silva, M.A., Frisch, C., Teubner, B., Sohl, G., Willecke, K., and Huston, J.P. (2004). Connexin30-deficient mice show increased emotionality and decreased rearing activity in the open-field along with neurochemical changes. European Journal of Neuroscience *18*, 629-638.

Dermietzel, R., Farooq, M., Kessler, J.A., Althaus, H., Hertzberg, E.L., and Spray, D.C. (1997). Oligodendrocytes express gap junction proteins connexin32 and connexin45. Glia *20*, 101-114.

Dermietzel, R., Hertberg, E.L., Kessler, J.A., and Spray, D.C. (1991). Gap junctions between cultured astrocytes: immunocytochemical, molecular, and electrophysiological analysis. Journal of Neuroscience *11*, 1421-1432.

Dermietzel, R., and Spray, D.C. (1993). Gap junctions in the brain: where, what type, how many and why? Trends Neurosci *16*, 186-192.

Dermietzel, R., Traub, O., Hwang, T.K., Beyer, E., Bennett, M.V., Spray, D.C., and Willecke, K. (1989). Differential expression of three gap junction proteins in developing and mature brain tissues. Proc Natl Acad Sci U S A *86*, 10148-10152.

Doetsch, F. (2003). The glial identity of neural stem cells. Nat Neurosci *6*, 1127-1134.

Doetsch, F., Caille, I., Lim, D.A., Garcia-Verdugo, J.M., and Alvarez-Buylla, A. (1999). Subventricular zone astrocytes are neural stem cells in the adult mammalian brain. Cell *97*, 703-716.

Elias, L.A., Wang, D.D., and Kriegstein, A.R. (2007). Gap junction adhesion is necessary for radial migration in the neocortex. Nature *448*, 901-907.

Emsley, J.G., Mitchell, B.D., Kempermann, G., and Macklis, J.D. (2005). Adult neurogenesis and repair of the adult CNS with neural progenitors, precursors, and stem cells. Prog Neurobiol *75*, 321-341.

Engelhardt, M., Bogdahn, U., and Aigner, L. (2005). Adult retinal pigment epithelium cells express neural progenitor properties and the neuronal precursor protein doublecortin. Brain Res *1040*, 98-111.

Enkvist, M.O., and McCarthy, K.D. (1994). Astroglial gap junction communication is increased by treatment with either glutamate or high K+ concentration. Journal of Neurochemistry *62*, 489-495.

Eriksson, P.S., Perfilieva, E., Bjork-Eriksson, T., Alborn, A.M., Nordborg, C., Peterson, D.A., and Gage, F.H. (1998). Neurogenesis in the adult human hippocampus. Nat Med *4*, 1313-1317.

Eriksson, P.S., and Wallin, L. (2004). Functional consequences of stress-related suppression of adult hippocampal neurogenesis - a novel hypothesis on the neurobiology of burnout. Acta Neurol Scand *110*, 275-280.

Ernst, C., and Christie, B.R. (2006). The putative neural stem cell marker, nestin, is expressed in heterogeneous cell types in the adult rat neocortex. Neuroscience *138*, 183-188.

Evirgen, N., Solak, M., Derekoy, S., Erdogan, M., Yildiz, H., Eser, B., Arikan, S., and Erkoc, A. (2008). Genotyping for Cx26 and Cx30 mutations in cases with congenital hearing loss. Genet Test *12*, 253-256.

Fraser, S.E., Green, C.R., Bode, H.R., and Gilula, N.B. (1987). Selective disruption of gap junctional communication interferes with a patterning process in hydra. Science *237*, 49-55.

Furshpan, E.J., and Potter, D.D. (1959). Transmission at the giant motor synapses of the crayfish. Journal of Physiology *145*, 289-325.

Gage, F.H. (2000). Mammalian neural stem cells. Science *287*, 1433-1438.

Gage, F.H., Ray, J., and Fisher, L.J. (1995). Isolation, characterization, and use of stem cells from the CNS. Annu Rev Neurosci *18*, 159-192.

Galarreta, M., and Hestrin, S. (1999). A network of fast-spiking cells in the neocortex connected by electrical synapses. Nature *402*, 72-75.

Giaume, C., and McCarthy, K.D. (1996). Control of gap-junctional communication in astrocytic networks. Trends Neurosci *19*, 319-325.

Giaume, C., Tabernero, A., and Medina, J.M. (1997). Metabolic trafficking through astrocytic gap junctions. GLIA *21*, 114-123.

Giaume, C., and Venance, L. (1995). Gap junctions in brain glial cells and development. Perspect Dev Neurobiol *2*, 335-345.

Gibson, J.R., Beierlein, M., and Connors, B.W. (1999). Two networks of electrically coupled inhibitory neurons in neocortex. Nature *402*, 75-79.

Giepmans, B.N. (2004). Gap junctions and connexin-interacting proteins. Cardiovasc Res *62*, 233-245.

Gilbert, M.E., Kelly, M.E., Samsam, T.E., and Goodman, J.H. (2005). Chronic developmental lead exposure reduces neurogenesis in adult rat hippocampus but does not impair spatial learning. Toxicol Sci *86*, 365-374.

Goldberg, G.S., Valiunas, V., and Brink, P.R. (2004). Selective permeability of gap junction channels. Biochim Biophys Acta *1662*, 96-101.

Gotz, M., Hartfuss, E., and Malatesta, P. (2002). Radial glial cells as neuronal precursors: a new perspective on the correlation of morphology and lineage restriction in the developing cerebral cortex of mice. Brain Res Bull *57*, 777-788.

Gould, E., Beylin, A., Tanapat, P., Reeves, A., and Shors, T.J. (1999). Learning enhances adult neurogenesis in the hippocampal formation. Nat Neurosci *2*, 260-265.

Gould, E., and Gross, C.G. (2002). Neurogenesis in adult mammals: some progress and problems. J Neurosci *22*, 619-623.

Gross, R.E., Mehler, M.F., Mabie, P.C., Zang, Z., Santschi, L., and Kessler, J.A. (1996). Bone morphogenetic proteins promote astroglial lineage commitment by mammalian subventricular zone progenitor cells. Neuron *17*, 595-606.

Guthrie, P.B., Knappenberger, J., Segal, M., Bennett, M.V., Charles, A.C., and Kater, S.B. (1999). ATP released from astrocytes mediates glial calcium waves. J Neurosci *19*, 520-528.

Guthrie, S.C., and Gilula, N.B. (1989). Gap junctional communication and development. Trends Neurosci *12*, 12-16.

Hastings, N.B., and Gould, E. (1999). Rapid extension of axons into the CA3 region by adult-generated granule cells. Journal of Comparative Neurology *413*, 146-154.

Henry, R.A., Hughes, S.M., and Connor, B. (2007). AAV-mediated delivery of BDNF augments neurogenesis in the normal and quinolinic acid-lesioned adult rat brain. Eur J Neurosci *25*, 3513-3525.

Hombach, S., Janssen-Bienhold, U., Sohl, G., Schubert, T., Bussow, H., Ott, T., Weiler, R., and Willecke, K. (2004). Functional expression of connexin57 in horizontal cells of the mouse retina. Eur J Neurosci *19*, 2633-2640.

Horner, P.J., and Palmer, T.D. (2003). New roles for astrocytes: the nightlife of an 'astrocyte'. La vida loca! Trends Neurosci *26*, 597-603.

Kalimi, G.H., and Lo, C.W. (1989). Gap junctional communication in the extraembryonic tissues of the gastrulating mouse embryo. J Cell Biol *109*, 3015-3026.

Kee, N., Sivalingam, S., Boonstra, R., and Wojtowicz, J.M. (2002). The utility of Ki-67 and BrdU as proliferative markers of adult neurogenesis. J Neurosci Methods *115*, 97-105.

Kempermann, G., Jessberger, S., Steiner, B., and Kronenberg, G. (2004). Milestones of neuronal development in the adult hippocampus. Trends Neurosci *27*, 447-452.

Kempermann, G., Kuhn, H.G., and Gage, F.H. (1997). More hippocampal neurons in adult mice living in an enriched environment. Nature *386*, 493-495.

Kuhn, H.G., Dickinson-Anson, H., and Gage, F.H. (1996). Neurogenesis in the dentate gyrus of the adult rat: age-related decrease of neuronal progenitor proliferation. J Neurosci *16*, 2027-2033.

Kuhn, H.G., Winkler, J., Kempermann, G., Thal, L.J., and Gage, F.H. (1997). Epidermal growth factor and fibroblast growth factor-2 have different effects on neural progenitors in the adult rat brain. J Neurosci *17*, 5820-5829.

Kunzelmann, P., Blumcke, I., Traub, O., Dermietzel, R., and Willecke, K. (1997). Coexpression of connexin45 and -32 in oligodendrocytes of rat brain. J Neurocytol *26*, 17-22.

Kunzelmann, P., Schroder, W., Traub, O., Steinhauser, C., Dermietzel, R., and Willecke, K. (1999). Late onset and increasing expression of the gap junction protein connexin30 in adult murine brain and long-term cultured astrocytes. Glia *25*, 111-119.

Landisman, C.E., Long, M.A., Beierlein, M., Deans, M.R., Paul, D.L., and Connors, B.W. (2002). Electrical synapses in the thalamic reticular nucleus. J Neurosci *22*, 1002-1009.

Lange, C., Mix, E., Rateitschak, K., and Rolfs, A. (2006). Wnt signal pathways and neural stem cell differentiation. Neurodegener Dis *3*, 76-86.

Lendahl, U., Zimmerman, L.B., and McKay, R.D. (1990). CNS stem cells express a new class of intermediate filament protein. Cell *60*, 585-595.

Lennington, J.B., Yang, Z., and Conover, J.C. (2003). Neural stem cells and the regulation of adult neurogenesis. Reprod Biol Endocrinol *1*, 99.

Leong, S.F., and Clark, J.B. (1984). Regional enzyme development in rat brain. Enzymes associated with glucose utilization. Biochem J *218*, 131-138.

Lim, D.A., and Alvarez-Buylla, A. (1999). Interaction between astrocytes and adult subventricularzone precursors stimulates neurogenesis. Proceedings of the National Academy of Sciences of the United States of America *96*, 7526-7531.

Lo, C.W. (1996). The role of gap junction membrane channels in development. J Bioenerg Biomembr *28*, 379-385.

Lu, Q.R., Park, J.K., Noll, E., Chan, J.A., Alberta, J., Yuk, D., Alzamora, M.G., Louis, D.N., Stiles, C.D., Rowitch, D.H., *et al.* (2001). Oligodendrocyte lineage genes (OLIG) as molecular markers for human glial brain tumors. PNAS *98*, 10851-10856.

Magavi, S.S., and Macklis, J.D. (2002). Induction of neuronal type-specific neurogenesis in the cerebral cortex of adult mice: manipulation of neural precursors in situ. Brain Res Dev Brain Res *134*, 57-76.

Mann-Metzer, P., and Yarom, Y. (1999). Electrotonic coupling interacts with intrinsic properties to generate synchronized activity in cerebellar networks of inhibitory interneurons. J Neurosci *19*, 3298-3306.

Manthey, D., Banach, K., Desplantez, T., Lee, C.G., Kozak, C.A., Traub, O., Weingart, R., and Willecke, K. (2001). Intracellular domains of mouse connexin26 and -30 affect diffusional and electrical properties of gap junction channels. J Membr Biol *181*, 137-148.

Mantz, J., Cordier, J., and Giaume, C. (1993). Effects of general anesthetics on intercellular communications mediated by gap junctions between astrocytes in primary culture. Anesthesiology *78*, 892-901.

Marshall, G.P., Reynolds, B.A., and Laywell, E.D. (2007). Using the neurosphere assay to quantify neural stem cells in vivo. Current Pharmaceutical Biotechnology *8*, 141-145.

Matsumoto, A., Arai, Y., Urano, A., and Hyodo, S. (1991). Cellular localization of gap junction mRNA in the neonatal rat brain. Neurosci Lett *124*, 225-228.

Maxeiner, S., Kruger, O., Schilling, K., Traub, O., Urschel, S., and Willecke, K. (2003). Spatiotemporal transcription of connexin45 during brain development results in neuronal expression in adult mice. Neuroscience *119*, 689-700.

Meier, C., and Dermietzel, R. (2006). Electrical synapses--gap junctions in the brain. Results Probl Cell Differ *43*, 99-128.

Melanson-Drapeau, L., Beyko, S., Dave, S., Hebb, A.L., Franks, D.J., Sellitto, C., Paul, D.L., and Bennett, S.A. (2003). Oligodendrocyte progenitor enrichment in the connexin32 null-mutant mouse. J Neurosci *23*, 1759-1768.

Menichella, D.M., Goodenough, D.A., Sirkowski, E., Scherer, S.S., and Paul, D.L. (2003). Connexins are critical for normal myelination in the CNS. J Neurosci *23*, 5963-5973.

Mollgard, K., and Moller, M. (1975). Dendrodendritic gap junctions: a developmental approach. Adv Neurol *12*, 79-89.

Montoro, R.J., and Yuste, R. (2004). Gap junctions in developing neocortex: a review. Brain Res Brain Res Rev *47*, 216-226.

Moorby, C., and Patel, M. (2001). Dual functions for connexins: Cx43 regulates growth independently of gap junction formation. Exp Cell Res *271*, 238-248.

Muroyama, Y., Kondoh, H., and Takada, S. (2004). Wnt proteins promote neuronal differentiation in neural stem cell culture. Biochem Biophys Res Commun *313*, 915-921.

Nadarajah, B., Jones, A.M., Evans, W.H., and Parnavelas, J.G. (1997). Differential expression of connexins during neocortical development and neuronal circuit formation. J Neurosci *17*, 3096-3111.

Nadarajah, B., Makarenkova, H., Becker, D.L., Evans, W.H., and Parnavelas, J.G. (1998). Basic FGF increases communication between cells of the developing neocortex. J Neuroscience *18*, 7881-7890.

Nagy, J.I., Dudek, F.E., and Rash, J.E. (2004). Update on connexins and gap junctions in neurons and glia in the mammalian nervous system. Brain Res Brain Res Rev *47*, 191-215.

Nagy, J.I., Ionescu, A.V., Lynn, B.D., and Rash, J.E. (2003a). Connexin29 and connexin32 at oligodendrocyte and astrocyte gap junctions and in myelin of the mouse central nervous system. J Comp Neurol *464*, 356-370.

Nagy, J.I., Ionescu, A.V., Lynn, B.D., and Rash, J.E. (2003b). Coupling of astrocyte connexins Cx26, Cx30, Cx43 to oligodendrocyte Cx29, Cx32, Cx47: Implications from normal and connexin32 knockout mice. Glia *44*, 205-218.

Nagy, J.I., Ochalski, P.A., Li, J., and Hertzberg, E.L. (1997). Evidence for the co-localization of another connexin with connexin-43 at astrocytic gap junctions in rat brain. Neuroscience *78*, 533-548.

Nagy, J.I., Patel, D., Ochalski, P.A., and Stelmack, G.L. (1999). Connexin30 in rodent, cat and human brain: selective expression in gray matter astrocytes, co-localization with connexin43 at gap junctions and late developmental appearance. Neuroscience *88*, 447-468.

Naus, C.C., and Bani-Yaghoub, M. (1998). Gap junctional communication in the developing central nervous system. Cell Biol Int *22*, 751-763.

Naus, C.C., Bechberger, J.F., Zhang, Y., Venance, L., Yamasaki, H., Juneja, S.C., Kidder, G.M., and Giaume, C. (1997). Altered gap junctional communication, intercellular signaling, and growth in cultured astrocytes deficient in connexin43. J Neurosci Res *49*, 528-540.

Nedergaard, M., Ransom, B., and Goldman, S.A. (2003). New roles for astrocytes: redefining the functional architecture of the brain. Trends Neurosci *26*, 523-530.

Neijssen, J., Pang, B., and Neefjes, J. (2007). Gap junction-mediated intercellular communication in the immune system. Prog Biophys Mol Biol *94*, 207-218.

Odermatt, B., Wellershaus, K., Wallraff, A., Seifert, G., Degen, J., Euwens, C., Fuss, B., Bussow, H., Schilling, K., Steinhauser, C., *et al.* (2003). Connexin 47 (Cx47)-deficient mice with enhanced green fluorescent protein reporter gene reveal predominant oligodendrocytic expression of Cx47 and display vacuolized myelin in the CNS. J Neurosci *23*, 4549-4559.

Olbina, G., and Eckhart, W. (2003). Mutations in the second extracellular region of connexin 43 prevent localization to the plasma membrane, but do not affect its ability to suppress cell growth. Mol Can Res *1*, 690-700.

Palmer, T.D., Ray, J., and Gage, F.H. (1995). FGF-2-responsive neuronal progenitors reside in proliferative and quiescent regions of the adult rodent brain. Mol Cell Neurosci *6*, 474-486.

Paul, D.L. (1995). New functions for gap junctions. Curr Opin Cell Biol *7*, 665-672.

Peinado, A., Yuste, R., and Katz, L.C. (1993). Gap junctional communication and the development of local circuits in neocortex. Cereb Cortex *3*, 488-498.

Penderis, J., Shields, S.A., and Franklin, R.J. (2003). Impaired remyelination and depletion of oligodendrocyte progenitors does not occur following repeated episodes of focal demyelination in the rat central nervous system. Brain *126*, 1382-1391.

Plumpe, T., Ehninger, D., Steiner, B., Klempin, F., Jessberger, S., Brandt, M., Romer, B., Rodriguez, G.R., Kronenberg, G., and Kempermann, G. (2006). Variability of doublecortin-associated dendrite maturation in adult hippocampal neurogenesis is independent of the regulation of precursor cell proliferation. BMC Neurosci *7*, 77.

Ramirez-Castillejo, C., Sanchez-Sanchez, F., Andreu-Agullo, C., Ferron, S.R., Aroca-Aguilar, J.D., Sanchez, P., Mira, H., Escribano, J., and Farinas, I. (2006). Pigment epithelium-derived factor is a niche signal for neural stem cell renewal. Nat Neurosci *9*, 331-339.

Rash, J.E., Yasumura, T., Davidson, K.G., Furman, C.S., Dudek, F.E., and Nagy, J.I. (2001). Identification of cells expressing Cx43, Cx30, Cx26, Cx32 and Cx36 in gap junctions of rat brain and spinal cord. Cell Commun Adhes *8*, 315-320.

Reynolds, B.A., and Rietze, R.L. (2005). Neural stem cells and neurospheres--re-evaluating the relationship. Nat Methods *2*, 333-336.

Reynolds, B.A., and Weiss, S. (1992). Generation of neurons and astrocytes from isolated cells of the adult mammalian central nervous system. Science *255*, 1707-1710.

Rouach, N., Avignone, E., Meme, W., Koulakoff, A., Venance, L., Blomstrand, F., and Giaume, C. (2002). Gap junctions and connexin expression in the normal and pathological central nervous system. Biol Cell *94*, 457-475.

Rouach, N., Koulakoff, A., and Giaume, C. (2004). Neurons set the tone of gap junctional communication in astrocytic networks. Neurochem Int *45*, 265-272.

Rozental, R., Campos de Carvalho, A.C., and Spray, D.C. (2000). Nervous system diseaes involving gap junctions. Brain Res Brain Res Rev *32*, 189-191.

Rozental, R., Morales, M., Mehler, M.F., Urban, M., Kremer, M., Dermietzel, R., Kessler, J.A., and Spray, D.C. (1998). Changes in the properties of gap junctions during neuronal differentiation of hippocampal progenitor cells. J Neurosci *18*, 1753-1762.

Seaberg, R.M., Smukler, S.R., and van der Kooy, D. (2005). Intrinsic differences distinguish transiently neurogenic progenitors from neural stem cells in the early postnatal brain. Dev Biol *278*, 71-85.

Shingo, T., Gregg, C., Enwere, E., Fujikawa, H., Hassam, R., Geary, C., Cross, J.C., and Weiss, S. (2003). Pregnancy-stimulated neurogenesis in the adult female forebrain mediated by prolactin. Science *299*, 117-120.

Shou, J., Rim, P.C., and Calof, A.L. (1999). BMPs inhibit neurogenesis by a mechanism involving degradation of a transcription factor. Nat Neurosci *2*, 339-345.

Slezak, M., and Pfrieger, F.W. (2003). New roles for astrocytes: regulation of CNS synaptogenesis. Trends Neurosci *26*, 531-535.

Sohl, G., Eiberger, J., Jung, Y.T., Kozak, C.A., and Willecke, K. (2001). The mouse gap junction gene connexin29 is highly expressed in sciatic nerve and regulated during brain development. Biological Chemistry *382*, 973-978.

Sohl, G., Maxeiner, S., and Willecke, K. (2005). Expression and functions of neuronal gap junctions. Nat Rev Neurosci *6*, 191-200.

Sohl, G., Odermatt, B., Maxeiner, S., Degen, J., and Willecke, K. (2004). New insights into the expression and function of neural connexins with transgenic mouse mutants. Brain Research - Brain Research Reviews *47*, 245-259.

Sohl, G., and Willecke, K. (2003). An update on connexin genes and their nomenclature in mouse and man. Cell Communication and Adhesion *10*, 173-180.

Sohl, G., and Willecke, K. (2004). Gap junctions and the connexin protein family. Cardiovasc Res *62*, 228-232.

Song, H., Stevens, C.F., and Gage, F.H. (2002). Astroglia induce neurogenesis from adult neural stem cells. Nature *417*, 39-44.

Sosinsky, G.E., and Nicholson, B.J. (2005). Structural organization of gap junction channels. Biochim Biophys Acta *1711*, 99-125.

Stout, C., Goodenough, D.A., and Paul, D.L. (2004). Connexins: functions without junctions. Current Opinion in Cell Biology *16*, 507-512.

Sutor, B., and Hagerty, T. (2005). Involvement of gap junctions in the development of the neocortex. Biochim Biophys Acta *1719*, 59-68.

Tabernero, A., Jimenez, C., Velasco, A., Giaume, C., and Medina, J.M. (2001). The enhancement of glucose uptake caused by the collapse of gap junction communication is due to an increase in astrocyte proliferation. Journal of Neurochemistry *78*, 890-898.

Tanapat, P., Hastings, N.B., Reeves, A.J., and Gould, E. (1999). Estrogen stimulates a transient increase in the number of new neurons in the dentate gyrus of the adult female rat. J Neurosci *19*, 5792-5801.

Teubner, B., Michel, V., Pesch, J., Lautermann, J., Cohen-Salmon, M., Sohl, G., Jahnke, K., Winterhager, E., Herberhold, C., Hardelin, J.P., *et al.* (2003). Connexin30 (Gjb6)-deficiency causes severe hearing impairment and lack of endocochlear potential. Hum Mol Genet *12*, 13-21.

Valiunas, V., Weingart, R., and Brink, P.R. (2000). Formation of heterotypic gap junction channels by connexins 40 and 43. Circ Res *86*, E42-49.

Venance, L., Rozov, A., Blatow, M., Burnashev, N., Feldmeyer, D., and Monyer, H. (2000). Connexin expression in electrically coupled postnatal rat brain neurons. Proc Natl Acad Sci U S A *97*, 10260-10265.

Verderio, C., Bruzzone, S., Zocchi, E., Fedele, E., Schenk, U., De Flora, A., and Matteoli, M. (2001). Evidence of a role for cyclic ADP-ribose in calcium signalling and neurotransmitter release in cultured astrocytes. J Neurochem *78*, 646-657.

Wallraff, A., Kohling, R., Heinemann, U., Theis, M., Willecke, K., and Steinhauser, C. (2006). The impact of astrocytic gap junctional coupling on potassium buffering in the hippocampus. J Neurosci *26*, 5438-5447.

Warner, A.E. (1987). The use of antibodies to gap junction protein to explore the role of gap junctional communication during development. Ciba Foundation Symposium *125*, 154-167.

Warner, A.E., Guthrie, S.C., and Gilula, N.B. (1984). Antibodies to gap-junctional protein selectively disrupt junctional communication in the early amphibian embryo. Nature *311*, 127-131.

Weissman, T.A., Riquelme, P.A., Ivic, L., Flint, A.C., and Kriegstein, A.R. (2004). Calcium waves propagate through radial glial cells and modulate proliferation in the developing neocortex. Neuron *43*, 647-661.

Weyer, A., and Schilling, K. (2003). Developmental and cell type-specific expression of the neuronal marker NeuN in the murine cerebellum. J Neurosci Res *73*, 400-409.

Zhang, Y.W., Kaneda, M., and Morita, I. (2003). The gap junction-independent tumor-suppressing effect of connexin 43. J Biol Chem *278*, 44852-44856.

Zhao, C., Deng, W., and Gage, F.H. (2008). Mechanisms and Functional Implications of Adult Neurogenesis. Cell *132*, 645-660.

Zhao, H.B., Kikuchi, T., Ngezahayo, A., and White, T.W. (2006). Gap junctions and cochlear homeostasis. J Membr Biol *209*, 177-186.

## APPENDIX I

**Table 1 Primary ab product details, specificity, concentrations, and dilutions that were used for immunolabelling in chapter 2 and chapter 3.**

| Primary Ab | Species raised in | Monoclonal or polyclonal | Supplier and /or location | Final dilution/ concentration used |
|---|---|---|---|---|
| BrdU | Mouse | Mono | Roche, Indianapolis, IN. | 6 μg/mL |
| BrdU-FITC | Rat | Mono | Cedarlane Laboratories Limited, Hornby, ON. | 1/50 |
| Cx30 | Mouse | Mono | Zymed, San Francisco, CA. | 1/50 |
| Cx30 | Rabbit | Poly | Zymed, San Francisco, CA. | 1 μg/mL |
| DCX | Guineapig | Poly | Chemicon, Temecula, CA. | 1/400 |
| GFAP-Cy3 | Mouse | Mono | Sigma, Saint Louis, Missouri. | 1/200 |
| GFAP | Rat | Mono | Zymed, San Francisco, CA. | 1/5 |
| Nestin | Mouse | Mono | Chemicon, Temecula, CA. | 1/25 |
| NeuN | Mouse | Mono | Chemicon, Temecula, CA. | 1/50 |
| NG2 | Rabbit | Poly | Chemicon, Temecula, CA. | 1/100 |
| PDGFαR | Rat | Mono | BD PharMingen. | 3/2000 |

**Table 2 Secondary ab details including specificity, product details, fluorophores that are conjugated, and dilutions used for immunolabelling in chapters 2, and 3.**

| Secondary Ab | Fluorophore conjugated | Species raised in | Supplier | Final Dilution |
|---|---|---|---|---|
| Guinea pig IgG | Cy3 | Donkey | Jackson | 1/400 |
| Mouse IgG | AMCA | Donkey | Jackson | 1/50 |
| Mouse IgG | Cy3 | Donkey | Jackson | 1/400 |
| Mouse IgG | Cy5 | Goat | Invitrogen | 1/100 |
| Mouse IgG | FITC | Donkey | Jackson | 1/50 |
| Rabbit IgG | Cy3 | Donkey | Jackson | 1/300 |
| Rabbit IgG | FITC | Donkey | Jackson | 1/50 |
| Rat IgG | Cy3 | Donkey | Jackson | 1/200 |

**Table 3 Primary and secondary ab details including specificity, final dilutions or concentrations, product details, and conjugated fluorophores for flow cytometry methods 2.2.4.**

| Primary or Secondary Ab | Fluorophore conjugated | Species raised in | Supplier | Final Dilution |
|---|---|---|---|---|
| Cx30 | - | Mouse | Invitrogen | 1/25 |
| Cx30 | - | Rabbit | Invitrogen | 1/25 |
| GFAP | - | Rat | Invitrogen | 1/25 |
| Nestin | - | Mouse | Chemicon | 1/20 |
| Mouse IgG | Cy5 | Goat | Invitrogen | 1/50 |
| Rabbit IgG | FITC | Donkey | Jackson | 1/50 |
| Rat IgG | RPE | Goat | AbD SeroTec | 1/10 |